

**VALIDATION AND APPLICATION OF
INTRAVASCULAR ULTRASOUND IN
ENDOVASCULAR TREATMENT OF
ABDOMINAL AORTIC ANEURYSM**


Jeroen Anne van Essen

I.S.B.N.: 90-9013750-5

Cover designed by A.W. Zwamborn

Type-setting: A.W. Zwamborn

Photographs: T. Rijsdijk

Printed by  Ridderprint B.V. Ridderkerk

(c) 2000, J.A. van Essen

All rights reserved. No part of this dissertation may be reproduced, stored in a retrieval system or transmitted in any other form or by any means, without the prior written permission of the author, or, when appropriate, of the publishers of the publications.

**VALIDATION AND APPLICATION OF
INTRAVASCULAR ULTRASOUND IN
ENDOVASCULAR TREATMENT OF
ABDOMINAL AORTIC ANEURYSM**

VALIDATIE EN TOEPASSING VAN
INTRAVASCULAIRE ECHOGRAFIE BIJ DE
ENDOVASCULAIRE BEHANDELING VAN HET
ABDOMINALE AORTA ANEURYSMA

PROEFSCHRIFT

Ter verkrijging van de graad van doctor
aan de Erasmus Universiteit Rotterdam
op gezag van de rector magnificus
Prof. dr. P.W.C. Akkermans M.A.
en volgens het besluit van het College voor Promoties

De openbare verdediging zal plaatsvinden op
Woensdag 28 juni 2000 om 11.45 uur


door
Jeroen Anne van Essen
geboren te Haarlem

Promotiecommissie

Promotoren: Prof. dr. H. van Urk
Prof. dr. P.M.T. Pattynama

Overige leden: Prof. dr. Ir. N. Bom
Prof. dr. J. Jeekel
Prof. dr. J.A. Reekers

Co-promotor: dr. E.J. Gussenhoven

Studies presented in this dissertation were supported by the Netherlands Heart Foundation (grant number 95.123 and 91.016),
and the Interuniversity Cardiology Institute of the Netherlands. 

This thesis was financially supported by the Interuniversity Cardiology Institute of the Netherlands, de Rotterdamse Vaatstichting, Endosonics Europe B.V., W.L. Gore & Associates and Medtronic B.V.

Chapter 1	General introduction and objectives	7
Chapter 2	Intravascular ultrasound allows accurate assessment of abdominal aortic aneurysm: an in vitro validation study. van Essen et al. <i>J Vasc Surg</i> 1998; 27: 347-353.	19
Chapter 3	Accurate assessment of abdominal aortic aneurysm by intravascular ultrasound: validation with spiral computed tomographic angiography. van Essen et al. <i>J Vasc Surg</i> 1999; 29: 631-638.	33
Chapter 4	Reliability and reproducibility of automated contour analysis in intravascular ultrasound images of femoropopliteal arteries. van der Lugt et al. <i>Ultrasound Med Biol</i> 1998; 24: 43-50.	47
Chapter 5	Validation of automated contour analysis of intravascular ultrasound images following vascular intervention. Hartlooper et al. <i>J Vasc Surg</i> 1998; 27: 486-491.	63
Chapter 6	Three-dimensional intravascular ultrasound assessment of the proximal and distal neck of abdominal aortic aneurysms. van Essen et al. <i>J Endovasc Ther</i> : in press.	75
Chapter 7	Intravascular ultrasound to guide endovascular treatment of abdominal aortic aneurysm. van Essen et al. Submitted.	91
Chapter 8	Endovascular repair of abdominal aortic aneurysms: The role of intravascular ultrasound.	107
Chapter 9	Summary	125
Chapter 10	Samenvatting	131

Contents

List of publications	139
Dankwoord	145
Curriculum vitae	149

INTRODUCTION AND OBJECTIVES

Introduction and objectives

ABDOMINAL AORTIC ANEURYSM

An abdominal aortic aneurysm (AAA) is a localized and permanent dilatation of the aorta that presents a clear danger for the patient because of the risk of rupture^{1,2}. The chance of rupture increases with the size of the aneurysm³. Mortality after rupture is high; 60-70% of patients with a ruptured AAA will not reach the hospital alive^{4,5}. Furthermore, surgical treatment of ruptured AAA carries an additional mortality of 45-55%⁶⁻⁸. Because of the poor prognosis of ruptured AAA, prophylactic exclusion of AAA is performed for AAA larger than 5.0 to 5.5 cm in diameter^{9,10}. The standard way of treating AAA is by elective open surgery. In this procedure, the diseased aortic segment is opened after proximal and distal clamping of the vessel and the contents of the aneurysm are removed. A synthetic prosthesis is placed inside the aneurysm. The proximal and distal ends of the prosthesis are anastomosed via continuous sutures to the normal aorta and/or iliac arteries, after which the aneurysm wall is closed around the prosthesis¹¹. Elective surgery itself carries a mortality of 5-7%^{6,8,12}; patients aged over 70 years, patients with congestive heart failure, cardiac ischemia, preexistent dysrhythmia, renal impairment or pulmonary impairment are known to have an increased mortality^{6,13,14}.

ENDOVASCULAR REPAIR OF ABDOMINAL AORTIC ANEURYSMS

Because of the rising incidence of AAA in older patients with increased co-morbidity and the associated morbidity and mortality of open repair, a new method of exclusion of AAA was sought. After successful experiments in sheep¹⁵ and dogs¹⁶, endovascular repair of AAA was introduced in 1991 in humans by Volodos et al. in Russia¹⁷ and Parodi et al. in Argentina¹⁸. In endovascular aneurysm repair, the AAA is excluded from the arterial circulation by means of a transfemorally inserted, intravascularly deployed stent-graft.

The procedure of stent-graft placement can be described as follows: the stent-graft is inserted via a cut-down in the femoral artery and is pushed upwards to the level of the AAA. The stent-graft is then deployed just distal to the renal arteries. Fixation is provided by means of the radial force of the stent, with or without hooks and barbs. In some cases balloon dilatation is performed to ensure fixation of hooks and barbs into the vessel wall.

The first generation stent-grafts for repair of AAA were homemade devices, constructed of polyester grafts with balloon expandable stents sewn to the proximal and distal ends, available in a tube graft configuration only. Nowadays, an increasing number of commercial endografts are available for clinical use¹⁹⁻²². These endografts come in tube, aorto-uni-iliac and bifurcated configurations, which potentially allows these grafts to be used in 60% of the patients presenting with AAA²³.

Endografts can be divided in custom-made and modular devices. The custom-made devices are prepared on the basis of computed tomographic (CT) imaging for each individual patient. Once inserted into the patient, no further modification is possible. The modular devices consist of multiple components that can be individually tailored in a variety of configurations during the procedure. Some devices enable the use of aortic and iliac extender cuffs to ensure complete exclusion. Therefore, after selection of appropriate patients, the final choice of dimensions of the stent-graft is done during the procedure.

Several studies have shown that endovascular repair of AAA is feasible and effective; with a technical success of 70-90% and an associated mortality and morbidity that is comparable to open surgical repair^{19-21, 24-26}.

Over the years, endovascular repair of AAA has presented a number of problems. During the intervention, a number of problems may arise that can threaten the success of the intervention. These include incorrect placement of the stent-graft leading to occlusion of renal or internal iliac arteries, incomplete apposition of the proximal or distal attachment system leading to insufficient fixation, migration and endoleaks, angulation of the iliac legs leading to kinking, thrombosis and dislodgement of stent-graft parts, and incomplete deployment of the stent-graft leading to stenosis or thrombosis of the iliac leg^{27,28}. After the intervention endoleakage may appear. In this condition, the aneurysm sac, not excluded from the circulation, will be under pressure and the chance of rupture is maintained²⁹⁻³¹. Currently, there is no uniform policy to treat endoleaks. However, if the endoleak persists for more than 3-6 months, or if the aneurysm increases in size, intervention is warranted³²⁻³⁴.

A recent report has shown that on the long term, endografts may be threatened by degradation of the Dacron graft material³⁵. The constant 'wear and tear' of the circulation may dislodge the stents from the stent-graft and these loose stents may damage the graft causing tears in the prosthesis, creating an endoleak. Shrinkage of the aneurysm may be responsible for kinking and dislodgement of stent-graft parts. Finally, continued expansion of the aortic neck after intervention, which may threaten long-term fixation of endografts, has been a source of concern^{36,37}. If necks continue to dilate, the fixation of the endograft may fail and new endoleaks may occur.

PARAMETERS OF ENDOVASCULAR REPAIR

In order to safely perform endovascular repair a number of parameters should be considered before intervention. The length and diameter of the proximal and distal fixation sites must be assessed, as well as the length of the aneurysm. Based on these parameters the type and size of the stent-graft may be selected. The presence of thrombus in the proximal neck must be

excluded as well as the presence of stenosis or occlusion in the iliac and common femoral arteries. The presence of accessory renal arteries must be documented. During the procedure itself, the proximal and distal fixation sites are imaged and the renal arteries and the internal iliac arteries should be identified in order to avoid occlusion. In case of modular stent-grafts, the final dimensions of the stent-graft may be chosen. After placement of the stent-graft the success of the procedure must be documented. Parameters that may threaten the success of the intervention should be acknowledged and, if necessary, treated. After the intervention the overall success can be assessed and the AAA should be monitored during follow-up.

IMAGING TECHNIQUES

The development of endovascular aneurysm repair and the introduction of modular stent-grafts, has prompted the need for accurate and detailed vascular imaging. Currently used techniques to define AAA are external ultrasound, angiography, CT angiography (CTA), magnetic resonance angiography (MRA) and intravascular ultrasound (IVUS)³⁸. External ultrasound, used to measure the maximum diameter of the aneurysm, is a cheap and easy method to document the progression of the aneurysmal disease. However, external ultrasound cannot be used to determine the dimensions of the aneurysmal necks, the length of the aneurysm and the dimensions of the stent-graft necessary for endovascular aneurysm repair. Angiography allows a broad imaging field, is easily accessible, but shows only the vessel lumen. Measurements of the length and diameter of the proximal and distal attachment sites may be influenced by the presence of thrombus, parallax and foreshortening. Although the use of calibrated angiography catheters may improve the length measurements, thrombus present in the AAA may give the false impression of a normal vessel suitable for endograft fixation. During intervention angiography/fluoroscopy remains the most frequently used imaging technique.

CTA is a noninvasive technique that provides relevant parameters for the selection of patients suitable for endovascular treatment. CTA is an acknowledged technique to provide accurate measurements on the dimensions of the AAA and the proximal and distal attachment sites. Therefore, CTA is currently considered to be the 'gold standard' in imaging patients potentially suitable for endovascular treatment of AAA³⁹. After intervention CTA can be used to document the success or failure of the intervention and to monitor the long-term efficacy of endovascular treatment^{40,41}.

An imaging technique with a potential for perioperative use is MRA. At this moment, however, MRA is only used in an experimental setting for preoperative imaging purposes⁴².

Finally, intravascular ultrasound (IVUS) is an acknowledged technique to provide information on lesion characteristics and vessel dimensions both in coronary and peripheral vessels, as well as providing information on the success of endovascular intervention⁴³⁻⁴⁶. With respect to the endovascular treatment of AAA, IVUS may overcome the limitations of angiography and CTA by providing cross-sectional images of the vessels before and after intervention. IVUS may be used to allow accurate depiction of the dimensions of the endograft necessary to exclude the aneurysm and to assess the success of the procedure.

OBJECTIVES OF THIS THESIS

Because no validation studies have been performed with IVUS in AAA, and little experience is available on the use of IVUS during endovascular AAA repair, the objectives of this thesis include:

1. To assess in vitro whether IVUS allows accurate assessment of AAA.
2. To validate IVUS measurements useful for endovascular treatment of AAA with CTA measurements.
3. To validate an automated contour analysis system for the assessment of vascular dimensions from a three-dimensional (3D) stack of IVUS images, and to define the potential role of 3D IVUS imaging to assess the proximal and distal neck of AAA.
4. To determine the role of IVUS during endovascular treatment of AAA.

CONTENTS OF THIS THESIS

In Chapter 2 we describe the accuracy of IVUS to detect lesion morphology and dimensions of AAA in an in vitro set-up.

In Chapter 3 we study the accuracy of IVUS to measure parameters useful for the endovascular treatment of AAA by comparison with CTA. In case of endovascular treatment, the diameter and length of the proximal and distal AAA neck as well as the length of the AAA itself, are important for the selection of endograft dimensions.

In Chapters 4-6 it is demonstrated that a (semi-) automated contour analysis system can be used to provide information on vascular dimensions. This system uses a three-dimensional (3D) stack of IVUS images in which the lumen contours are detected by minimal cost algorithm. The system is tested first in femoropopliteal arteries before and after endovascular interventions, and is subsequently used to define the proximal and distal necks of AAA.

In Chapter 7 the role of IVUS before and after endograft placement is determined in 29 patients using different stent-grafts. Before placement, the position of renal arteries, accessory renal arteries, aortic bifurcation and internal iliac arteries is documented. If a modular device is used, the diameter and length of the device is determined. After placement, the

apposition at the proximal and distal ends of the stent-graft is determined. Possible occlusion of renal arteries, accessory renal arteries and internal iliac arteries is checked. Stenosis of the iliac legs of the stent-graft and damage to the iliac arteries as a result of the introduction of the device is determined and treated if necessary.

In Chapter 8 the results of endovascular repair of AAA are reviewed, and the role of IVUS and other, alternative, imaging methods are discussed.

REFERENCES

1. A. Hollier LH, Rutherford RB. Infrarenal aortic aneurysms. In: Rutherford RB (ed), *Vascular Surgery*. WB Saunders Company, London 1989: 909-927.
2. Johnston KW, Rutherford RB, Tilson D, Shah DM, Hollier L, Stanley JC. Suggested standards for reporting on arterial aneurysms. *J Vasc Surg* 1991; 13: 444-450.
3. Ernst CB. Abdominal aortic aneurysm. *N Engl J Med* 1993; 328: 1167-1172.
4. Ingoldby CJH, Wujanto R, Mitchell JE. Impact of vascular surgery on community mortality from ruptured aortic aneurysms. *Br J Surg* 1986; 73: 551-553.
5. Bengtsson H, Bergqvist D. Ruptured abdominal aortic aneurysm: a population-based study. *J Vasc Surg* 1993; 18: 74-80.
6. Katz DJ, Stanley JC, Zelenock GB. Operative mortality rates for intact and ruptured abdominal aortic aneurysms in Michigan: an eleven-year statewide experience. *J Vasc Surg* 1994; 19: 804-817.
7. Dardik A, Burleyson GP, Bowman H, Gordon TA, Williams M, Webb TH, Perler BA. Surgical repair of ruptured abdominal aortic aneurysms in the state of Maryland: factors influencing outcome among 527 recent cases. *J Vasc Surg* 1998; 28: 413-421.
8. Sayers RD, Thompson MM, Nasim A, Healey P, Taub N, Bell PRF. Surgical management of 671 abdominal aortic aneurysms: a 13 year review from a single center. *Eur J Vasc Endovasc Surg* 1997; 13: 322-327.
9. Hollier LH, Taylor LM, Ochsner J. Recommended indications for operative treatment of abdominal aortic aneurysms. Report of a subcommittee of the Joint Council of the Society for Vascular Surgery and the North American Chapter of the International Society for Cardiovascular Surgery. *J Vasc Surg* 1992; 15: 1046-1056.
10. Greenhalgh RM, Forbes JF, Fowkes FGR, Powel JT, Ruckley CV, Brady AR, Brown LC, Thompson SG. The UK Small Aneurysm Trial Participants Steering Committee. Early elective open surgical repair of small abdominal aortic aneurysms is not recommended: results of the UK small aneurysm trial. *Eur J Vasc Endovasc Surg* 1998; 16: 462-464.
11. Yao JST, Flinn WR, Bergan JJ. Technique for repairing infrarenal abdominal aortic aneurysms. In: Nyhus LM and Baker RJ (eds), *Mastery of Surgery*. Little, Brown and Company, Boston 1992: 1699-1704.
12. Akkersdijk GJM, Graaf van der Y, Bockel van HJ, Vries de AC, Eikelboom BC. Mortality rates associated with operative treatment of infrarenal abdominal aortic aneurysm in The Netherlands. *Br J Surg* 1994; 81: 706-709.
13. Steyersberg EW, Kievit J, Mol van Otterloo de JCA, Bockel van JH, Eijkemans MJC, Habbema JDF. Perioperative mortality of elective abdominal aortic aneurysm surgery. A clinical prediction rule based on literature and individual patient data. *Arch Intern Med* 1995; 155: 1998-2004.
14. Poldermans D, Arnese M, Fioretti PM, Salustri A, Boersma E, Thomson IR, Roelandt JR, Urk van H. Improved cardiac risk stratification in major vascular

- surgery with dobutamine-atropine stress echocardiography. *J Am Coll Cardiol* 1995; 26: 648-653.
15. Balko A, Piasecki GJ, Shah DM, Carney WI, Hopkins RW, Jackson BT. Transfemoral placement of intraluminal polyurethane prosthesis for abdominal aortic aneurysm. *J Surg Res* 1986; 40: 305-309.
 16. Mirich D, Wright KC, Wallace S, Yoshioka T, Lawrence DD, Charnsangavej C, Gianturco C. Percutaneously placed endovascular grafts for aortic aneurysms: feasibility study. *Radiology* 1989; 170: 1033-1037.
 17. Volodos NL, Karpovich IP, Troyan VI, Kalashnikova YV, Shekhanin VE, Ternyuk NE, Neoneta AS, Ustinov NI, Yakovenko LF. Clinical experience of the use of self-fixing synthetic prostheses for remote endoprosthetics of the thoracic and the abdominal aorta and iliac arteries through the femoral artery and as intraoperative endoprosthesis for aorta reconstruction. *Vasa* 1991; 33 (suppl): 93-95.
 18. Parodi JC, Palmaz JC, Barone HD. Transfemoral intraluminal graft implantation for abdominal aortic aneurysms. *Ann Vasc Surg* 1991; 5: 491-499.
 19. Broeders IAMJ, Blankensteijn JD, Eikelboom BC. The Endovascular Technologies system. In Hopkinson B, Yusuf W, Whitaker S, Veith F (eds), *Endovascular Surgery for Aortic Aneurysms*. WB Saunders Company, London 1997: 105-121.
 20. Blum U, Voshage G, Lammer J, Beyersdorf F, Töllner D, Kretschmer G, Spillner G, Polterauer P, Nagel G, Hölzenbein T, Thurnher S, Langer M. Endoluminal stent-grafts for infrarenal abdominal aortic aneurysms. *N Engl J Med* 1997; 336: 13-20.
 21. Uflacker R, Robison JG, Brothers TE, Pereira AH, Sanvitto PC. Abdominal aortic aneurysm treatment: preliminary results with the Talent Stent-Graft system. *JVIR* 1998; 9: 51-60.
 22. Allen RC, White RA, Zarins CK, Fogarty TJ. What are the characteristics of the ideal endovascular graft for abdominal aortic aneurysm exclusion? *J Endovasc Surg* 1997; 4: 195-202.
 23. Armon MP, Hopkinson BR. How much does an aorto-uni-iliac stent-graft increase the endovascular options for abdominal aortic aneurysm repair? In: Greenhalgh RM (ed), *Indications in Vascular and Endovascular Surgery*. WB Saunders Company, London 1998: 221-227.
 24. May J, White GH, Yu W, Ly CN, Waugh R, Stephen MS, Arulchelvam M, Harris JP. Concurrent comparison of endoluminal versus open repair in the treatment of abdominal aortic aneurysm: analysis of 303 patients by life table method. *J Vasc Surg* 1998; 27: 213-221.
 25. Brewster DC, Geller SC, Kaufman JA, Cambria RP, Gertler JP, LaMuraglia GM, Atamian S, Abbott WM. Initial experience with endovascular aneurysm repair: comparison of early results with outcome of conventional open repair. *J Vasc Surg* 1998; 27: 992-1005.
 26. Zarins CK, White RA, Schwarten D, Kinney E, Dietrich EB, Hodgson KJ, Fogarty TJ. AneuRx stent graft versus open repair of abdominal aortic aneurysms: multicenter prospective clinical trial. *J Vasc Surg* 1999; 29: 292-308.

27. Parodi JC, Barone A, Piraino R, Schonholz C. Endovascular treatment of abdominal aortic aneurysms: lessons learned. *J Endovasc Surg* 1997; 4: 102-110.
28. Naslund TC, Edwards WH, Neuzil DF, Martin RS, Snyder SO, Mulherin JL, Failor M, McPherson K. Technical complications of endovascular abdominal aortic aneurysm repair. *J Vasc Surg* 1997; 26: 502-510.
29. Lumsden AB, Allen RC, Chaikof EL, Resnikoff M, Moritz MW, Gerhard H, Castronuovo JJ. Delayed rupture of aortic aneurysms following endovascular stent grafting. *Am J Surg* 1995; 170: 174-178.
30. Torsello GB, Klenk E, Kasprzak B, Umscheid T. Rupture of abdominal aortic aneurysm previously treated by endovascular stentgraft. *J Vasc Surg* 1998; 28: 184-187.
31. Schurink GWH, Aarts NJM, Wilde J, Baalen van JM, Chuter TAM, Schultze Kool LJ, Bockel van JH. Endoleakage after stent-graft treatment of abdominal aortic aneurysm: implications on pressure and imaging - an in vitro study. *J Vasc Surg* 1998; 28: 234-241.
32. Beebe HG, Bernhard VM, Parodi JC, White GH. Leaks after endovascular therapy for aneurysm: detection and classification. *J Endovasc Surg* 1996; 3: 445-448.
33. Golzarian J, Struyven J, Abada HT, Wery D, Dussaussois L, Madani A, Ferreira J, Dereume JP. Endovascular aortic stent-grafts: transcatheter embolization of persistent perigraft leaks. *Radiology* 1997; 202: 731-734.
34. Makaroun M, Zajko A, Sugimoto H, Eskandari M, Webster M. Fate of endoleaks after endoluminal stent grafting of abdominal aortic aneurysms with the EVT device. *European Society for Vascular Surgery, XII Annual Meeting, 1998: 152.*
35. Alimi YS, Chakfe N, Rivoal E, Slimane KK, Valerio N, Riepe G, Kretz JG, Juhan C. Rupture of an abdominal aortic aneurysm after endovascular graft placement and aneurysm size reduction. *J Vasc Surg* 1998; 28: 178-183.
36. Illig KA, Green RM, Ouriel K, Riggs P, Bartos S, DeWeese JA. Fate of the proximal aortic cuff: implications for endovascular aneurysm repair. *J Vasc Surg* 1997; 26: 492-501.
37. Matsumura JS, Chaikof EL. Continued expansion of aortic necks after endovascular repair of abdominal aortic aneurysms. *J Vasc Surg* 1998; 28: 422-431.
38. Beebe HG. Imaging modalities for aortic endografting. *J Endovasc Surg* 1997; 4: 111-123.
39. Balm R, Leeuwen van MS, Noordzij J, Eikelboom BC. Spiral CT for aortic aneurysms. In: Greenhalgh RM (ed), *Vascular Imaging for Surgeons*, WB Saunders Company, London 1995: 191-202.
40. Balm R, Kaatee R, Blankensteijn JD, Mail WPTM, Eikelboom BC. CT-angiography of abdominal aortic aneurysms after Transfemoral Endovascular Aneurysm Management. *Eur J Vasc Endovasc Surg* 1996; 12: 182-188.
41. Broeders IAMJ, Blankensteijn JD, Gvakharia A, May J, Bell PRF, Swedenborg J, Collin J, Eikelboom BC. The efficacy of Transfemoral Endovascular Aneurysm

-
- Management: a study on size changes of the abdominal aorta during mid-term follow-up. *Eur J Vasc Endovasc Surg* 1997; 14: 84-90.
42. Nasim A, Thompson MM, Sayers RD, Boyle JR, Hartshorne T, Moody AR, Bell PRF. Role of magnetic resonance angiography for assessment of abdominal aortic aneurysm before endoluminal repair. *Br J Surg* 1998; 85: 641-644.
 43. Gussenhoven WJ, Essed CE, Lancée CT, Mastik F, Frietman P, Egmond van FC, Reiber J, Bosch H, Urk van H, Roelandt J, Bom N. Arterial wall characteristics determined by intravascular ultrasound imaging: an in vitro study. *J Am Coll Cardiol* 1989; 14: 947-952.
 44. The SHK, Gussenhoven WJ, Zhong Y, Li W, Egmond van FC, Pieterman H, Urk van H, Gerritsen P, Borst C, Wilson RA, Bom N. Effect of balloon angioplasty on femoral artery evaluated with intravascular ultrasound imaging. *Circulation* 1992; 86: 483-493.
 45. Lugt van der A, Gussenhoven EJ, Pasterkamp G, Stijnen T, Reekers JA, Berg van der FG, Tielbeek AV, Seelen JL, Pieterman H. Intravascular ultrasound predictors of restenosis after balloon angioplasty of the femoropopliteal artery. *Eur J Vasc Endovasc Surg* 1998; 16: 110-119.
 46. Sambeek van MRHM, Gussenhoven EJ, Overhagen van H, Honkoop J, Lugt van der A, Bois du NAJJ, Urk van H. Intravascular ultrasound in endovascular stent-grafts for peripheral aneurysm: a clinical study. *J Endovasc Surg* 1998; 5: 106-112.

Introduction and objectives _____

**INTRAVASCULAR ULTRASOUND ALLOWS
ACCURATE ASSESSMENT OF ABDOMINAL
AORTIC ANEURYSM: AN IN VITRO
VALIDATION STUDY**

**Jeroen A. van Essen, MD¹, Aad van der Lugt, MD, PhD²,
Elma J. Gussenhoven, MD, PhD¹, Trude C. Leertouwer, MD¹,
Pieter Zondervan, MD³, Marc R.H.M. van Sambeek, MD, PhD⁴.**

From the Departments of Cardiology¹, Radiology², Pathology³ and
Vascular Surgery⁴ of the University Hospital Rotterdam-Dijkzigt and
the Erasmus University Rotterdam, the Netherlands.

Supported by grants from the Interuniversity Cardiology Institute, the
Netherlands and the Netherlands Heart Foundation (no. 95.123 and 91.016).

J Vasc Surg 1998; 27: 347-353

ABSTRACT

Objectives:

To acquire insight in the interpretation of intravascular ultrasound images of the abdominal aorta and to assess to what extent this technique can provide useful parameters for the endovascular treatment of abdominal aortic aneurysm.

Study-design:

This was a descriptive study.

Methods:

Fifteen abdominal aortic specimens (normal, atherosclerotic or aneurysmal) were studied. Ultrasonic images and corresponding histologic sections were compared for vessel wall characteristics, lesion morphology and for lumen diameter. The length of the aneurysm and the length of the proximal and distal neck were measured and compared with external measurements. Tomographic images were reconstructed to a three-dimensional format.

Results:

Normal aortic wall was seen as a two- or three-layered structure corresponding with intima, media and adventitia. A distinction could be made between fibrous lesion, calcified lesion and thrombus and between normal and aneurysmal aorta. Correlation between the histologic specimens and intravascular ultrasound for lumen diameter measurements was high ($r=0.93$; $p<0.001$). Similarly, correlation between external measurements and intravascular ultrasound measurements on the length of the aneurysm and its proximal and distal neck was high ($r=0.99$; $p<0.001$). Three-dimensional analysis enhanced interpretation of the tomographic images by visualizing the spatial position of anatomic structures and contributed to understanding the shape and dimensions of the aneurysm.

Conclusions:

Intravascular ultrasound provides accurate information on the vessel wall, lesion morphology and quantitative parameters of the abdominal aorta. Spatial information supplied by three-dimensional analysis contributes to a more realistic interpretation of the tomographic images.

INTRODUCTION

Since the introduction of the endoluminal stent-graft for the treatment of abdominal aortic aneurysm¹, several studies have demonstrated the feasibility of this therapy²⁻⁹. This kind of endovascular intervention depends increasingly on accurate and detailed visualization of the anatomy of the abdominal aorta. Intravascular ultrasound (IVUS) which permits detailed high-quality imaging of coronary and peripheral vessels¹⁰⁻¹², may be suitable to provide information before and during endovascular treatment of aneurysmal abdominal aorta. This in vitro study was undertaken to acquire insight in the interpretation of IVUS images of normal and diseased abdominal aorta and to examine the accuracy of IVUS assessed parameters that may be useful during endovascular aneurysm repair.

METHODS

Human specimens.

Human aortic specimens, removed at autopsy from patients over 60 years of age, and classified on external appearance as normal ($n=5$), atherosclerotic with calcification ($n=5$) or aneurysmal (diameter 3.5-7 cm, $n=5$) were studied in vitro. Side-branches were tied off with sutures and the proximal and distal ends were connected to sheaths fixed to a waterbath which was maintained at room temperature. During the study the aorta was pressurized at 100 mmHg by means of a fluid reservoir containing water connected to the side-arm of the distal sheath (Fig. 1). The investigation was approved by the Local Committee on Human Research.

Intravascular ultrasound.

Mechanical IVUS systems used were: the Microsound system with a Princeps 30 MHz 4.3F catheter (Endosonics, Rijswijk, the Netherlands) and the HP-Sonos Intravascular Imaging System (Hewlett Packard, Andover, MA, USA) with a Sonicath Side-Saddle 12.5 MHz 6.2 F catheter (Boston Scientific Corp., Watertown, MA, USA). Because the Microsound system permits a maximum radius of 30 mm, this system was only used in normal and atherosclerotic aortae. A displacement sensing device was used to match IVUS images with corresponding histologic sections, to assess the distance between the major side-branches and to determine the length of the aneurysm and proximal and distal neck; in addition the displacement sensing device was used to reconstruct a three-dimensional (3D) image of the aorta¹³. The displacement of the IVUS catheter tip in steps of 0.01 cm was related to the reference site (i.e. the proximal sheath) and mixed automatically with the ultrasound information on the video screen (Fig. 1). IVUS images were stored on video-tape (S-VHS) for further analysis.

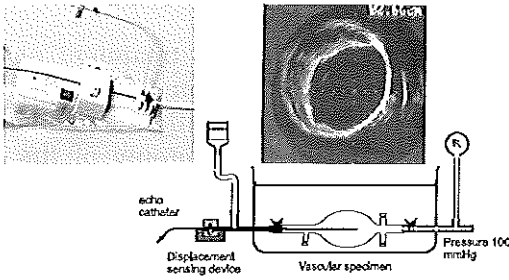


Fig. 1. In vitro set-up showing the intravascular ultrasound catheter advanced through the sensing unit of the displacement sensing device and sheath toward the pressurized vascular specimen. The catheter tip position in relation to the proximal sheath is indicated in the right upper corner. The displacement sensing device is seen in the insert in the left upper panel. Calibration: 5 mm.

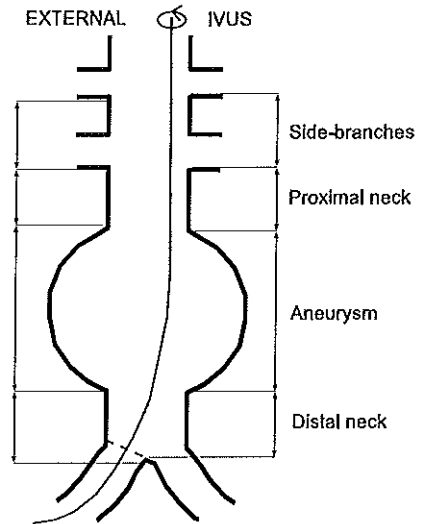


Fig. 2. Artist's rendition of an abdominal aortic aneurysm illustrating the side-branches, the aneurysm and the proximal and distal neck. On the left the measurements as performed externally, on the right the measurements with intravascular ultrasound (IVUS). The intraluminal line represents the ultrasound catheter.

Histology.

Immediately following the IVUS examination the aortic specimens were fixed under pressure (100 mm Hg) in 10% buffered formalin for two hours. The distance between the aortic bifurcation and major side-branches, i.e. coeliac trunk, superior and inferior mesenteric arteries and renal arteries, was measured externally, as was the distance between consecutive major side-branches. Similarly, in aneurysmal aortae, the length of the aneurysm as well as the length of the proximal and distal neck was measured (Fig. 2). The specimens were subsequently decalcified in a standard RDO solution (Apex Inc., Plainfield, Illinois, USA) for five hours and further processed for routine paraffin embedding. Transverse sections (5 μ m thick) were cut at 10 mm intervals for normal and atherosclerotic aortae and at 5 mm intervals for aneurysmal aortae. The sections were stained with elastic van Gieson and hematoxylin-eosin techniques.

Qualitative data analysis.

IVUS images obtained were photographed at increments of 5 mm. For comparison with the corresponding histologic sections data from the displacement sensing device and anatomic markers such as side-branches were used. Aortic wall characteristics and lesion morphology assessed with IVUS were verified with the corresponding histology.

Quantitative data analysis.

For each specimen a set of five infrarenal histologic sections and their corresponding IVUS cross-sections, taken at increments of 2 cm, were quantitatively analyzed. Given the fact that the histologic sections did not

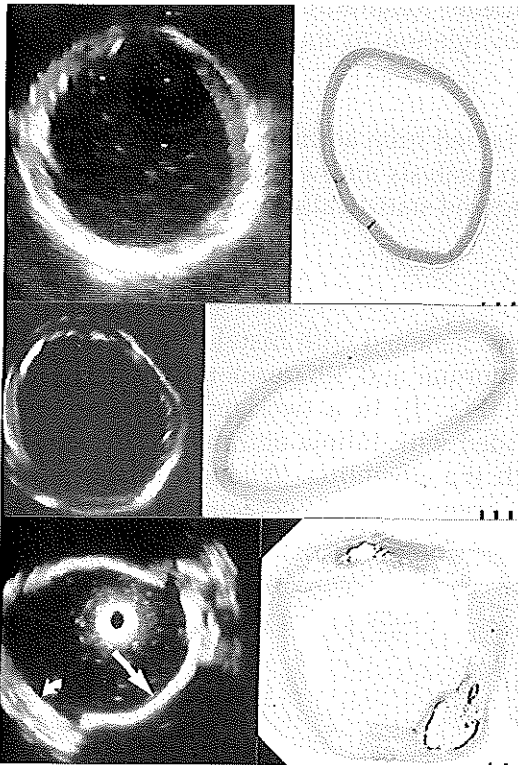


Fig. 3. Intravascular ultrasound cross-sections and histologic counterparts (staining: hematoxylin-eosin). (*Upper panel*) shows a normal aorta with a two-layered structure. (*Middle panel*) shows a normal aorta with a three-layered structure. (*Lower panel*) shows an atherosclerotic aorta with a calcified lesion at 4 o'clock (*straight arrow*) and a fibrous lesion at 8 o'clock (*curved arrow*). Note the absence of a circular shape in the histologic section in the middle panel. Calibration: 5 mm (IVUS) and 1 mm (histology).

maintain a circular shape due to the processing procedure, the lumen diameter was calculated from the lumen circumference, both on histology and IVUS. For this purpose a digital video analyzing system was used¹⁴. Distances between the major

side-branches and the aortic bifurcation measured externally, along the central axis of the vessel with the use of a pair of compasses, were compared with the distances measured with IVUS. The caudal borders of the side-branches and the border of the aortic bifurcation were used as reference (Fig. 2). Furthermore, the distances between consecutive major side-branches measured externally and with IVUS were compared, as were the length of the aneurysm and the length of the proximal and the distal

neck. The proximal neck was defined as the distance between the caudal border of the most distal renal artery and the cranial border of the aneurysm; the distal neck was defined as the distance between the caudal border of the aneurysm and the aortic bifurcation (Fig. 2). Measurements on the length of aneurysm and proximal and distal neck were compared together because of the small number of measurements.

Three-dimensional analysis.

In order to create a 3D model of the aorta the IVUS images were digitized at a resolution of 800x600x8 Bits by a frame grabber (DT-3852) and aligned and stacked longitudinally^{15,16}. Up to 200 images were acquired with a given interval (0.5-1.0 mm). In the resulting model two planes parallel to the linear axis of the vessel were selected to create longitudinal images that display position and size of the aneurysm in relation to major side-branches and aortic bifurcation.

Statistical analysis.

Diameter and axial measurements obtained from aortic specimens and IVUS were compared with linear regression analysis and with the paired samples *t*-test. A *p*-value below 0.05 was considered statistically significant.

RESULTS

Qualitative analysis.

A total of 285 IVUS cross-sections were matched with histologic sections for qualitative analysis. IVUS identified normal and atherosclerotic vessel wall as a two- or three-layered structure (Fig. 3). In a two-layer structure the inner, less echogenic layer corresponded with intima and media; the outer, hyperechoic layer, corresponded with the adventitia. When a three-layered aspect was encountered, the intima appeared as a hyperechoic layer on the inside, the adventitia as an echo-bright layer on the outside, and the media as a hypoechoic layer between intima and adventitia (Fig. 3).

In the presence of a lesion, IVUS was able to distinguish fibrous lesions from calcified lesions. Fibrous lesion appeared as an echogenic structure through which the underlying wall was visible; calcified lesion was seen as a hyperechoic structure with peripheral shadowing preventing visualization of the vessel wall

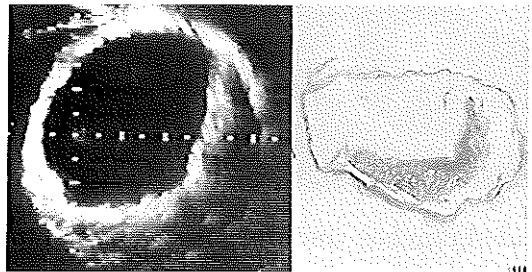


Fig. 4. Intravascular ultrasound cross-section and histologic counterpart of an aneurysmal aorta showing thrombus from 1 to 7 o'clock. Calibration: 5 mm (IVUS) and 1 mm (histology). Staining: hematoxylin-eosin.

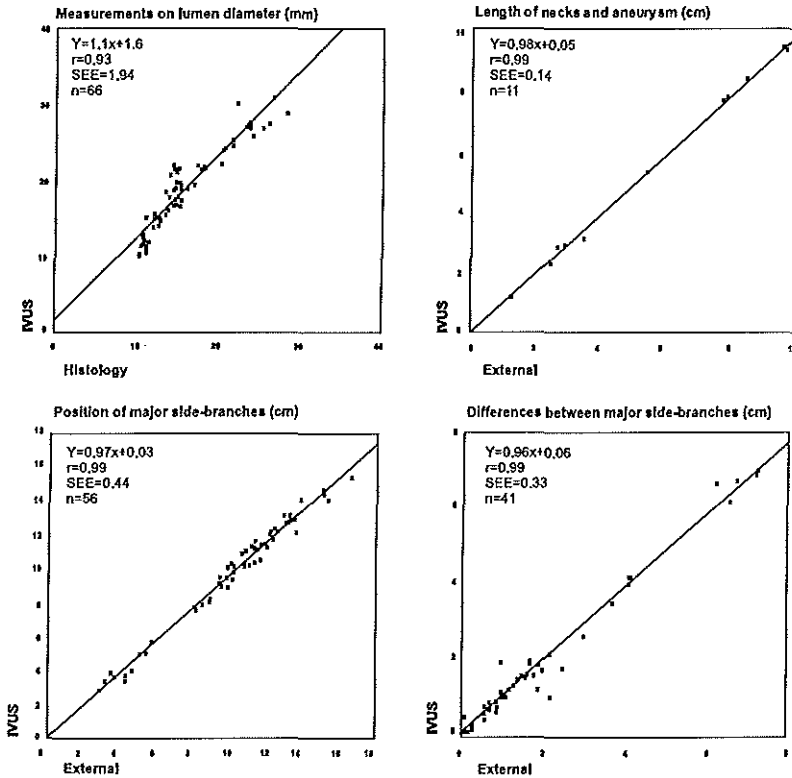


Fig. 5. Comparison between histologic and external measurements and intravascular ultrasound measurements.

(Fig. 3). Thrombus, seen in three out of five aneurysms, was identified as a hypoechoic structure attached to the arterial wall (Fig. 4). Because the thrombotic lesions attenuated the signal, rather than reflecting it, thrombus was distinguished from the echogenic reflection observed in fibrous lesions and the hyperechoic reflection with shadowing in calcified lesions. The two- or three-layered aspect of the aortic wall disappeared in the aneurysmal part of the aortae, though microscopy revealed a very thin media to be present in all histologic sections. Side-branches were seen with IVUS as a distinct interruption of the vessel wall. Besides major side-branches, small side-branches (lumbar arteries) could be identified as well.

Quantitative analysis.

Lumen diameter was assessed in 66 histologic and IVUS cross-sections; in nine histologic sections lumen diameter could not be assessed due to damage incurred during histologic processing. Comparison between histology and IVUS on lumen diameter showed a high correlation ($r=0.93$;

$p < 0.001$, Fig.5). Histologic lumen diameters were consistently smaller (17%) than the corresponding IVUS measured diameters (mean difference: -3.1 ± 2.0 mm; $p < 0.001$).

A total of 56 major side-branches could be identified. Fifteen side-branches were absent in the studied specimens, and the inferior mesenteric artery was not identified with IVUS in four instances; in three instances an aneurysmal aorta was involved and in one an atherosclerotic aorta. Measurements on the distance of the major side-branches in relation to the aortic bifurcation obtained externally, correlated well with IVUS measurements ($r = 0.99$; $p < 0.001$, Fig.5). External measurements were larger than those obtained with IVUS, the mean difference between both groups was significant (0.32 ± 0.45 cm; $p < 0.001$). Distance between the consecutive side-branches showed a high correlation ($r = 0.99$; $p < 0.001$, Fig.5), with no significant difference (mean difference of 0.03 ± 0.34 cm; $p = 0.59$). Measurements on length of the aneurysm and the proximal and distal neck showed a high correlation ($r = 0.99\%$; $p < 0.001$, Fig.5) with a mean difference of 0.06 ± 0.15 cm ($p = 0.22$). The proximal neck was present in all specimens, the distal neck was present in two specimens.

Three-dimensional reconstruction.

In the longitudinal images derived from 3D analysis, the major side-branches and the aneurysm were manifest (Fig. 6). The longitudinal image positioned through the renal arteries and the aortic bifurcation displayed the aneurysm and the proximal and distal neck. Compared to the single tomographic images, the transition from non-aneurysmal to aneurysmal aorta was better appreciated in the longitudinal (3D) reconstructions.

DISCUSSION

With the introduction of the endovascular treatment of abdominal aortic aneurysms, new demands are made on vascular surgeons and interventional radiologists. Success and safety of this new form of treatment require accurate and detailed pre- and intra-operative visualization of the abdominal aorta, its side-branches and characteristic features of the aneurysm¹⁷.

Techniques such as angiography and contrast CT scanning, have been used so far to evaluate the anatomy of aortic aneurysm^{18,19}. Angiography, however, only outlines the vessel lumen and fails to show the outline of the aneurysm, the presence of thrombus and the precise relation of the aneurysm to the side-branches, thereby failing to define the length of the proximal and distal neck.

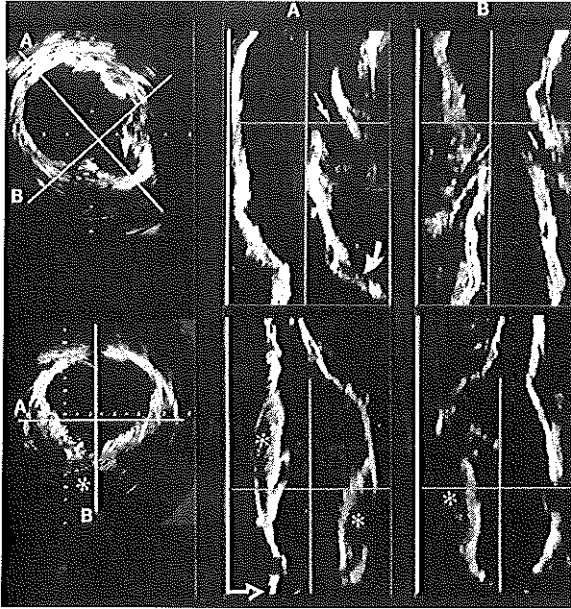


Fig. 6. Three-dimensional reconstruction of an aneurysmal aorta. (*Line A and B*) represent longitudinal reconstructed sections (*right panels*), which stand perpendicular on each other as demonstrated in the axial image (*left panel*). (*Upper panel*) shows the proximal neck with the superior mesenteric artery (*large arrow*), the renal arteries (*small arrows*) and the proximal part of the aneurysm (*curved arrow*). (*Lower panel*) shows the proximal neck, the aneurysm with thrombus (*asterisk*) and the aortic bifurcation (*open arrow*).

CT scanning, on the other hand, provides all the aforementioned information on aneurysms, but provides little information on vessel wall condition and cannot be used during the intervention²⁰.

Recently, IVUS was recognized to determine luminal morphology, quantitate dimensions for device sizing and ensure secure device placement at the time of intervention²¹⁻²³. White et al.²¹ reported a single patient study in which pre-operative IVUS compared to CT scanning in abdominal aortic aneurysm was capable to provide accurate information on aortic wall characteristics and on the position of the visceral and renal arteries in relation to the aneurysm. Verbin et al.²² demonstrated that IVUS used in normal and aneurysmal canine aortae following stent-graft placement could identify stent-aorta interfaces, thrombus formation and graft folding, characteristics missed by angiography and postinterventional CT scanning. Lyon et al.²³ reported on the clinical use of IVUS in endovascular procedures. IVUS was found to be more sensitive in detecting major arterial and graft lesions, which could result in graft thrombosis or technical failure, than intraoperative angiography. IVUS, however, was less sensitive in detecting endoleaks than post-operative CT.

The present validation study performed *in vitro* demonstrates the capacity of IVUS to identify the different morphologic and quantitative characteristics of normal, atherosclerotic and aneurysmal aorta. A distinction could be made between fibrous and calcified lesion and thrombus, which allows

definition and characterization of the proximal and distal neck. This information might be valuable during the endovascular treatment of abdominal aortic aneurysms. The comparison between histology and IVUS on lumen diameter and axial measurements showed a high correlation. The observation that lumen diameter in the histologic sections was smaller than in the IVUS cross-sections was attributed to shrinkage of histologic specimens during fixation, a process also observed by other investigators²⁴. The observation that the distance between major side-branches and aortic bifurcation was larger (0.3 cm) on external measurements than measured with IVUS can be ascribed to the curved nature of the pull back of the ultrasound catheter (Fig. 2). This assumption is supported by the finding that no significant difference was observed in the distance between the consecutive major side-branches where no curvation occurred. More importantly, the length of the aneurysm and the length of the proximal and distal neck were adequately assessed with IVUS.

The 3D reconstructions and longitudinal images enhance the spatial insight in the aneurysm. The perpendicular cuts show a better continuity between the consecutive images and therefore have an additional value in the interpretation of IVUS images. Similarly, White et al.²¹ reported that 3D IVUS imaging facilitated interpretation of the tomographic images.

Given the results of the present study and considering the high costs of IVUS catheters we opine that in the future IVUS should be used during the endovascular treatment of abdominal aortic aneurysm and not as a diagnostic device prior to intervention only. Immediately before stent-graft placement IVUS will be able to assess the relevant quantitative parameters of the aneurysm; after intervention IVUS can be used to document position and deployment of the stent-graft. Additional interventions may be performed during the same session, based on information obtained with IVUS. These features give IVUS a headstart since neither angiography nor CT-scanning can supply all the necessary information on the position and deployment of the stent-graft during intervention. IVUS would be the most appropriate choice for interventional imaging.

STUDY LIMITATIONS

It should be acknowledged that the number of aneurysmal specimens studied was limited and that the aneurysms studied were clinically not suspected. Three of the aneurysms were smaller than 5 cm. In addition, this study was performed without pulsatile blood flow, its presence will have consequences on the quality of 3D reconstruction.

CONCLUSIONS

IVUS provides accurate information on vessel wall and lesion morphology of the abdominal aorta. The precise identification of the major side-branches, aortic bifurcation and aneurysm allows accurate assessment of the length of the aneurysm and the proximal and distal neck. Three-dimensional reconstruction facilitates spatial insight in the aneurysm and surrounding vascular structures.

ACKNOWLEDGEMENT

The authors thank H. van Seyen and G. Verheyen for their support in harvesting the aortic specimens. Dr R. Berger is acknowledged for supplying the HP IVUS system.

REFERENCES

1. Balko A, Piasecki GJ, Shah DM, Carney WI, Hopkins RW, Jackson BT. Transfemoral placement of intraluminal polyurethane prosthesis for abdominal aortic aneurysm. *J Surg Res* 1986; 40: 305-309.
2. Mirich D, Wright KC, Wallace S, Yoshioka T, Lawrence DD, Charnsangavej C, et al. Percutaneously placed endovascular grafts for aortic aneurysms: feasibility study. *Radiology* 1989; 170: 1033-1037.
3. Parodi JC, Palmaz JC, Barone HD. Transfemoral intraluminal graft implantation for abdominal aortic aneurysms. *Ann Vasc Surg* 1991; 5: 491-499.
4. Lazarus HM. Endovascular grafting for the treatment of abdominal aortic aneurysms. *Surg Clin N Am* 1992; 72: 959-968.
5. Chuter TAM, Green RM, Ouriel K, Fiore WM, DeWeese JA. Transfemoral endovascular aortic graft placement. *J Vasc Surg* 1993; 18: 185-197.
6. Moore WS, Vescera CL. Repair of abdominal aortic aneurysm by transfemoral endovascular graft placement. *Ann Surg* 1994; 220: 331-341.
7. Parodi JC. Endovascular repair of abdominal aortic aneurysms and other arterial lesions. *J Vasc Surg* 1995; 21: 549-555.
8. Balm R, Eikelboom BC, May J, Bell PRF, Swedenborg J, Collin J. Early experience with Transfemoral Endovascular Aneurysm Management (TEAM) in the treatment of aortic aneurysms. *Eur J Vasc Endovasc Surg* 1996; 11: 214-220.
9. Blum U, Voshage G, Lammer J, Beyersdorf F, Töllner D, Kretschmer G, et al. Endoluminal stent-grafts for infrarenal abdominal aortic aneurysms. *N Engl J Med* 1997; 336: 13-20.
10. Losordo DW, Rosenfield K, Pieczek A, Baker K, Harding M, Isner JM. How does angioplasty work? Serial analysis of human iliac arteries using intravascular ultrasound. *Circulation* 1992; 86: 1845-1858.
11. Gussenhoven EJ, Lugt van der A, Pasterkamp G, Berg van der FG, Sie LH, Vischjager M, et al. Intravascular ultrasound predictors of outcome after peripheral balloon angioplasty. *Eur J Vasc Endovasc Surg* 1995; 10: 279-288.
12. Lugt van der A, Gussenhoven EJ, Stijnen T, Strijen van M, Driel van E, Egmond van FC, et al. Comparison of intravascular ultrasonic findings after coronary balloon angioplasty evaluated in vitro with histology. *Am J Cardiol* 1995; 76: 661-666.
13. Gussenhoven EJ, Lugt van der A, Strijen van M, Li W, Kroeze H, The SHK, et al. Displacement sensing device enabling accurate documentation of catheter tip position. In: Roelandt J, Gussenhoven EJ, Bom N, eds. *Intravascular Ultrasound*. Dordrecht: Kluwer Academic Press, 1993: 157-166.
14. Wenguang L, Gussenhoven WJ, Zhong Y, The SHK, Di Mario C, Madretsma S, et al. Validation of quantitative analysis of intravascular ultrasound images. *Int J Card Imaging* 1991; 6: 247-253.
15. Li W, Bom N, Egmond van FC. Three-dimensional quantification of intravascular ultrasound images. *J Vasc Invest* 1995; 1: 57-61.
16. Wenguang L, Bom N, Birgelen von C, Steen van der TFW, Korte de CL, Gussenhoven EJ, et al. State of the art in ICUS quantitation. In Reiber JHC, Wall

-
- van der EE eds. Cardiovascular imaging. Dordrecht: Kluwer Academic Publishers, 1996: 79-82.
17. Moritz JD, Rotermund S, Keating DP, Oestmann JW. Infrarenal abdominal aortic aneurysms: implications of CT evaluation of size and configuration for placement of endovascular aortic grafts. *Radiology* 1996; 198: 463-466.
 18. Rubin GD, Walker PJ, Dake MD, Napel S, Jeffrey B, McDonnell CH, et al. Three-dimensional spiral computed tomographic angiography: an alternative imaging modality for the abdominal aorta and its branches. *J Vasc Surg* 1993; 18: 656-665.
 19. Siegel CL, Cohan RH. CT of abdominal aortic aneurysms. *AJR* 1994; 163: 17-29.
 20. Balm R, Kaatee R, Blankensteijn JD, Mali WPTM, Eikelboom BC. CT-angiography of abdominal aortic aneurysms after Transfemoral Endovascular Aneurysm Management. *Eur J Vasc Endovasc Surg* 1996; 12: 182-188.
 21. White RA, Scoccianti M, Back M, Kopchok G, Donayre C. Innovations in vascular imaging: arteriography, three-dimensional CT scans, and two- and three-dimensional intravascular ultrasound evaluation of an abdominal aortic aneurysm. *Ann Vasc Surg* 1994; 8: 285-289.
 22. Verbin C, Scoccianti M, Kopchok G, Donayre C, White RA. Comparison of the utility of CT scans and intravascular ultrasound in endovascular aortic grafting. *Ann Vasc Surg* 1995; 9: 434-440.
 23. Lyon RT, Veith FJ, Berdejo GL, Okhi T, Sanchez LA, Wain RA, et al. Utility of intravascular ultrasound for assessment of endovascular procedures. Society for Vascular Surgery and North American Chapter, International Society for Cardiovascular Surgery, Joint Annual Meeting, 1997: 43.
 24. Gussenhoven EJ, Lugt van der A, Steen van der AFW, Ligtvoet KM. What have we learned from in vitro intravascular ultrasound? *Am Heart J* 1996; 132: 702-710.

**ACCURATE ASSESSMENT OF ABDOMINAL
AORTIC ANEURYSM BY INTRAVASCULAR
ULTRASOUND: VALIDATION WITH
COMPUTED TOMOGRAPHIC ANGIOGRAPHY**

**Jeroen A. van Essen, MD¹, Elma J. Gussenhoven, MD, PhD¹,
Aad van der Lugt, MD, PhD², Paul C. Huijsman¹,
Johannes M. van Muiswinkel, MD²,
Marc R.H.M. van Sambeek, MD, PhD³,
Lukas C. van Dijk, MD, PhD²,
Hero van Urk, MD, PhD³.**

From the Departments of Cardiology¹, Radiology² and
Vascular Surgery³ of the University Hospital Rotterdam-Dijkzigt and
the Erasmus University Rotterdam, the Netherlands.

Supported by grants from the Netherlands Heart Foundation (no 95.123) and
the Interuniversity Cardiology Institute, the Netherlands.

ABSTRACT

Purpose:

To assess the accuracy of intravascular ultrasound (IVUS) parameters of abdominal aortic aneurysm, used for endovascular grafting, by comparison with computed tomographic angiography (CTA).

Study-design:

Descriptive.

Methods:

Between March 1997 and March 1998, 16 patients with abdominal aortic aneurysm were studied with angiography, IVUS (12.5 MHz) and CTA. The length of the aneurysm and the length and lumen diameter of the proximal and distal neck, obtained with IVUS were compared with the data obtained with CTA. Measurements with IVUS were repeated by a second observer to assess the reproducibility. Tomographic IVUS images were reconstructed into a longitudinal format.

Results:

IVUS identified 31 out of 32 renal arteries and four out of five accessory renal arteries. Comparison of the length measurements of the aneurysm and the proximal and the distal neck, obtained with IVUS and CTA revealed a correlation of 0.99 ($p < 0.001$), with a coefficient of variation of 9%; IVUS tended to underestimate the length compared to CTA (0.48 ± 0.52 cm; $p < 0.001$). Comparison of lumen diameter measurements of the proximal and distal neck, derived from IVUS and CTA, showed a correlation of 0.93 ($p < 0.001$), with a coefficient of variation of 9%; IVUS tended to underestimate aneurysm neck diameter compared to CTA (0.68 ± 1.76 mm; $p = 0.006$). Interobserver agreement of IVUS length and diameter measurements showed a very good correlation ($r = 1.0$; $p < 0.001$), with coefficients of variation of 3% and 2%, respectively, and no significant differences (0.0 ± 0.16 cm and 0.06 ± 0.36 mm, respectively). The longitudinal IVUS images displayed the important vascular structures and improved the spatial insight in aneurysmal anatomy.

Conclusions:

Intravascular ultrasound provided accurate and reproducible measurements of abdominal aortic aneurysm. Longitudinal reconstruction of IVUS images provided additional knowledge on the anatomy of the aneurysm and its proximal and distal neck.

INTRODUCTION

The feasibility of endoluminal stent-grafts in the treatment of abdominal aortic aneurysm has been demonstrated¹⁻⁴. The success of this technique is closely related to accurate knowledge of critical parameters of aortic morphology. Intravascular ultrasound (IVUS) is acknowledged as an important imaging technique to provide information on lesion characteristics and vessel dimensions of coronary and peripheral arteries, and of the abdominal aorta⁵⁻⁷. Although IVUS is currently used for intra-operative imaging of abdominal aortic aneurysm during endovascular treatment, no study has focused on the clinical validation of IVUS parameters⁸⁻¹⁰. The purpose of this study was to assess the accuracy of IVUS parameters of abdominal aortic aneurysm by comparison with computed tomographic angiography (CTA).

METHODS

Patients.

Between March 1997 and March 1998, 17 consecutive patients with an abdominal aortic aneurysm scheduled for operation were asked to participate in the study. One patient refused. The remaining 16 patients (12 male, four female, age range 42-84 years, mean age 68 years) were studied with routine angiography, IVUS and CTA. The study was approved by the Local Committee on Human Research; written consent was obtained from all patients.

Subtraction angiography.

Routine anteroposterior (AP) views were obtained using a pigtail catheter (Royal Flesh II pigtail aneurysm swing catheter, WA Cook Australia PTY. LTD., Queensland) placed at the level of the renal arteries via a common femoral artery puncture. A single bolus of 35 ml of contrast fluid (Omnipaque, Nycomed Ireland Ltd., Cork) was injected at 14 ml/s with a power injector. Then the catheter was placed above the aortic bifurcation and a second bolus of contrast was injected.

Intravascular ultrasound.

A HP-Sonos Intravascular Imaging System (Hewlett Packard, Andover, MA, USA) was used with a mechanical driven Sonicath Side-Saddle 12.5 MHz 6.2 F catheter (Boston Scientific Corp, Watertown, MA, USA). The catheter was introduced over a 0.025 inch Terumo angled hydrophilic coated guide-wire (Terumo Europe NV, Leuven, Belgium) through an 8F sheath into the aorta up to the level of the celiac trunk. To monitor the position of the IVUS catheter, a displacement sensing device was used. This device consists of a small, sterile, disposable sensing unit. The movement of the catheter activates a rotating wheel that converts the linear movement into an electronic pulse train signal so that the advancement or withdrawal of the

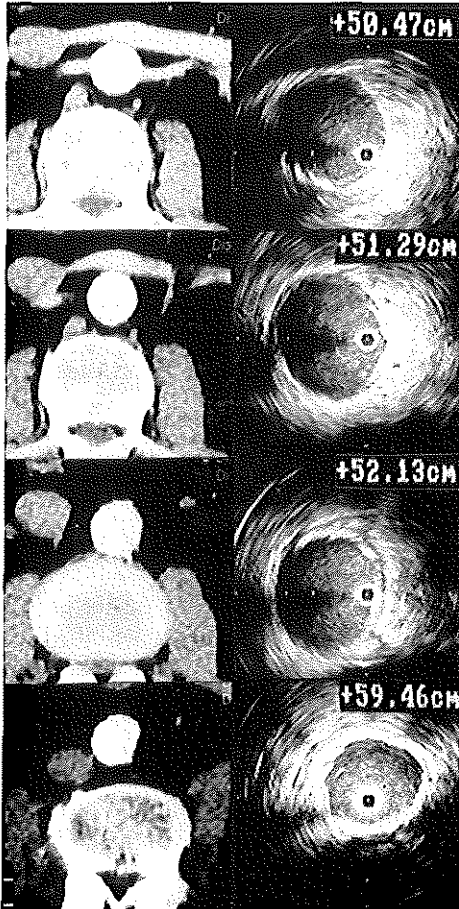


Fig. 1. Intravascular ultrasound cross-sections and computed tomographic angiography counterparts of the proximal and distal neck of an abdominal aortic aneurysm. *Upper panel* shows the cross-section 0.2 cm below the most distal renal artery. The *second panel* shows a cross-section halfway in the proximal neck. The *third panel* shows a cross-section 0.2 cm proximal to the aneurysm. The *lower panel* shows a cross-section 1 cm distal to the aneurysm. *Inserts* show the reading from the displacement sensing device. Calibration on CTA: 10 mm. Calibration on IVUS: 5 mm.

catheter is digitized and wirelessly registered by a sterilizable unit to which the sensing unit is mounted¹¹. The display of the displacement of the IVUS catheter tip in steps of 0.01 cm was mixed together with the ultrasound information on the videoscreen. IVUS images were stored on videotape (S-VHS) for further quantitative analysis and longitudinal reconstruction.

Longitudinal IVUS reconstruction.

The IVUS images were digitized off-line at a resolution of 800x600x8 bits by a frame grabber (DT-3852) and aligned and stacked longitudinally¹². Up to 200 images were acquired with a given interval (0.5-1.0 mm). In the resulting model two panels parallel to the vessel axis were selected to create longitudinal images.

Computed tomographic angiography.

Spiral-CTA was performed with a Siemens Somatom 4 Scanner (Siemens Medical Systems, Iselin NJ). After frontal scout projection a single dose of 130 ml of intravenous contrast (Omnipaque, Nycomed Ireland Ltd, Cork) was injected through a catheter in the antecubital vein at 2.0 ml/s with a scan delay of 35 seconds. A slice thickness of 5 mm and a table speed of 5 mm/s was chosen with a reconstruction interval of 2 mm. The volume scanned was from the celiac axis down to the level of the proximal femur.

Data analysis.

The presence of renal and accessory renal arteries was documented on angiography, IVUS and CTA.

For angiographic assessment both subtracted and unsubtracted images were reviewed from film by an independent radiologist (LCvD).

The length of the aneurysm and the length and diameter of the proximal and distal neck, seen with IVUS (JAvE) and CTA (AvdL) was determined. The *proximal neck* was defined as the distance between the lower border of the most distal renal artery and the proximal border of the aneurysm. The *distal neck* was defined as the distance between the distal border of the aneurysm and the aortic bifurcation. If the aneurysm extended into the iliac arteries, the *distal neck* was defined as the distance between the distal border of the

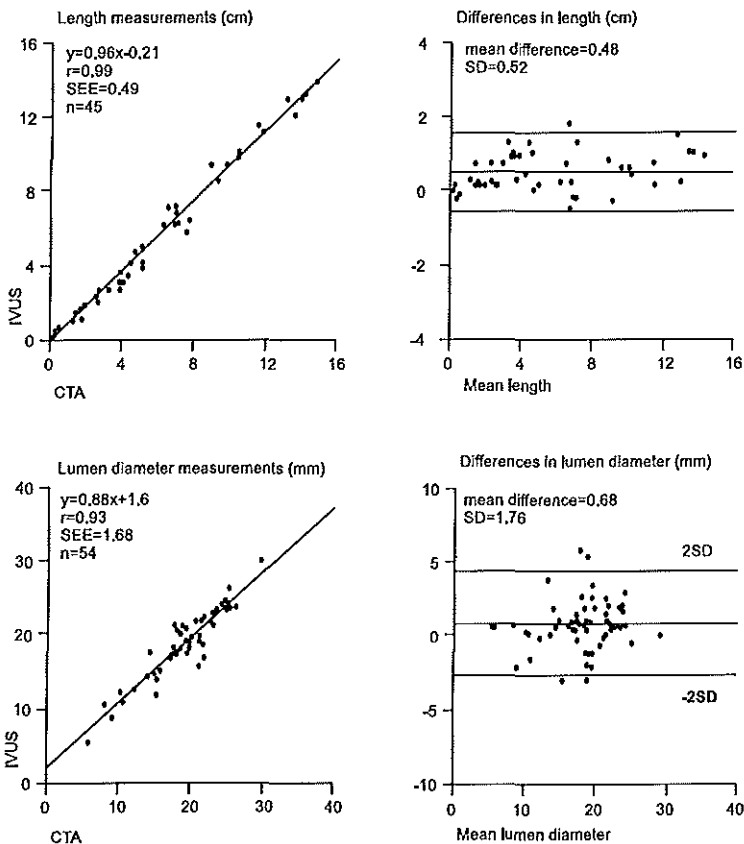


Fig. 2. Comparison between intravascular ultrasound (IVUS) and computed tomographic angiography (CTA) for length measurements of the aneurysm, the proximal and distal neck and lumen diameter measurements of the proximal and distal neck. SEE: standard error of estimate; SD: standard deviation.

aneurysm and the iliac bifurcation at the side of access. Length measurements on IVUS were obtained using the information provided by the displacement sensing device. Length measurements using CTA were performed on a Siemens Magic View Workstation (Sienet VA 31B) using multiplanar reformats. The length was determined by manually counting the number of steps, which were 1 mm apart, necessary to cross the distance to be investigated (i.e. the neck, the aneurysm, the iliac artery) along the central lumen line.

In the presence of a proximal neck > 1 cm in length on CTA, the lumen diameter was measured with IVUS and CTA at three positions: 0.2 cm distal from the renal artery, in the mid portion of the proximal neck and 0.2 cm

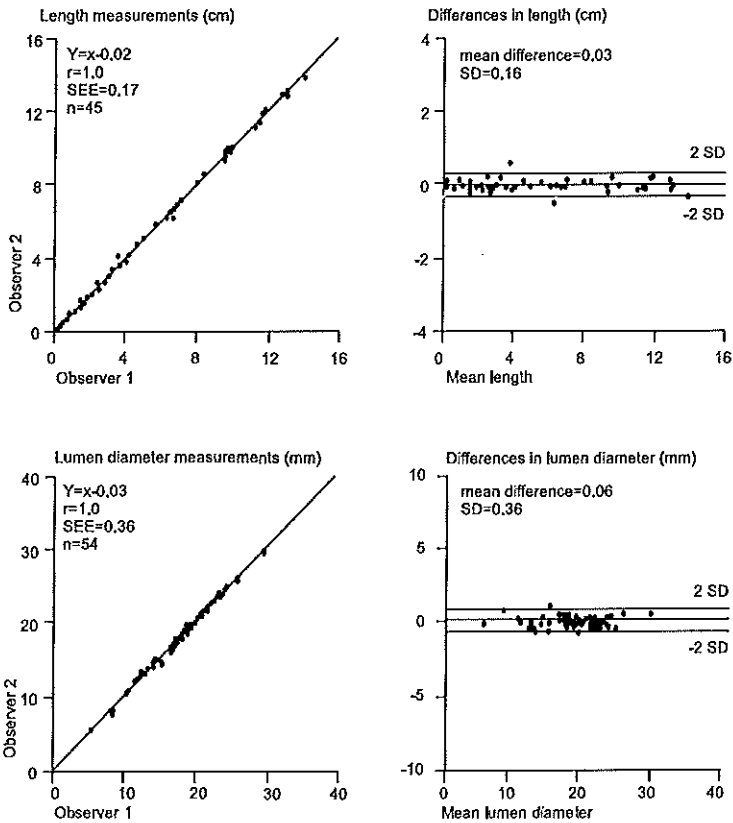


Fig. 3. Comparison between observer 1 and 2 for length and lumen diameter measurements. SEE: standard error of estimate; SD: standard deviation.

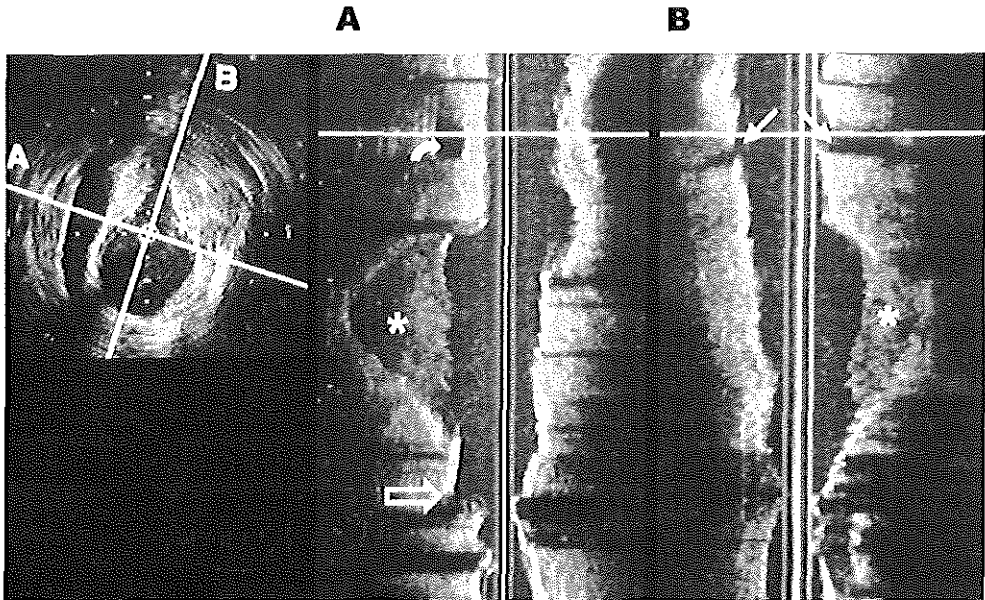


Fig. 4. Longitudinal IVUS reconstructions of an aneurysmal aorta. *Lines A and B* represent the longitudinal reconstructed sections (*right panels*) which stand perpendicular to each other, as demonstrated in the axial image (*left panel*). Both renal arteries are visible (*small arrows*), as well as the renal vein (*curved arrow*), thrombus in the aneurysm (*asterisk*) and the aortic bifurcation (*large arrow*).

proximal from the aneurysm (Fig. 1). If the proximal neck was < 1 cm in length on CTA only one cross-section, taken 0.2 cm distal from the renal artery, was selected for lumen diameter assessment. The diameter of the distal neck was measured 1 cm distal from the distal border of the aneurysm in the aorta. If the distal aortic neck > 1 cm in length on CTA the cross-section selected for analysis was 1 cm distal from the aneurysm in the aorta. In the presence of a too short distal aortic neck (< 1 cm), not suitable for endograft placement, the diameter of the iliac artery was measured 1 cm distal from the bifurcation. If the aneurysm extended into the iliac arteries the selected cross-section was 1 cm distal from the aneurysm in the iliac artery.

The selected IVUS cross-sections were digitized and the minimum lumen diameter was calculated from the manual traced lumen area contour and its geometrical center using a digital video analyzer¹³. The minimum lumen diameter was used for analysis given the fact that the IVUS catheter may be in a non coaxial position: such a cross-section will have an oval shape instead of a circular one. As a consequence the mean lumen diameter of

such a cross-section may overestimate the lumen dimension. On CTA, the lumen diameter measurements were performed on cross-sections taken perpendicular to the central lumen line, using electronic calipers on the Siemens Workstation. For every cross-section, the diameter was measured in four directions; the mean lumen diameter was taken.

To assess the interobserver variability of IVUS measurements, the images were reviewed by a second independent observer (PCH).

Statistical analysis.

Linear regression analysis was performed to assess the strength of the relation between IVUS and spiral CTA measurements, and between the observer's measurements. Systematic differences between the IVUS and spiral CTA measurements and between the observer measurements, were analyzed with the Student t-test for paired observations; the agreement was expressed as a coefficient of variation, defined as the standard deviation (SD) of the paired differences divided by the mean of the absolute value¹⁴. A p-value <0.05 was considered statistically significant.

RESULTS

In 15 patients data obtained with angiography, IVUS and CTA were complete; in one patient CT scanning was only performed from the celiac trunk down to the aortic bifurcation.

With angiography 32 renal arteries and two accessory renal arteries were identified. IVUS identified 31 renal arteries and four accessory renal arteries; one renal artery was missed on IVUS due to the shadow of the guide-wire. CTA identified 32 renal and five accessory renal arteries.

Angiographically, a distinct aneurysm was identified in 12 patients; in four patients the angiogram showed a local dilatation and elongation of the abdominal aorta, suggestive of aneurysmal disease. Both IVUS and CTA showed a distinct abdominal aortic aneurysm in all 16 patients. On IVUS and CTA the length of the proximal neck was > 1 cm in 13 patients and < 1 cm in three patients. Similarly, the length of the distal aortic neck was > 1 cm in five patients and < 1 cm in two patients who both had normal iliac arteries. In six other patients the aneurysm extended from the aorta up to the aortic bifurcation with a normal iliac artery, and in the three remaining patients the aneurysm extended down to the iliac bifurcation.

In the 12 patients where angiography identified an aneurysm, seven out of nine proximal necks \geq 1 cm were seen. In one out of three patients in whom the proximal neck was absent on IVUS and CTA, the neck was deemed to be present angiographically. IVUS and CTA showed thrombus obscuring the lumen of the aneurysm. Angiography failed to identify three out of five distal necks \geq 1 cm. Four of the necks that were missed on the angiogram

showed a conical shape on IVUS and CTA and were considered part of the aneurysm on angiography.

Comparison of IVUS and CTA measurements on the length of the aneurysm and the proximal and distal neck revealed a correlation of 0.99 ($p < 0.001$). Student *t*-test showed a significant difference between the measurements of 0.48 ± 0.52 cm ($p < 0.001$): IVUS tended to underestimate the length compared to CTA. The coefficient of variation was 9% (Fig. 2). Comparison between IVUS and CTA for total measured length in all patients revealed a correlation of 0.96, a difference of 1.2 ± 0.9 cm and a coefficient of variation of 6%. Comparison of the lumen diameter obtained revealed a correlation of 0.93 ($p < 0.001$). The difference between the measurements was 0.68 ± 1.76 mm ($p = 0.006$); diameters derived from IVUS tended to underestimate compared to CTA. The coefficient of variation was 9% (Fig. 2).

Interobserver IVUS measurements revealed a correlation of 1.0 ($p < 0.001$) for both length and lumen diameter measurements, with a difference of 0.0 ± 0.16 cm and 0.06 ± 0.36 mm and a coefficient of variation of 3% and 2%, respectively (Fig. 3).

Longitudinal reconstruction. Creating longitudinal reconstructions of IVUS data available required three minutes. In the longitudinal images, the renal arteries, the proximal neck, the aneurysm and the distal neck were manifest (Fig. 4). Compared to the single cross-sectional images, the transition from neck into aneurysm was better appreciated in the longitudinal images, especially when the neck showed a more conical shape. The longitudinal reconstructions contributed to a better understanding of the aneurysmal anatomy.

DISCUSSION

Endovascular grafting of abdominal aortic aneurysm presents a minimally invasive technique, in which accurate visualization of the abdominal aorta before, during and after placement of stent-graft is of eminent importance. Currently used techniques are angiography, IVUS and CTA. Angiography allows a broad imaging field, is easily accessible, but shows only the vessel lumen. Measurements of the length and diameter of the proximal and distal attachment sites may be influenced by the presence of thrombus, parallax and foreshortening. Therefore, caution should be applied when sizing the stent-graft solely on angiographic measurements¹⁵. In contrast, CTA is a noninvasive technique that provides relevant parameters for the selection of patients suitable for endovascular treatment and to decide on the dimensions of the stent-graft to be used¹⁶. However, CTA can not be used during intervention. Recently, IVUS has been introduced as an alternative modality to be used during endovascular treatment⁸⁻¹⁰. In a recent validation study we have shown that IVUS can provide accurate information on the

morphology and quantitative dimension of abdominal aortic aneurysm in vitro⁷. However, no study has focused on the validation of this technique in a clinical situation.

The present study confirms the insufficiency of angiography to adequately determine the morphology of the aneurysm. Although angiography revealed a distinct aneurysm in 12 patients, and abnormalities suggestive of aneurysmal disease in four other patients, precise determination of the nature of the proximal and distal neck failed in five patients (three proximal and four distal). Although calibrated angiography may be unsuitable to determine the length of individual segments of the aneurysm, in practice it can be used to determine the distance between the renal and iliac arteries.

This study demonstrates the capability of IVUS to identify pertinent structures such as renal arteries, aneurysm and aortic bifurcation. Comparison of length measurements of the aneurysm and the proximal and distal neck revealed a difference of 0.48 ± 0.52 cm between IVUS and CTA, with IVUS measurements being smaller than those of CTA. Both the stiffness and the non-coaxial position of the IVUS catheter may be responsible for the fact that the path of the IVUS catheter does not correspond with the path of the central lumen line: the endograft may not follow either path. Although a significant difference was found between IVUS and CTA length measurements, the coefficient of variation indicates a good agreement, while the differences encountered may be a consequence of measurement faults of both imaging modalities. The difference in length encountered between IVUS and CTA indicates that device sizing based on IVUS measurements will be appropriate, given that stent-graft sizes are determined by the centimeter, and, in practice, only the minimum length to cross the aneurysm into the iliac arteries is required. The appropriate length of the stent-graft may be assessed with either a displacement sensing device or a sterile ruler held along the IVUS catheter.

Comparison between IVUS and CTA revealed a small, yet significant difference for lumen diameter. IVUS diameters tended to be 3.5% smaller than seen with CTA. This may be due to the fact that the minimum lumen diameter was chosen for the IVUS cross-sections, and no correction was used for systolic and diastolic changes. It should be emphasized that we used the minimum lumen diameter in order to correct for the non coaxial position of the IVUS catheter during imaging. However, if the mean lumen diameter was used for analysis the difference found between IVUS and CTA was 1% (0.22 ± 1.9 mm) and not significant; showing an identical correlation ($r= 0.93$) and coefficient of variation (9.4%) as found for minimum lumen diameter. Another factor that may contribute to the difference in lumen diameter obtained with IVUS and CTA may be that CTA can overestimate the diameter because of the slice thickness and filtering

techniques. Taken into account the difference in diameter between IVUS and CTA of 3.5%, and the selection of 10-15% oversized stent-grafts commonly used for implantation, we opine that IVUS can be used in a clinical setting to determine the appropriate stent-graft diameter.

Longitudinal IVUS imaging enhanced the spatial insight in the aneurysm by showing the continuity between consecutive images. These longitudinal images used as a quick reference in the interpretation of the axial cross-sections may have an additional value in the interpretation of IVUS images in the clinical setting. The recognition of the shape of the aortic neck may improve and the transition from neck into the aneurysm may be clarified¹⁸. In case of a conical shaped neck, the transition from neck into aneurysm may be obscured. Conical shaped necks may also give difficulties in sizing the appropriate endograft. Using longitudinal imaging a cut-off point may be chosen where the neck stops and the aneurysm starts.

It should be remembered that the longitudinal IVUS images are reconstructed relative to the catheter tip. They do not present an true three-dimensional (3D) view of the aorta. It should be acknowledged that 3D reconstruction using CTA will be able to show the angulation of the iliac arteries and necks in relation to the aneurysm, features that can not be obtained with IVUS.

In other studies, the use of IVUS to assess the dimensions of abdominal aortic aneurysm and to guide stent-graft delivery has been described⁸⁻¹⁰. In 1997 Lyon et al.⁸ reported the use of IVUS following endovascular procedures and found that IVUS was more sensitive than angiography to detect arterial and graft lesions (92% vs 50%). Based on IVUS, additional intervention was required in 33% of the lesions detected. IVUS was, however, less sensitive in detecting endoleaks compared to post-operative CTA. White et al.⁹ reported the use of IVUS before and after intervention. They concluded that "IVUS was the most accurate way to determine the morphology of vascular structures (i.e. calcium, thrombus)"⁹. In addition, the final choice of device dimensions and fixation sites was determined by IVUS interrogation. Finally, Vogt et al.¹⁰ reported the use of IVUS before, during and after intervention. Before stent-graft placement the location of renal arteries and the renal vein was determined with IVUS and the position of the catheter tip on fluoroscopy in relation to a radiopaque ruler was documented. After the deployment the expansion and the adaptation of both the distal and the proximal stents were evaluated, as was the position of the proximal stent in relation to the renal arteries. IVUS showed to be unsuitable for the monitoring during stent-graft deployment.

Nowadays, most stent-grafts are modular systems, allowing the interventionalist to select the appropriate modules during the intervention. Therefore, an intraoperative imaging technique that can accurately

quantitate the dimensions of the stent-graft may be profitable¹⁷. The present study indicates that IVUS used for endovascular treatment for abdominal aortic aneurysm can provide relevant information on the parameters necessary to exclude the aneurysm successfully. After the intervention, IVUS may be used to document the position and assess proper deployment of the device. Future clinical studies have to prove the efficacy of IVUS during intervention, for the benefit of the individual patient.

CONCLUSIONS

Intravascular ultrasound provides accurate and reproducible information on the dimensions of abdominal aortic aneurysm. Longitudinal reconstruction provides additional knowledge on the anatomy of the aneurysm.

ACKNOWLEDGEMENTS

The authors thank J. Honkoop for his continuous support during the clinical studies and Dr R. Berger for supplying the HP IVUS system.

REFERENCES

1. Parodi JC. Endovascular repair of abdominal aortic aneurysms and other arterial lesions. *J Vasc Surg* 1995; 21: 549-557.
2. Balm R, Eikelboom BC, May J, Swedenborg J, Collin J. Early experience with transfemoral endovascular aneurysm management (TEAM) in the treatment of abdominal aortic aneurysms. *Eur J Vasc Endovasc Surg* 1996; 11: 214-220.
3. Blum U, Langer M, Spillner G, Mialhe C, Beyersdorf F, Buitrago-Tellez C, et al. Abdominal aortic aneurysms: preliminary technical and clinical results with transfemoral placement of endovascular self-expanding stent-grafts. *Radiology* 1996; 198: 25-31.
4. May J, White GH, Yu W, Ly CN, Waugh R, Stephen MS, et al. Concurrent comparison of endoluminal versus open repair in the treatment of abdominal aortic aneurysms: analysis of 303 patients by life table method. *J Vasc Surg* 1998; 27: 213-221.
5. Lugt van der A, Gussenhoven EJ, Stijnen T, Li W, Strijen van M, Driel van E, et al. Comparison of intravascular ultrasound findings after coronary balloon angioplasty evaluated in vitro with histology. *Am J Cardiol* 1995; 76: 661-666.
6. Gussenhoven EJ, Lugt van der A, Pasterkamp G, Berg van den FG, Sie LH, Vischjager M, et al. Intravascular ultrasound predictors of outcome after peripheral balloon angioplasty. *Eur J Vasc Endovasc Surg* 1995; 10: 279-288.
7. Essen van JA, Lugt van der A, Gussenhoven EJ, Leertouwer TC, Zondervan P, Sambek van MRHM. Intravascular ultrasound allows accurate assessment of abdominal aortic aneurysm: an in vitro validation study. *J Vasc Surg* 1998; 27: 347-353.
8. Lyon RT, Veith FJ, Berdejo GL, Okhi T, Sanchez LA, Wain RA, et al. Utility of intravascular ultrasound for assessment of endovascular procedures. Society for Vascular Surgery and North American Chapter, International Society for Cardiovascular Surgery, Joint Annual Meeting, 1997: 43.
9. White RA, Donayre C, Kopchok G, Walot I, Wilson E, deVirgilio C. Intravascular ultrasound: the ultimate tool for abdominal aortic aneurysm assessment and endovascular graft delivery. *J Endovasc Surg* 1997; 4: 45-55.
10. Vogt KC, Brunkwall J, Malina M, Ivancev K, Lindblad B, Risberg B, et al. The use of intravascular ultrasound as control procedure for the deployment of endovascular stented grafts. *J Vasc Endovasc Surg* 1997; 13: 592-596.
11. Gussenhoven EJ, Lugt van der A, Strijen van M, Li W, Kroeze H, The SHK, et al. Displacement sensing device enabling accurate documentation of catheter tip position. In Roelandt J, Gussenhoven EJ, Bom N (eds). *Intravascular ultrasound*. Kluwer Academic Publishers Dordrecht; 1993: 157-166.
12. Li W, Bom N, Egmond van FC. Three-dimensional quantification of intravascular ultrasound images. *J Vasc Invest* 1995; 1: 57-61.
13. Wenguan L, Gussenhoven WJ, Zhong Y, The SHK, Di Mario C. Validation of quantitative analysis of intravascular ultrasound images. *Int J Card Imag* 1991; 6: 247-253.
14. Bland JM, Altman DG. Statistical methods for assessing agreement between two methods of clinical measurement. *Lancet* 1986; 1(8476): 307-310.

15. Beebe HG. Imaging modalities for aortic endografting. *J Endovasc Surg* 1997; 4: 111-123.
16. Balm R, Stokking R, Kaatee R, Blankensteijn JD, Eikelboom BC, Leeuwen van MS. Computed tomographic angiographic imaging of abdominal aortic aneurysms: implications for transfemoral endovascular aneurysm management. *J Vasc Surg* 1997; 26: 231-237.
17. Allen RC, White RA, Zarins CK, Fogarty TJ. What are the characteristics of the ideal endovascular graft for abdominal aortic aneurysm exclusion. *J Endovasc Surg* 97; 4: 195-202.

**RELIABILITY AND REPRODUCIBILITY OF
AUTOMATED CONTOUR ANALYSIS IN
INTRAVASCULAR ULTRASOUND IMAGES OF
FEMOROPOPLITEAL ARTERIES**

**Aad van der Lugt¹, Aran Hartlooper², Jeroen A. van Essen^{2,4},
Wenguang Li², Clemens von Birgelen², Johan H.C. Reiber^{3,4},
Elma J. Gussenhoven^{2,4}.**

Departments of Radiology¹ and Cardiology²,
University Hospital Rotterdam-Dijkzigt, Rotterdam,
Laboratory for Clinical and Experimental Imaging³,
University Hospital Leiden, and the
Interuniversity Cardiology Institute of the Netherlands (ICIN)⁴

This study was supported by grants from the Interuniversity Cardiology
Institute of the Netherlands and the Netherlands Heart Foundation (91.016).

ABSTRACT

An automated contour analysis system was previously developed to increase reproducibility and facilitate quantitative analyses of intravascular ultrasound (IVUS) images. The aim of this study was to compare measurements by this automated system with those obtained by conventional manual tracing, and to determine the intra- and interobserver variability of the automated system. IVUS images obtained in the femoropopliteal artery (n=12) were analyzed with both systems. Area measurements by the automated system agreed well with the results obtained by manual tracing displaying low coefficients of variation (8.5 to 15.7%) and high correlation coefficients ($r = 0.92$ to 0.98).

Intra- and interobserver comparison of lumen area, vessel area, plaque area and percentage area stenosis showed low coefficients of variation (6.0 to 15.3% and 5.7 to 14.0%, respectively) and high correlation coefficients (both: $r = 0.93$ to 0.99).

These data indicate that the automated analysis system is a reliable tool for the quantitative assessment of vessel dimensions in IVUS images obtained during clinical examination of peripheral arteries.

INTRODUCTION

Intravascular ultrasound (IVUS) imaging is a relatively new technique that enables real-time visualization of the vascular anatomy from inside the vessel. While angiography displays a planar view of the vessel lumen only, IVUS provides a cross-sectional view of the vessel with information about lumen and vessel area, and plaque characteristics¹⁻³. At present, IVUS guided vascular interventions in femoropopliteal arteries are based on the relatively subjective visual estimation of lumen and vessel dimensions. Assessment of lumen and vessel area can be performed on an individual IVUS cross-section with a manual contour tracing system⁴. However, analysis with this system is time consuming and is mainly used off-line for research purposes⁵. In addition, manually assessed measurements are liable to interobserver variability^{6,7}. Recently, an automated system was developed that has the potential to provide reproducible measurements on-line, enabling its use in the clinical setting⁸⁻¹⁰. The aim of the present study was to validate this automated system in IVUS images obtained in peripheral arteries by:

- A. comparing measurements obtained with the automated analysis system with those obtained by manual contour tracing; and
- B. evaluating the intra- and interobserver variability of the automated analysis system.

MATERIAL AND METHODS

Study group.

The study group comprised 12 patients with symptomatic femoropopliteal artery disease eligible for balloon angioplasty (8 men, 4 women; age range 51-88 (median 65) years). Patients were studied with IVUS before balloon angioplasty.

Intravascular ultrasound imaging.

The IVUS studies were performed using a mechanical system based on a single ultrasound element (30 MHz); the tomographic image is produced by a rotating element mounted on a guidewire-tipped 4.3F catheter (Du-MED, Rotterdam, The Netherlands, 0.035").

The ultrasound catheter was antegradely introduced through a sheath into the femoropopliteal artery. After the cathetertip was advanced distal to the region of interest, the catheter was pulled back manually. A displacement sensing device was used to document the relative position of the cathetertip in steps of 0.1 mm¹¹. The images were displayed on the monitor via a video-scanned memory and stored on a S-VHS recorder.

Automated analysis system.

The analysis program uses the Microsoft Windows operating system on a Pentium (100 MHz) personal computer with 32 Mbytes of internal RAM. A framegrabber (DT-3852; resolution 800 x 600 x 8 bits) digitizes a user-defined region of interest from a maximum of 200 IVUS images. Selection of the IVUS images was performed by manually choosing the appropriate images from the videotape using the distance information provided by the catheter displacement sensing device. Images were selected and digitized every 0.2 mm.

The automated contour detection is based on the minimum-cost algorithm. By this approach the digitized IVUS images are resampled according to a radial image reconstruction (64 radii in the cross-sectional image; 200 rows in the longitudinal sections). A cost matrix that represents the edge strength is calculated from the image data. For the detection of the boundary between lumen and plaque (lumen area), the cost value is defined by the spatial first derivate. To detect the external boundary of the total vessel (vessel area) a pattern-matching process by cross-correlation is adopted for the cost-calculations. Through the cost-matrixes a path with the smallest accumulated value is determined by dynamic programming techniques¹⁰. Analysis of the IVUS data consists of three steps⁸⁻¹⁰ (Fig. 1).

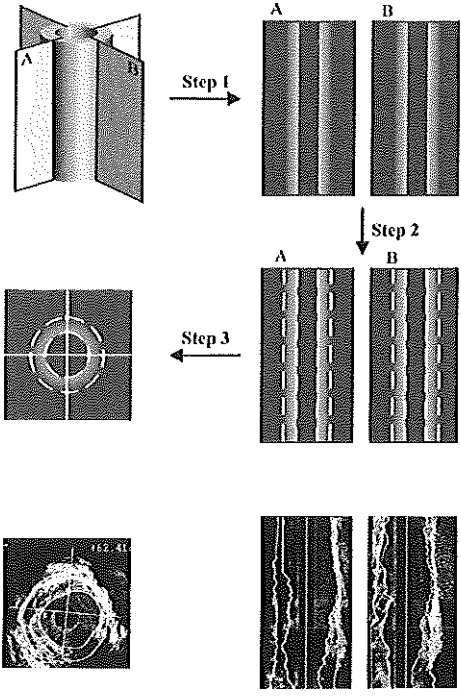


Fig. 1. Principle of the automated contour detection. The intravascular ultrasound images, obtained during pull-back of the catheter, are used to reconstruct two longitudinal sections from the voxel space (step 1). Automated longitudinal contour detection of the intimal leading edge and the external boundary of the vessel is performed (step 2). The longitudinal contours are represented as individual edge points in the cross-sectional images. These points define center and range of the final contour detection process on the cross-sectional images (step 3). Lower panels: an example of contour detection from in vivo IVUS images.

1. A sequence of digitized IVUS images is stored in a voxel space. Two perpendicular cut planes parallel to the longitudinal axis of the vessel are selected to reconstruct longitudinal sections (Fig. 1). These longitudinal reconstructions use the IVUS data located at the intersection of the cut planes with the voxel space. The position and the rotation angle of the two cut planes can be changed interactively by the user to obtain an optimal quality of the longitudinal sections.
2. The longitudinal contours of lumen and vessel are detected in these longitudinal images (Fig. 1). The program starts with an automatically detected contour by the minimum-cost algorithm. The user is then free to set markers in the longitudinal images and force the contour to pass through these sites. This step is achieved by setting the cost matrix of the manually defined sites at a very low value. By applying dynamic programming techniques, the optimal path is then redefined for the modified cost matrix. During the entire user-interactive procedure the longitudinal contours are visible and updated in the longitudinal sections.
3. The contours in the cross-sectional images are detected with information from the longitudinal contours. By transforming the contours from the two longitudinal planes to the transverse plane, four predefined points are available for each cross-section (Fig. 1). These edge points guide the contour detection in the transverse images by defining the center and range of the boundary searching process. The cross-sectional images are then transformed to a polar format. A cost matrix having very low values at the four predefined positions is generated from the resampled data, and an optimal path passing through the four edge points is obtained by applying the minimum cost algorithm. The optimal path is interpolated, and converted back to the original coordinates to form the cross-sectional contours. The position of an individual transverse plane in the longitudinal section is indicated by a horizontal cursor line which can be used to scroll through the whole series of transverse images. The detected contours are checked by the user and, if necessary, manually corrected.

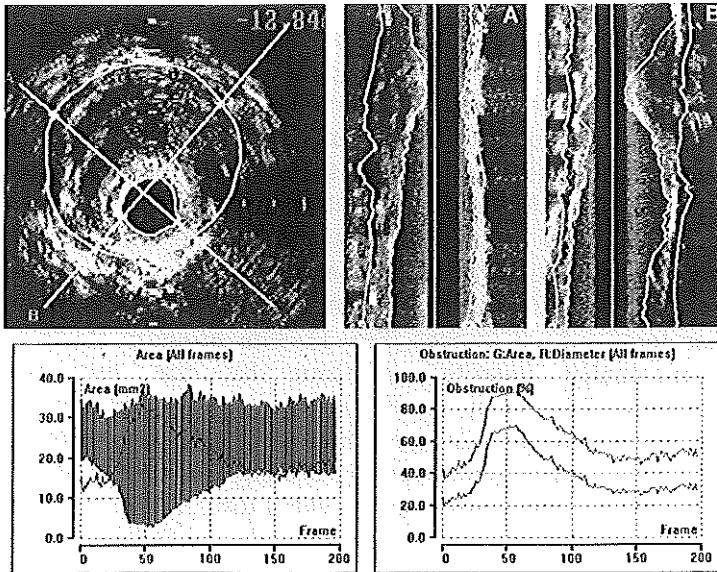


Fig. 2. Two longitudinally reconstructed sections (A and B; left and middle top panel), which stands perpendicular on each other as demonstrated in the transverse image (left top panel). Lower panels: standard display of results. Left lower panel: Area measurements of lumen, vessel and plaque area. Gray area represents atherosclerotic plaque. Upper and lower boundaries of the gray zone correspond to dimensions of vessel and lumen. Absolute value of plaque dimension is given as a single function. Right lower panel: Functions of diameter stenosis and area stenosis.

Table 1. Measurements of lumen area, vessel area, plaque area and percentage area stenosis assessed with automated and manual contour tracing systems, the mean differences and the coefficient of variation.

	Automated	Manual	Δ (Automated - manual)	Coefficient of variation (%)	<i>p</i> value	<i>r</i>
Lumen area (mm ²)	15.8 ± 8.2	16.0 ± 8.2	-0.2 ± 1.8	11.3	0.12	0.98
Vessel area (mm ²)	32.7 ± 12.0	33.1 ± 12.2	-0.4 ± 3.0	9.2	0.18	0.97
Plaque area (mm ²)	16.4 ± 6.2	16.6 ± 6.4	-0.2 ± 2.6	15.7	0.34	0.92
% Area stenosis	51.8 ± 13.8	51.8 ± 13.3	0.0 ± 4.4	8.5	0.99	0.95

Values are mean ± SD; Δ = differences; *r* = correlation coefficient.

In principle, the algorithm is automatic. In practice, the automated system requires a certain degree of user-interactive correction depending upon the image quality; the derived data are, therefore, a result of a semi-automatic process. The measurements on lumen, vessel and plaque area and percentage area stenosis were presented in a graph containing the data on each individual cross-section (Fig. 2).

Manual analysis system.

This analysis system has been described previously¹². Briefly, the analysis system operates on an IBM compatible PC/AT. A DT 2851 framegrabber is used to digitize IVUS recordings from a standard VHS videotape into a 512 x 512 x 8 bits digital image. Manual tracings of the circumferential outline are processed by the computer to produce a smoothed, connected closed contour.

Area measurements.

Measurements of lumen and vessel area were performed with both the automated analysis system and the manual analysis system. Lumen area was defined as the area encompassed by the inner boundary of the intimal surface (characterized also by the presence of blood flow); vessel area was defined as the boundary between the hypoechoic medial layer and the adventitia. Plaque area was calculated by subtracting the lumen from the vessel area. Percentage area stenosis was calculated as plaque area divided by vessel area. To facilitate the discrimination of the luminal boundary the IVUS images were replayed in real-time on an additional video monitor. Measurements were not considered for analysis:

1. when image quality was inadequate;
2. in the presence of a sidebranch; or
3. in case of a total occlusion. Vessel area, plaque area and percentage area stenosis were not considered for analysis when extensive dropouts due to plaque calcification were encountered, preventing visualisation of the underlying vessel wall.

For automated analysis, IVUS images were selected at 0.2 mm intervals based on the information provided by the displacement sensing device, enabling the analysis of an arterial segment of four centimeters. Every 25th IVUS cross-section analyzed with the automated analysis system was subsequently analyzed with the manual contour tracing system. Measurements in the cross-sections traced with both systems were compared to evaluate potential differences between the automated analysis system and the manual system.

Automated analysis was subsequently repeated by the same observer six weeks later and by a second observer. All available cross-sections were used to assess the intra- and interobserver variability in the measurements obtained with the automated system.

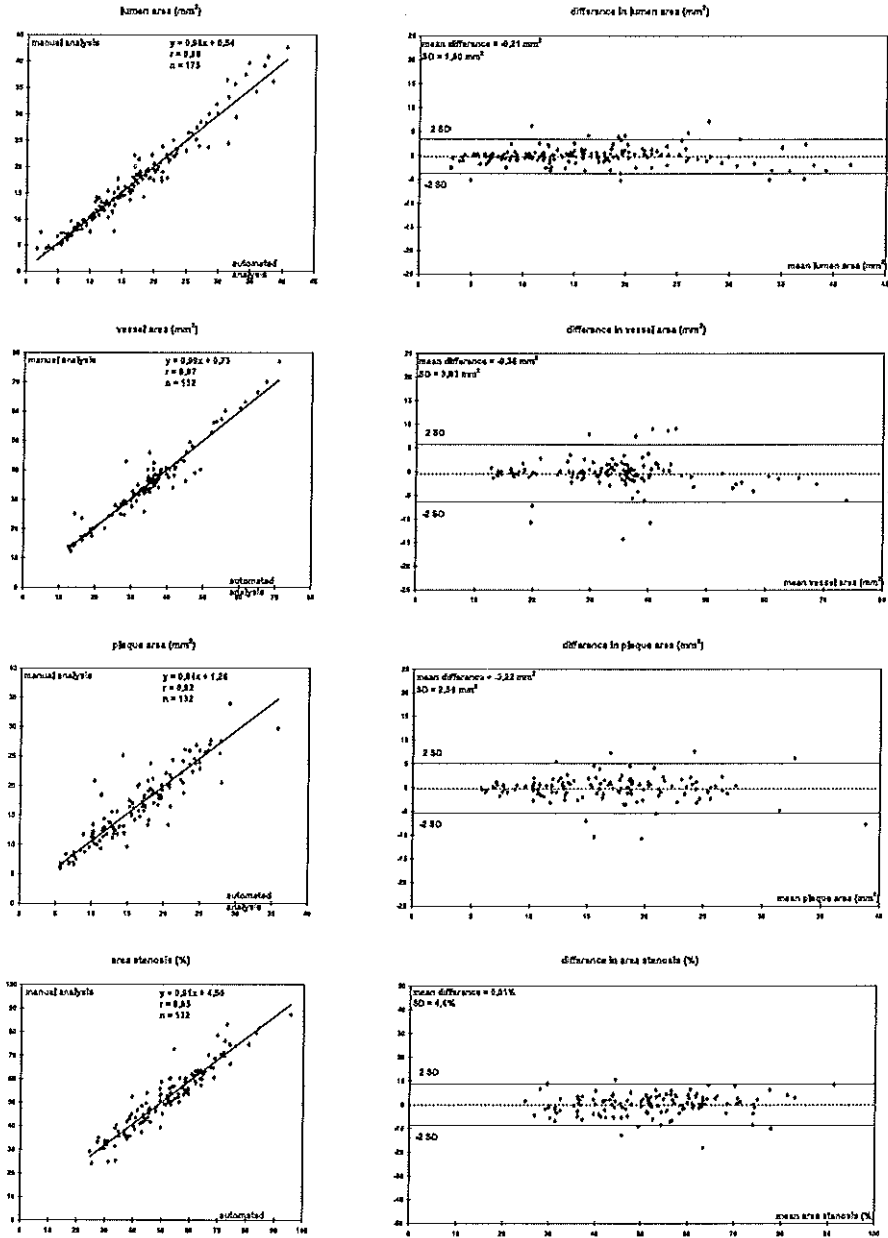


Fig. 3. Left panels: the results of the linear regression analyses, comparing lumen area, vessel area, plaque area and area stenosis, obtained with the automated and manual contour tracing system. Right panels: differences between the two systems plotted against mean of two measurements.

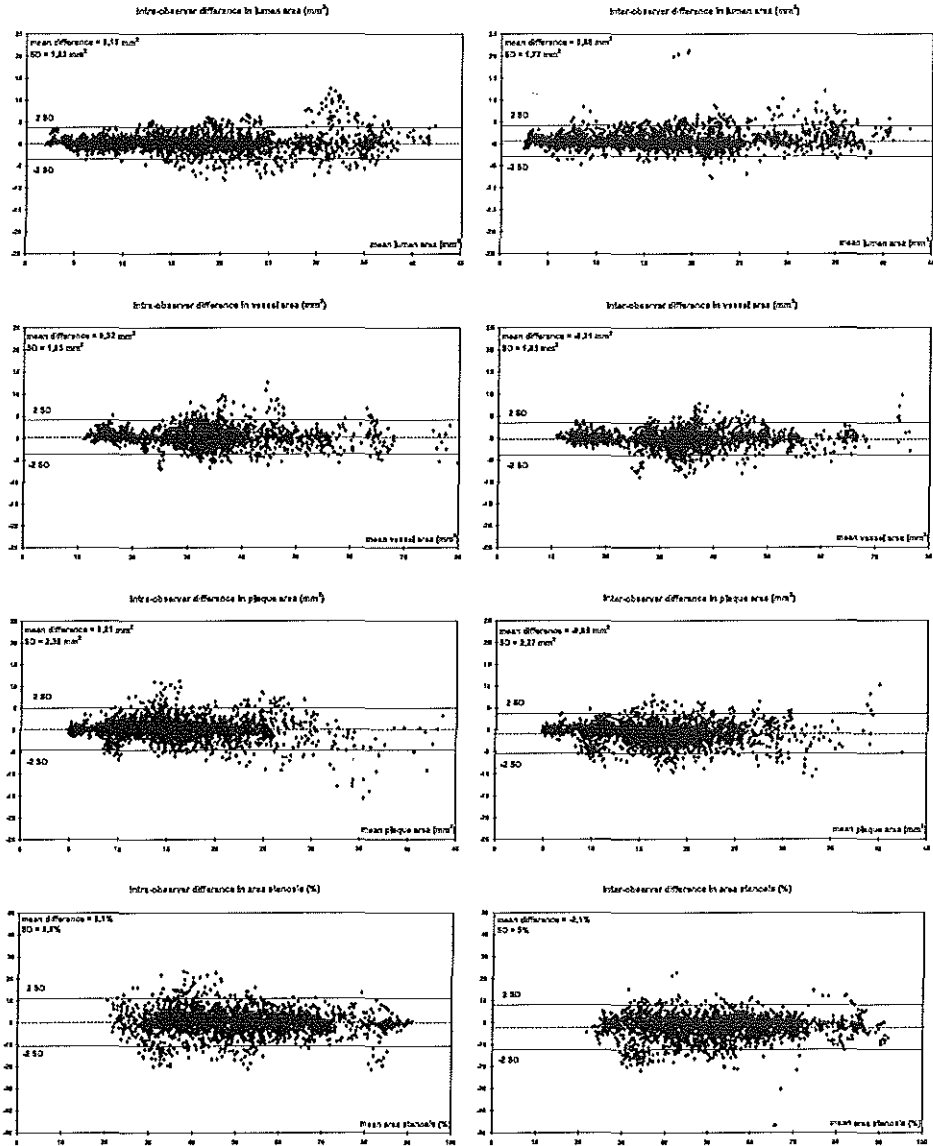


Fig. 4. Intra- and inter-observer variability of area measurements. Intraobserver differences (left panels) and interobserver differences (right panels) are plotted against the mean of two measurements.

Table 2. Intra- and interobserver analyses with the automated contour analysis: measurements of lumen area, vessel area, plaque area and percentage area stenosis, the mean differences and the coefficients of variation.

	Observer 1, Observation 1	Observer 1, Observation 2	Observer 2	Δ Intraob- server	Coefficient of variation (%)	Δ Inter- observer	Coefficient of variation
Lumen area (mm ²)	16.1 \pm 8.5	15.9 \pm 8.4	15.4 \pm 8.2	0.2 \pm 1.8 †	11.4	0.7 \pm 1.8 †	11.3
Vessel area (mm ²)	32.1 \pm 11.8	31.8 \pm 11.9	32.3 \pm 11.8	0.3 \pm 1.9 †	6.0	-0.2 \pm 1.8 †	5.7
Plaque area (mm ²)	15.7 \pm 6.0	15.5 \pm 6.3	16.6 \pm 6.3	0.2 \pm 2.4 †	15.3	-0.9 \pm 2.3 †	14.0
% Area stenosis	50.8 \pm 14.6	50.7 \pm 15.0	52.9 \pm 14.4	0.1 \pm 5.5	10.8	-2.1 \pm 5.1 †	10.6

Values are mean \pm SD; Δ = differences; † p < 0.001.

Data analysis.

To compare the measurements obtained with the two systems, mean and standard deviation (SD) of the paired differences were calculated. Systematic differences between automated and manual measurements and between the intra- and inter-observer measurements were analyzed with the Student *t*-test for paired observations. The degree of variation was presented as a coefficient of variation, defined as the SD of the paired difference divided by the mean of the absolute value. Linear regression analysis was performed to assess the strength of the relation between the two methods and between the intra- and inter-observer measurements. A *p*-value < 0.05 was considered statistically significant. Results are given as mean \pm SD, or as a median and range when appropriate.

RESULTS

In 10 patients image quality of the IVUS recordings was adequate for analysis. In the other two patients, analysis of lumen and vessel area could not be performed because of low image quality in one patient and technical failure of the displacement sensing device in the other patient. The length of the arterial segments analyzed ranged from 4 to 16 cm (median = 7.9 cm). The number of cross-sections analyzed automatically per segment ranged from 200 to 800 (median = 394).

Automated versus manual contour tracing.

A total of 217 IVUS cross-sections were selected for analysis (range 11 - 38 per arterial segment, median 21). Forty-two cross-sections were not considered for analysis due to low image quality (n=8), sidebranches (n=10), and total occlusion (n=24). In 43 other cross-sections vessel area,

plaque area and percentage area stenosis were not considered for analysis due to plaque calcification which prevented visualisation of the media. This resulted in 175 paired measurements of lumen area and 132 paired measurements of vessel area, plaque area and percentage area stenosis available for analysis. Results of automated and manual contour tracing on IVUS cross-sections are summarized in Table 1. Correlation coefficients were high ($r = 0.92 - 0.98$). No significant difference between the two methods was found for the area measurements. The coefficient of variation for lumen area, vessel area and percentage area stenosis was smaller than for plaque area (11.3, 9.2, 8.5 and 15.7%, respectively)(Fig. 3).

Observer variability.

A total of 4303 IVUS cross-sections were selected for analysis. There were 834 IVUS cross-sections not considered for analysis due to low image quality ($n=178$), sidebranches ($n=152$), and total occlusion ($n=504$). In 878 IVUS cross-sections vessel area, plaque area and percentage area stenosis were not considered for analysis due to plaque calcification which prevented visualisation of the media. This resulted in 3469 paired measurements of lumen area and 2591 paired measurements of vessel area, plaque area and percentage area stenosis available for observer analysis.

The correlation of the intraobserver measurements of lumen area, vessel area, plaque area and percentage area stenosis was high with correlation coefficients of 0.98, 0.99, 0.93 and 0.93, respectively. The mean differences between the repeated measurements by the same observer was low (range 0.1 - 0.3 mm²)(Fig. 4; Table 2). The coefficient of variation was higher for plaque area measurements than for lumen area, vessel area and percentage area obstruction (15.3 versus 11.4, 6.0 and 10.8%, respectively).

The interobserver correlation coefficients for lumen area, vessel area, plaque area and percentage area stenosis ($r=0.98, 0.99, 0.93$ and 0.94 , respectively) were in the same order as the intraobserver correlation coefficients. The mean interobserver differences were slightly larger than the intraobserver differences (range -2.1 - 0.7 mm²)(Fig. 4; Table 2). The coefficients of variation of the interobserver measurements were in the same order as the coefficients of variation of the intraobserver measurements.

DISCUSSION

Reliable assessment of lumen and vessel area on IVUS images obtained during percutaneous vascular intervention is important for guiding the procedure and evaluation of the results of intervention. For example: the location of the smallest lumen area and the extent of plaque assessed before intervention determines the site of intervention (balloon angioplasty); estimation of lumen area and/or vessel area influence the choice of

balloonsize and/or stentsize¹³; the dimensions of the treated segment after intervention define the success of intervention¹⁴.

An automated analysis system was developed to facilitate the quantitative assessment of vessel dimensions with reduction of the time of analysis and improvement of the reproducibility of quantitative IVUS analyses¹⁰. Previously, this automated contour analysis system was validated in IVUS images of diseased coronary arteries obtained both *in vitro* and *in vivo*^{8,9}. In the present study, the system was validated using clinical IVUS examination of atherosclerotic femoropopliteal arteries.

The results of this study show firstly good agreement between the automated and manual analysis system for quantitative assessment of IVUS images, and secondly a high intra- and interobserver reproducibility of the automated contour analysis system. The larger variability of plaque area measurements, derived from measurements of lumen and vessel area, reflects the combined variability of these two measurements.

Previous studies.

The coefficients of variation between automated and manual analysis in the present study were larger than those reported by von Birgelen et al.⁸ *in vitro* (11.3 versus 2.2% for lumen area; 9.2 versus 1.9% for vessel area). This may be explained by the difference in study design. The study by von Birgelen et al.⁸ was performed *in vitro* in mildly diseased coronary arteries which were filled with saline facilitating easier detection of the lumen-plaque interface. In our study, data were obtained during clinical intervention where blood, cyclic vessel movement and a guidewire, which causes dropout, hampered identification of the luminal boundary.

Sonka et al.¹⁵ devised an alternative approach to contour detection of lumen and vessel boundary. Their automatic contour detection is based on two-dimensional information, without guidance from the additional information provided by contour detection on longitudinally reconstructed IVUS images. In their coronary *in vitro* study the correlation ($r = 0.96, 0.95$ and 0.93 for lumen area, plaque area and percentage area stenosis, respectively) between measurements obtained with automatic and manual contour tracing was comparable to the results obtained in our *in vivo* study. The performance of the system used by Sonka et al.¹⁵ remains to be confirmed in the analysis of *in vivo* images.

It is noteworthy that the coefficient of variation between automated and manual analysis for lumen and vessel area in the present study was in the same range as the interobserver variability of manual analysis assessed in a clinical study by van der Lugt et al.⁶. However, the interobserver variability of the automated contour tracing system in the present study was lower than the values found by van der Lugt et al.⁶ for manual tracing (17.2 versus 11.3% for lumen area; 10.5 versus 5.7% for vessel area). The same

improvement in reproducibility with automated analysis in comparison to manual contour tracing was observed in coronary arteries in vivo^{9,16}. These findings underline that automated contour tracing has the potential to replace conventional manual analysis in the future.

Limitations.

Besides the exclusion of IVUS images for analysis because of low image quality, side-branches and occluded segments the main limitation of this study is the exclusion of IVUS images caused by the presence of extensive calcification. Especially manual analysis is hampered by the large dropouts. The automated contour analysis system, however, allows better interpolation of the vessel boundary behind calcium and thus may be more reliable than manual tracing of a single IVUS image.

A maximum of 200 IVUS images which can be analyzed simultaneously at an interval of 0.2 mm (in this study), results in an analyzed vessel segment of maximally 4 cm. However, diseased segments in femoropopliteal arteries are often longer than 4 cm. Increasing the interval between IVUS images to be grabbed may extend the vessel length to be studied, but this may influence the accuracy of the automated system. In addition, increasing processor speed and use of large memory chips might be another solution. Another limitation of the automated approach is that the images were manually acquired from videotape. This can be improved by automated image acquisition techniques. Finally, it should be acknowledged that this study was limited by the fact that IVUS recordings were obtained prior to intervention.

CONCLUSION

These data indicate that the automated contour analysis system provides reliable and reproducible measurements of vessel dimensions in IVUS images obtained during clinical examination of peripheral arteries.

REFERENCES

1. Gussenhoven EJ, Essed CE, Lancée CT, et al. Arterial wall characteristics determined by intravascular ultrasound imaging: an in vitro study. *J Am Coll Cardiol* 1989; 14: 947-952.
2. Potkin BN, Bartorelli AL, Gessert JM, et al. Coronary artery imaging with intravascular high-frequency ultrasound. *Circulation* 1990; 81: 1575-1585.
3. Tobis JM, Mallery J, Mahon D, et al. Intravascular ultrasound imaging of human coronary arteries in vivo. Analysis of tissue characterizations with comparison to in vitro histological specimens. *Circulation* 1991; 83: 913-926.
4. Li W, Gussenhoven WJ, Zhong Y, et al. Validation of quantitative analysis of intravascular ultrasound images. *Int J Card Imag* 1991; 6: 247-253.
5. The SHK, Gussenhoven EJ, Zhong Y, et al. The effect of balloon angioplasty on the femoral artery evaluated with intravascular ultrasound imaging. *Circulation* 1992; 86:483-493.
6. Lugt van der A, Gussenhoven EJ, Pasterkamp G, et al. Interobserver reproducibility of qualitative and quantitative analysis of intravascular ultrasound images before and after peripheral balloon angioplasty. *Ultrasound Med Biol* 1996; 22:399-404.
7. Peters RJG, Kok WEM, Rijsterborgh H, et al. Reproducibility and beat-to-beat variation of quantitative measurements on intracoronary ultrasound images. Thesis, University of Amsterdam, 1994: 55-72.
8. Birgelen von C, Lugt van der A, Nicosia A, et al. Computerized assessment of coronary lumen and atherosclerotic plaque dimensions in three-dimensional intravascular ultrasound correlated with histomorphometry. *Am J Cardiol* 1996; 78: 1202-1209.
9. Birgelen von C, Di Mario C, Li W, et al. Morphometric analysis in three-dimensional intracoronary ultrasound: An in vitro and in vivo study performed with a novel system for the contour detection of lumen and plaque. *Am Heart J* 1996; 132: 516-527.
10. Li W, Birgelen von C, Di Mario C, et al. Semi-automatic contour detection for volumetric quantification of intracoronary ultrasound. In: *Computers in Cardiology 1994*. Los Alamitos, CA: IEEE Computer Society Press, 1994: 277-280.
11. Gussenhoven EJ, Lugt van der A, Strijen van M, et al. Displacement sensing device enabling accurate documentation of catheter tip position. In: Roelandt JRTC, Gussenhoven EJ, Bom N, eds. *Intravascular Ultrasound*. Dordrecht: Kluwer Academic Publishers, 1993: 157-166.
12. Wenguang L, Gussenhoven WJ, Bosch JG, et al. A computer-aided analysis system for the quantitative assessment of intravascular ultrasound images. *Proc Comput Cardiol* 1990: 333-336.
13. Stone GW, Hodgson JM, StGoar FG, et al. Improved procedural results of coronary angioplasty with intravascular ultrasound-guided balloon sizing: The CLOUT Pilot Trial. *Circulation* 1997; 95: 2044-2052.

14. Gussenhoven EJ, Lugt van der A, Pasterkamp G, et al. Intravascular ultrasound predictors of outcome after peripheral balloon angioplasty. *Eur J Vasc Endovasc Surg* 1995; 10: 279-288.
15. Sonka M, Zhang X, Siebes M, et al. Segmentation of intravascular ultrasound images: A knowledge-based approach. *IEEE Trans Med Imag* 1995; 14: 719-732.
16. Haase J, Ozaki Y, Di Mario C, et al. Can intracoronary ultrasound correctly assess the luminal dimensions of coronary artery lesions? A comparison with quantitative angiography. *Eur Heart J* 1995; 16: 112-119.

**VALIDATION OF AUTOMATED CONTOUR
ANALYSIS OF INTRAVASCULAR
ULTRASOUND IMAGES FOLLOWING
VASCULAR INTERVENTION**

**Aran Hartlooper, MSc¹, Jeroen A. van Essen, MD¹,
Elma J. Gussenhoven, MD, PhD¹, Aad van der Lugt, MD, PhD²,
Marc R.H.M. van Sambeek, MD, PhD³,
Hans van Overhagen, MD, PhD².**

From the Departments of Cardiology¹, Radiology² and Vascular
Surgery³ of the University Hospital Rotterdam-Dijkzigt and the
Erasmus University Rotterdam, the Netherlands

Supported by grants from the Interuniversity Cardiology Institute of the
Netherlands and the Netherlands Heart Foundation (no. 91.016)

ABSTRACT

Objective:

To determine the feasibility of automated contour analysis of intravascular ultrasound images obtained after vascular intervention.

Study design:

Descriptive.

Methods:

Intravascular ultrasound images obtained from patients following balloon angioplasty (n=10), stent (n=10) or stentgraft placement (n=10) were analyzed. A comparison was made between lumen area measured with an automated and a manual system. The location showing the smallest lumen area derived from the automated system was compared with the smallest lumen area selected by visual estimation.

Results:

Images containing a dissection as result of balloon angioplasty could not be analyzed by the automated system. The coefficient of variation between the lumen area measurements obtained with the automated system and the manual tracing system of images with a stent (n=76) or stentgraft (n=79) was 2.7% and 2.1%, respectively. Correlation between the two systems was high ($r = 1.00$; $p < 0.01$) both for images containing stents or stentgrafts. Minimum lumen area measured with the automated analysis system was smaller than minimum lumen area selected by visual estimation (mean difference 0.8 mm^2 (4.9%) for stents and 2.4 mm^2 (10.9%) for stentgrafts). The location of the smallest lumen area determined with both systems was the same ($< 1.0 \text{ cm}$) in 16 cases, and differed more than 1.0 cm in 4 other cases.

Conclusions:

The automated analysis system shows good agreement with manual contour analysis of lumen area in images with a stent or stentgraft and is a reliable tool for determination of the smallest lumen area. The system is not able to analyze an irregular-shaped lumen area caused by a dissection.

INTRODUCTION

Intravascular ultrasound (IVUS) enables visualization of the blood vessel anatomy before and after intervention¹⁻⁴. Quantitative IVUS parameters may be used to guide a procedure and evaluate the results. At present, accurate measurements can be obtained after digitizing the individual cross-sections with a manual contour tracing system^{5,6}. Because analysis with this system is time consuming, an automated analysis system has been developed which has the potential to provide reproducible measurements instantaneously, enabling its use in the clinical setting⁷.

A good agreement between the automated and manual contour tracing system was established for assessment of lumen and vessel area on IVUS images obtained clinically before intervention in coronary and peripheral arteries^{8,9}. Our current objective is to focus on the value of the automated system in peripheral arteries showing vascular damage (i.e. dissections) after balloon angioplasty and in peripheral arteries where endovascular prostheses were placed (i.e. stents or stentgrafts).

METHODS

Study group.

The study group comprised 30 patients with peripheral arterial disease who underwent a vascular intervention: balloon angioplasty resulting in a dissection (n=10), stent placement (n=10) or stentgraft placement (n=10). There were 21 men and 9 women; the median age was 62 years (range 47-86 years). All patients have given their informed consent for the procedures.

The location of the treated lesion included the femoropopliteal artery (n=23), iliac artery (n=2), renal artery (n=3), carotid artery (n=1) and coeliac artery (n=1). Patients were scheduled for intervention based on angiographic proven obstructive vascular disease (diameter stenosis > 50%) (n=25) or an aneurysm (n=5).

Balloon angioplasty was performed with 4 cm long 6 mm balloons (Opta, Cordis Europe, Roden, The Netherlands).

The following stents were used: Palmaz (Johnson and Johnson Interventional Systems, Warren, NJ) in seven patients, Memotherm (Angiomed, Nitinol, Karlsruhe, Germany) in two patients and a Wallstent (Schneider, Zurich, Switzerland) in one patient.

Stentgrafts used were composed of one or more stents (Palmaz) and a thin-walled polytetrafluoroethylene graft (ePTFE) (W.L. Gore & Associated, Flagstaff, Az). The length of the treated segment was recorded with the help of a radiopaque ruler.

IVUS imaging.

The IVUS studies were performed using a mechanical IVUS system based on a single ultrasound element (30 MHz); the tomographic image is produced by a rotating element, which is mounted on a guidewire-tipped 4.3F catheter (DuMED, Rijswijk, The Netherlands). The axial resolution of the system is 80 μm and the lateral resolution is better than 225 μm at a depth of 1 mm.

The ultrasound catheter was introduced through a sheath via the guide-wire into the artery distal to the region of interest. During slow pullback of the ultrasound catheter its location was compared with the radiopaque ruler using fluoroscopy. The fluoroscopic image was mixed with the IVUS information. The resulting images were recorded on an S-VHS videotape.

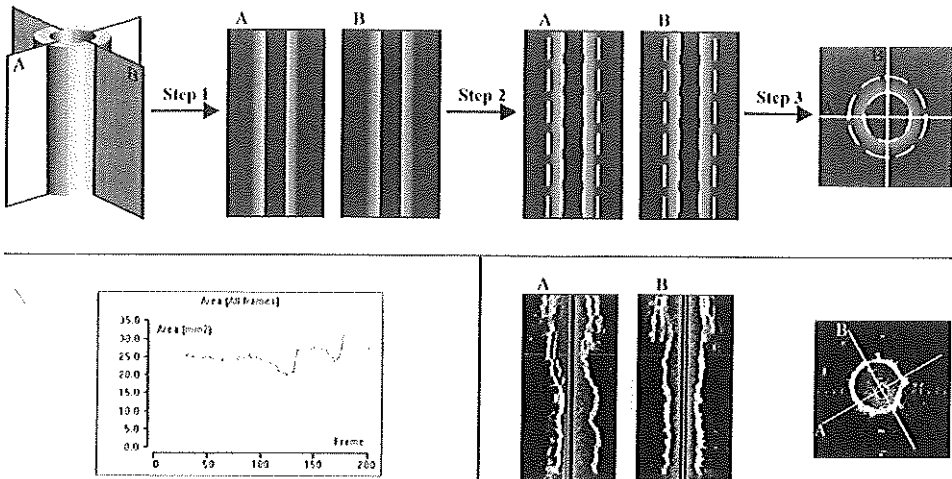


Fig.1. Automated contour detection of intravascular ultrasound (IVUS) images. **Upper panel:** two perpendicular planes are used to reconstruct two longitudinal sections (A and B) from the digitized IVUS images (step 1). Automated contour detection of the intimal leading edge and the external boundary of the vessel is performed on these longitudinal sections (step 2). The longitudinal contours are represented as individual edge points in the cross-sectional images. These points define centre and range of the final contour detection process on the cross-sectional images (step 3). **Lower left panel** presents a standard display of lumen area measurements derived from a stentgraft. **Lower right panel:** The two reconstructed longitudinal sections (A and B), correspond to the perpendicular planes seen in the cross-section.

Automated analysis.

The automated analysis system⁷ uses a Pentium (100 MHz) system with 32 Mbytes of internal RAM memory. IVUS data were acquired continuously from the S-VHS video with a framegrabber (DT-3852; resolution 800 x 600 x

8 bits). Images obtained in the dilated segment, stent and stentgraft were selected for analysis (from proximal to distal border). A maximum of 200 IVUS cross-sections was stored per vessel segment. In short, the analysis procedure could be divided into 3 steps (Fig. 1). First, a sequence of IVUS images was digitized and two perpendicular planes, parallel to the longitudinal axis of the vessel, were selected to reconstruct longitudinal views. The user was able to select the angle and location of the perpendicular planes within the arterial lumen. Second, the program defined the contours of lumen and vessel area on these longitudinal planes by applying a minimum cost algorithm. In brief, a matrix is yielded from the digitized images, producing low values (costs) for large changes in echo intensity. Through this matrix, the algorithm determined a path with the smallest accumulated cost which represents the contours. Third, the longitudinal contour information was transformed to the cross-sections defining four guiding points. These points were used to facilitate contour detection of lumen and vessel area on each individual cross-section. During all steps the analysis could be refined by the user. The results were presented in a graph containing the measurements of each individual cross-section⁷ (Fig. 1).

Manual contour analysis.

This analysis system, developed on an IBM compatible PC/AT, uses a DT 2851 framegrabber and a PC mouse for manual contour tracing^{5,6}. The analysis program consists of 3 main steps: image acquisition, contour tracing and parameter calculation. For image acquisition, video signals from the VHS videotape were converted into 512 x 512 x 8 bits digital images using a framegrabber and stored on the hard disk of the PC. Manual tracings of the circumferential outline were processed by the computer to produce a smoothed, connected closed contour. Parameter calculations were automatically performed after the contour was completed or modified.

Quantitative analysis.

Measurement of lumen area was performed with both the automated analysis system and the manual analysis system. Lumen area was defined as the area encompassed by the inner boundary of the intimal surface (characterized also by the presence of flowing blood), or the inner surface of the stent or stentgraft. Within the selected vessel segment, a maximum of 200 images was analyzed with the automated system. Because the length of the selected vessel segments was not fixed, the interval between consecutive images in each vessel segment differed. The location and size of the smallest lumen area were selected from these images by the automated analysis system. From each vessel segment 6-8 cross-sections were analyzed manually at a 0.5-1.0 cm interval, including the visually determined smallest lumen area within each artery. To assess the interobserver

variability for lumen area of the automated system, the analysis was repeated by a second blinded observer.

Data analysis.

Systematic differences between the automated and manual contour measurements and between the interobserver measurements were analyzed with the Student *t*-test for paired observations; the agreement was expressed as a coefficient of variation, defined as the standard deviation (SD) of the paired difference divided by the mean of the absolute value. Linear regression analysis was performed to assess the strength of the relation between the two methods and between the interobserver measurements. A *p*-value < 0.05 was considered statistically significant. Values are given as mean \pm SD.

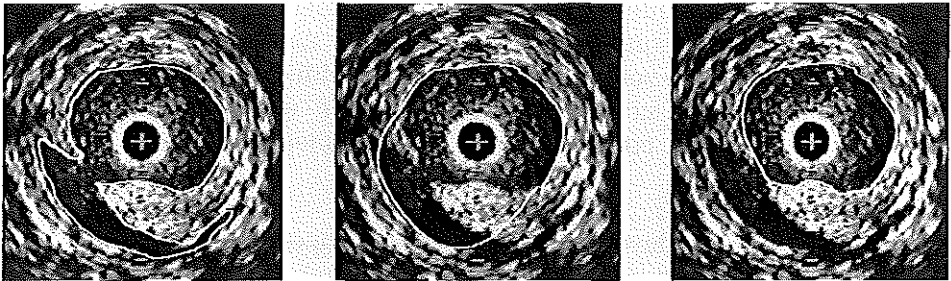


Fig.2. Identical intravascular ultrasound cross-sections showing a dissection with the results of manual and automated analysis. **Left panel** shows the manually assessed contour of lumen area. **Middle and right panel** show 2 incorrect analyses of lumen area derived with the automated system.

RESULTS

Automated versus manual.

In all patients with dissection following balloon angioplasty (median length 10.5 cm), automated analysis of lumen area could not be achieved due to the inability of the automated system to follow the irregular lumen contour (Fig. 2). In contrast, irregular lumen contours could be traced by the manual analysis system.

The IVUS recordings were adequate for automated analysis in patients with stent (n=10) or stentgraft (n=10). The median length of the stents was 2.0 cm (range 1.5 - 9.0 cm); the median length of the stentgrafts was 8.0 cm (range 2.5 - 15 cm). Results of the automated and manual contour tracing are summarized in Table I. Automated analysis resulted in significantly smaller lumen area than manual analysis (mean difference $0.24 \pm 0.59 \text{ mm}^2$ and $0.57 \pm 0.70 \text{ mm}^2$, respectively for stents and stentgrafts; $p < 0.01$);

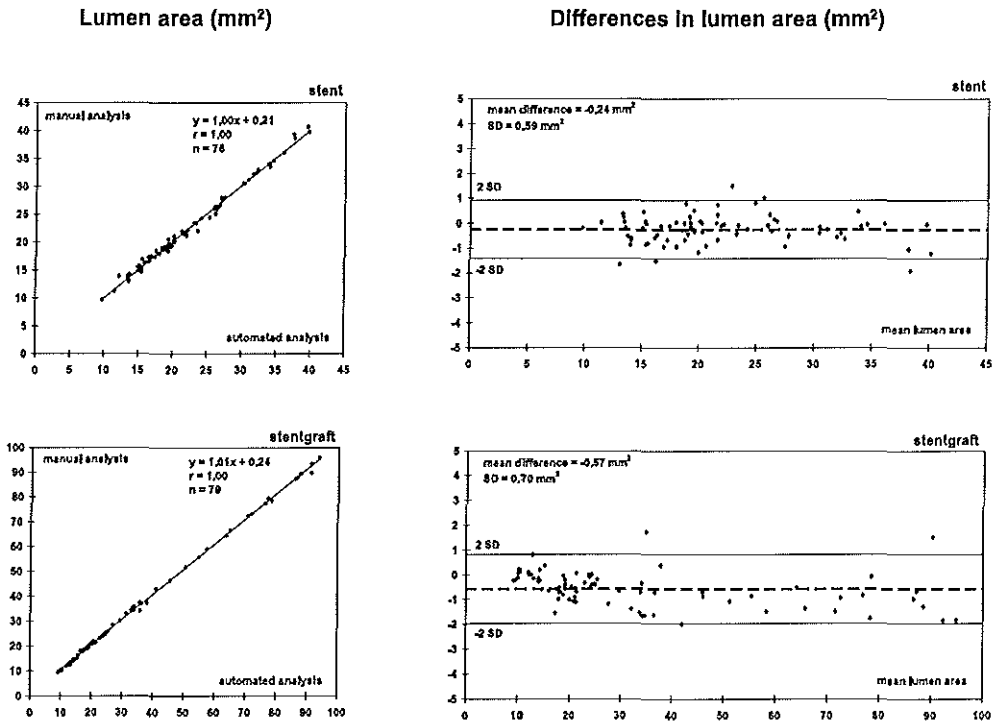


Fig.3. Comparison of automated and manual analysis of lumen area in stents and stentgrafts. **Left panel:** linear regression analyses comparing lumen area obtained with the automated and manual contour tracing system. **Right panel:** differences between the measurements obtained with the two systems plotted against the mean of two measurements.

the coefficients of variation were low (2.7% and 2.1%, respectively). The correlation between the two systems for lumen area measurement was high ($r=1.00$) (Fig. 3).

Smallest lumen area.

Minimum lumen area measured with the automated analysis system was smaller than measured with the manual analysis system, both for stents (mean difference $0.8 \pm 1.1 \text{ mm}^2$) and stentgrafts (mean difference $2.4 \pm 1.7 \text{ mm}^2$). The location of the smallest lumen area as determined by the automated system and by visual estimation corresponded closely in 16 instances (difference $< 1.0 \text{ cm}$). In 4 stentgrafts the distance found for the site with the smallest lumen area was 1.0 cm, 1.3 cm, 6 cm and 8 cm,

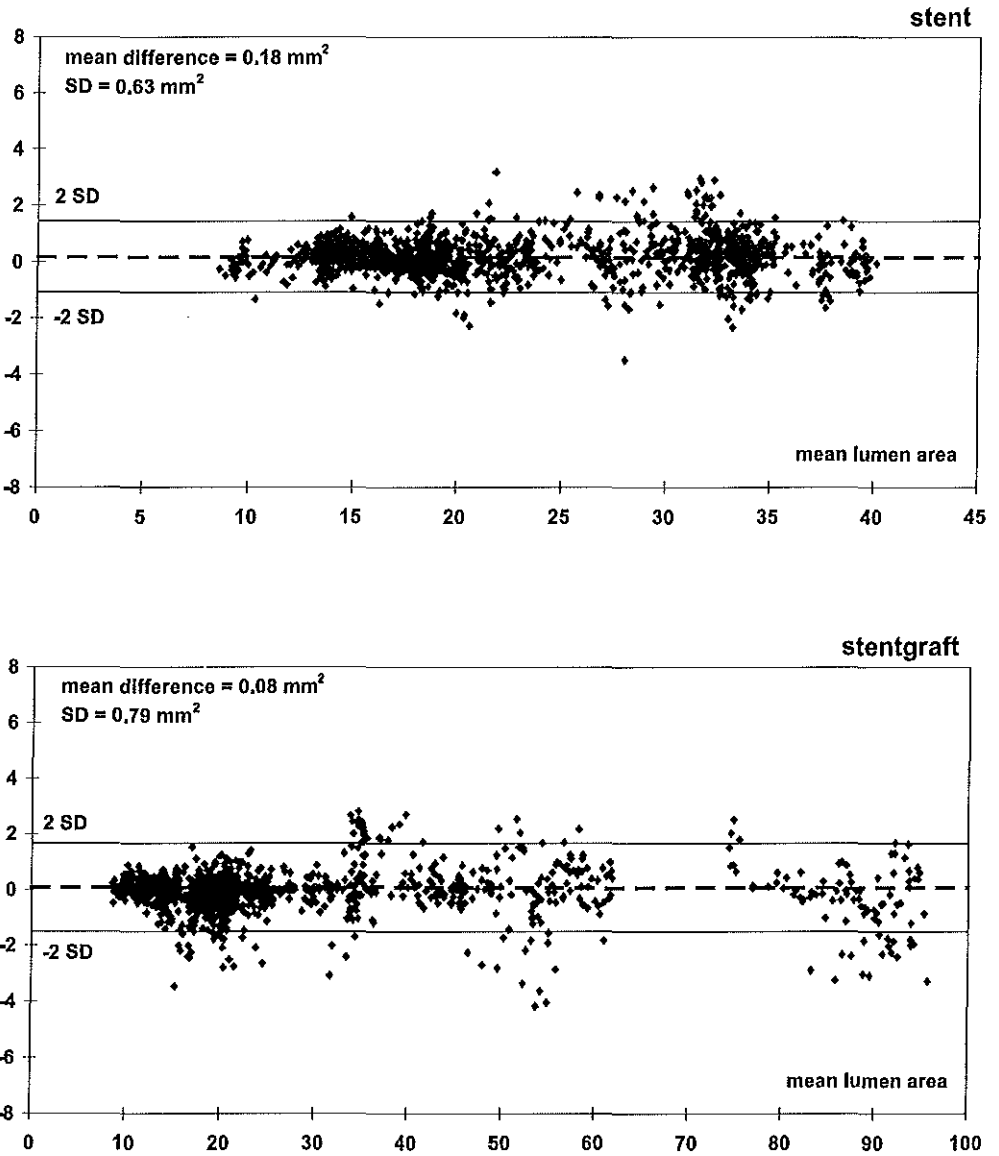


Fig.4. Interobserver variability of lumen area (mm²) measurements in stents and stentgrafts. Interobserver differences are plotted against the mean of two measurements.

Table 1. Paired difference and coefficient of variation between the lumen area measurements obtained by automated analysis and manual contour tracing

	Lumen area (mm ²)	
	Stents (n=76)	Stentgrafts (n=79)
Automated	21.78 ± 7.34	32.68 ± 23.90
Manual	22.00 ± 7.38	33.25 ± 24.15
Paired difference	-0.24 ± 0.59	-0.57 ± 0.70
Coefficient of variation	2.7%	2.1%
p-value	< 0.01	< 0.01
correlation coefficient (r)	1.00	1.00

respectively; the difference in lumen area at these sites was 3.0 mm² (22.2%), 1.1 mm² (13.1%), 0.6 mm² (3.6%) and 2.0 mm² (12.7%), respectively.

Interobserver variability.

The mean difference for lumen area measurements of the automated system was less than 1% in both stents and stentgrafts (0.18 ± 0.63 mm² and 0.08 ± 0.79 mm², respectively; $p < 0.01$) (Fig. 4); the coefficient of variation was 2.8% for lumen area in stents and 2.9% for lumen area in stentgrafts.

DISCUSSION

Intravascular ultrasound is a valuable tool in clinical practice to assist in decision making during vascular procedures. In order to objectively determine vessel dimensions on-line an automated analysis system has been developed. This system enables to calculate vascular dimensions of an individual cross-section as well as of the complete recorded vessel. Previous studies indicated that automated contour analysis provides reliable and reproducible measurements of vessel dimensions in IVUS images obtained prior to vascular intervention of coronary and peripheral arteries^{8,9}. In the present study, the reliability of the automated analysis system for area measurement in IVUS images obtained after intervention was studied. We learned that automatic analysis of lumen area in IVUS images showing a dissection was not feasible; this was due to the minimum cost algorithm.

Sharp edges in the lumen or media border could not be followed and protrusions inside the lumen were missed. These problems may be overcome in the future by use of edge detection algorithms that are currently being developed^{10,11}. In contrast, in the presence of smooth-shaped lumen borders as seen in stents and stentgrafts, the variability between the automated and manual contour tracing system for lumen area was low (coefficient of variation is 2.7% and 2.1%, respectively); these data are similar to those calculated from coronary arteries studied *in vitro* (2.2%)⁸. In peripheral arteries studied in humans before intervention a higher coefficient of variation (11.3%) was found⁹, likely due to the presence of flowing blood and the absence of a clear lumen-wall interface. Although the present study revealed that the automated analysis system draws significantly smaller area contours than manual contour analysis it seems that the practical difference between the two systems was too small to influence the interpretation of the measurements.

In addition, the difference in smallest lumen area found between the automated and the manual analysis systems was larger than the differences between the two systems for all analyzed cross-sections. This suggests that the automated analysis system is able to accurately locate the smallest lumen area and that visual estimation can miss the actual smallest lumen area. Although manual estimation of smallest lumen area was within 1.0 cm of the location assessed by the automated system in 16 cases, the distance was larger in 4 of the studied stentgrafts. It should be noted that visual estimation of the location of minimum lumen area is subjective, which might preclude distinguishing area differences < 20%.

In this study the interobserver variability of automated analysis after stent or stentgraft placement was excellent (coefficient of variation was 2.8% and 2.9%, respectively). Similar values were found in coronary arteries studied *in vivo* (2.6%)¹². In peripheral arteries studied before intervention a higher interobserver variability was reported (11.3%)⁹; this might be attributed to the distinct lumen/wall border in stents and stentgrafts compared to native vessels.

CONCLUSIONS

The automated analysis system is a reliable tool to determine lumen area in peripheral vessels where endovascular prostheses were placed. Accurate data on the size of the stent and stentgraft and on the location of the smallest lumen area may assist in decision making during vascular procedures. The automated system cannot be used in vessels with a dissection due to an irregular-shaped lumen area.

REFERENCES

1. Gussenhoven EJ, Essed CE, Lancee CT, Mastik F, Frietman P, Egmond van FC, Reiber J, Bosch H, Urk van H, Roelandt J, Bom N. Arterial wall characteristics determined by intravascular ultrasound imaging: an in vitro study. *J Am Coll Cardiol* 1989; 14: 947-952.
2. Fitzgerald PJ, Yock PG. Mechanisms and outcomes of angioplasty and atherectomy assessed by intravascular ultrasound imaging. *J Clin Ultrasound* 1993; 21: 579-588.
3. Lugt van der A, Gussenhoven EJ, Stijnen T, Strijen van M, Driel van E, Egmond van FC, Suylen RJ, Urk v H. Comparison of intravascular ultrasound findings after coronary balloon angioplasty with histology. *Am J Cardiol* 1995;76:661-666.
4. Mintz GS, Popma JJ, Pichard AD, Kent KM, Satler LF, Chuang YC, Griffin J, Leon MB. Intravascular ultrasound predictors of restenosis after percutaneous transcatheter coronary revascularization. *J Am Coll Cardiol* 1996;27:1678-1687.
5. Wenguang L, Gussenhoven WJ, Bosch JG, Mastik F, Reiber JHC. A computer-aided analysis system for the quantitative assessment of intravascular ultrasound images. *Proc Comput Cardiol* 1990: 333-336.
6. Wenguang L, Gussenhoven WJ, Zhong Y, The SHK, Di Mario C. Validation of quantitative analysis of intravascular ultrasound images. *Int J Card Imag* 1991; 6: 247-253.
7. Li W, Birgelen von C, Di Mario C, Boersma E, Gussenhoven EJ, Putten van der N, Bom N. Semi-automatic contour detection for volumetric quantification of intracoronary ultrasound. In: *Computers in Cardiology 1994*. Los Alamitos, CA: IEEE Computer Society Press, 1994: 277-280.
8. Birgelen von C, Lugt van der A, Nicosia A, Mintz GS, Gussenhoven EJ, Vrey de E, et al. Computerized assessment of coronary lumen and atherosclerotic plaque dimension in three-dimensional intravascular ultrasound correlated with histomorphometry. *Am J Cardiol* 1996;78:1202-1209.
9. Lugt van der A, Hartlooper A, Wenguang L, Birgelen von C, Reiber JHC, Gussenhoven EJ. Reliability and reproducibility of automated contour analysis in intravascular ultrasound images of femoropopliteal arteries. *Ultrasound Med Biol* 1998; 24: 43-50.
10. Li W, Steen van der AFW, Lancee CT, Honkoop J, Gussenhoven EJ, Bom N. Temporal correlation of blood scattering signals in vivo from radiofrequency intravascular ultrasound. *Ultrasound Med Biol* 1996; 5: 583-590.
11. Zwet van der PM, Reiber JH. A new approach for quantification of complex lesion morphology: the gradient field transform; principles and validation results. *J Am Coll Cardiol* 1994; 24: 216-224.
12. Birgelen von C, Di Mario C, Li W, Schuurbijs JCH, Slager CJ, Feyter de PJ et al. Morphometric analysis in three-dimensional intracoronary ultrasound: An in vitro and in vivo study performed with a novel system for the contour detection of lumen and plaque. *Am Heart J* 1996; 132: 516-527.

**THREE-DIMENSIONAL INTRAVASCULAR
ULTRASOUND ASSESSMENT OF THE
PROXIMAL AND DISTAL NECK OF
ABDOMINAL AORTIC ANEURYSMS**

**Jeroen A. van Essen, MD¹, Elma J. Gussenhoven, MD, PhD¹,
Jan D. Blankensteijn, MD, PhD⁴, Jan Honkoop, MSc¹,
Lukas C. van Dijk, MD, PhD², Marc R.H.M. van Sambeek, MD, PhD³,
Aad van der Lugt, MD, PhD².**

From the Departments of Cardiology¹, Radiology² and Vascular Surgery³ of the University Hospital Rotterdam-Dijkzigt and the Erasmus University Rotterdam, and Vascular Surgery⁴ of the University Medical Center Utrecht, the Netherlands.

Supported by grants from the Netherlands Heart Foundation (no 95.123) and the Interuniversity Cardiology Institute, the Netherlands.

J Endovasc Ther: In press

ABSTRACT

Purpose:

To document the accuracy of an automated analysis system to determine lumen diameter and length of proximal and distal necks of abdominal aortic aneurysm (AAA) from intravascular ultrasound (IVUS) images and to describe additional features associated with three-dimensional (3D) IVUS imaging.

Materials and methods:

Twenty-two AAA were studied with IVUS. Lumen diameter obtained from 2 IVUS cross-sections in each neck using the automated and manual analysis system was compared. Length of the neck obtained with automated analysis was compared with length assessed by the displacement sensing device. Automated analyses were repeated by a second observer.

Results:

Twenty proximal aortic, 6 distal aortic and 3 iliac necks were available for analysis. Comparison between automated and manual analysis for lumen diameter revealed a difference of 0.45 ± 0.42 mm ($p < 0.001$, $r = 0.99$, coefficient of variation = 2.1%); for length measurements a difference of 0.05 ± 0.12 cm ($p = 0.04$, $r = 0.99$, coefficient of variation = 4.1%) was found. Interobserver difference for lumen diameter was 0.13 ± 0.66 mm ($p < 0.001$, $r = 0.99$ and coefficient of variation = 3.4%); and for length measurements 0.05 ± 0.11 cm ($p = 0.02$, $r = 0.99$ and coefficient of variation = 3.5%). 3D IVUS imaging allowed identification of the shape of the neck.

Conclusions:

Automated analysis of IVUS images allows accurate measurement of lumen diameter of the proximal and distal neck of AAA and gives similar length measurements compared to manual analysis. Longitudinal display of IVUS images facilitates anatomic understanding of neck anatomy.

INTRODUCTION

Accurate knowledge of the dimensions of the proximal and distal neck of abdominal aortic aneurysm (AAA) is important for planning endovascular treatment¹⁻³. Intravascular ultrasound (IVUS) has been acknowledged as a powerful imaging tool, providing information regarding dimensions of the abdominal aorta and vessel wall morphology⁴⁻⁶. It has been proposed that three-dimensional IVUS imaging may have clinical potential in the assessment of AAA dimensions^{7,8}. We developed an automated analysis system that provides longitudinal information of the vessel interrogated which may be used in a clinical setting to assess measurements in a 3D stack of IVUS images⁹. The purpose of this study was to validate this automated analysis system to document lumen diameter and length of the proximal and distal neck of AAA and to describe the features associated with 3D IVUS imaging.

MATERIAL AND METHODS

In vitro.

Aneurysmal abdominal aortic specimens (n=6; aged 61-88 years; five male), removed at autopsy, were studied in an in vitro setup⁵.

In vivo.

Patients (n=16; aged 59-81 years; all male) with AAA were studied with IVUS at the time of preoperative angiographic assessment or immediately before endovascular treatment⁶.

Intravascular ultrasound.

Two IVUS systems were used; the HP-Sonos Intravascular Imaging System (Hewlett Packard, Andover, MA, USA) with a 12.5 MHz Sonicath Side-Saddle catheter (Boston Scientific Corp, Watertown, MA, USA) or the Endosonics Visions PV Five-64 system with a 10 MHz Computed Intraluminal Sonography Imaging Catheter (Endosonics Corp, Rancho Cordova, CA, USA). The IVUS catheter was pulled back manually, and a displacement sensing device was used to document the position of the cathetertip [Fig 1]. This information was mixed automatically with the ultrasound information on the videoscreen¹⁰. To enable automatic acquisition of the IVUS images, a computerized position registry device with audiofeedback, coupled to the displacement sensing device, was used. The computerized position registry translates the data obtained from the displacement sensing device to an audiosignal that is used by the automated analysis system to acquire the IVUS images with a given interval¹¹. IVUS images were stored on videotape (S-VHS) for further analysis.

Automated IVUS analysis.

The automated analysis system uses a Pentium (100 MHz) system with 32 Mbytes of internal RAM memory. IVUS cross-sections of the proximal and

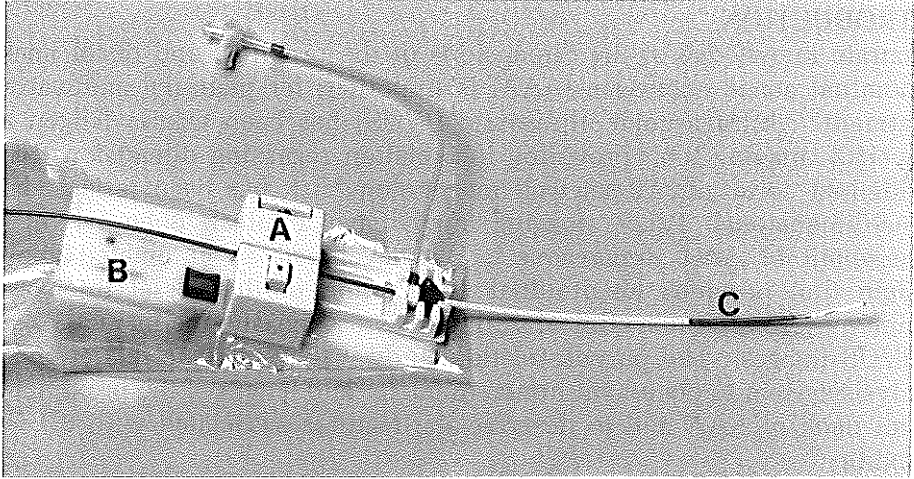


Fig. 1. Displacement sensing device showing the disposable sterile sensing unit (A) and the registration unit (B) which is packed in a plastic, sterile bag. The ultrasound catheter (C) is advanced via the sensing unit and the sheath.

distal aortic neck, including the adjacent part of the aneurysm, were acquired continuously from S-VHS video with a framegrabber (DT-3852; resolution 800 x 600 x 8 bits) and stored on the computer. A maximum of 200 IVUS images could be stored with an interval of 0.3 or 0.6 mm, depending on the total length of the segment to be studied⁹.

Basically, the analysis can be divided into 3 steps (Fig. 2). First, a sequence of IVUS cross-sections was digitized and stacked longitudinally. Two perpendicular planes, parallel to the longitudinal axis of the vessel, were selected to reconstruct the longitudinal IVUS images (step 1). The user was able to select the location of the perpendicular planes within the lumen. Second, the program defined the contours of the lumen on these longitudinal images by applying a minimum cost algorithm (step 2). The algorithm detects changes in echo intensity representing the boundaries (contours) of the arterial structures. Third, the longitudinal contour information was transformed to the cross-sections defining four guiding points, which were used to facilitate automated contour detection of the lumen area in each individual cross-section (step 3). During all steps the automated detected contours could be refined by the user. For assessment of the lumen diameter and length of the neck, the observer could manually exclude cross-sections from analysis showing the aneurysm, the renal arteries or the aortic bifurcation. The results were presented in a graph containing the measurements of each analyzed cross-section.

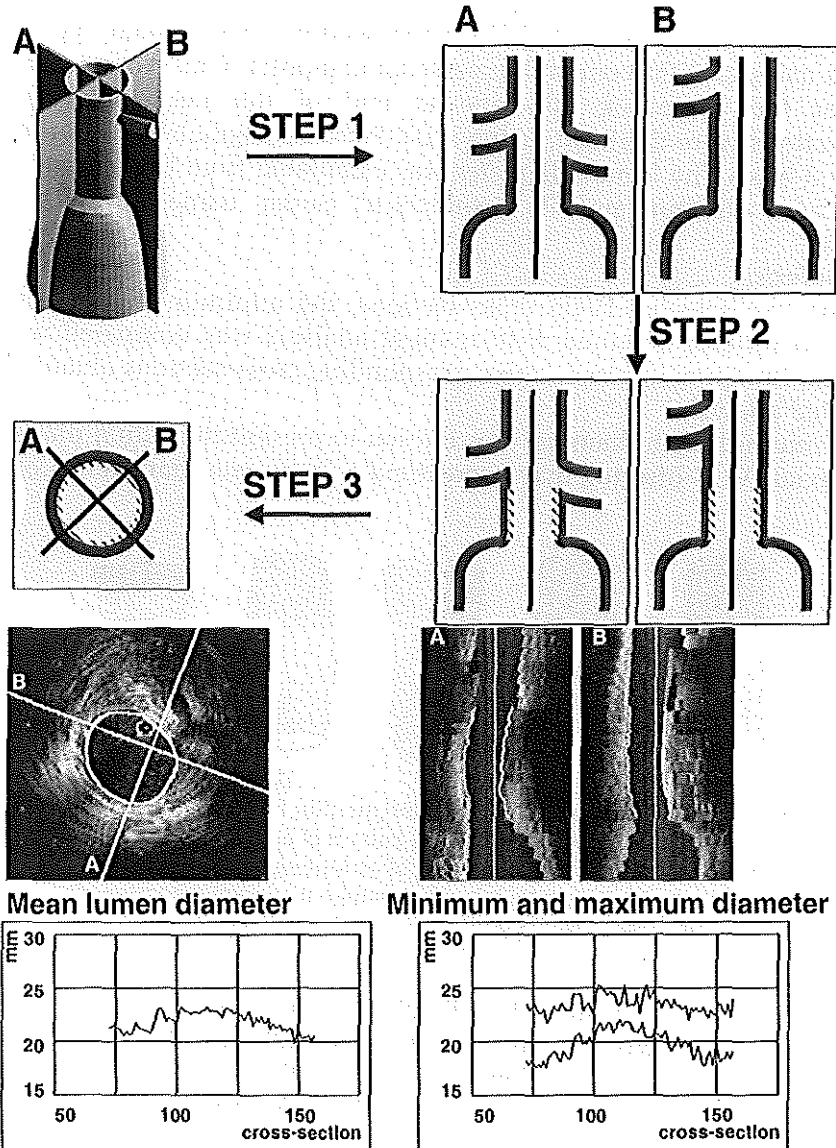


Fig. 2. Automated contour detection of intravascular ultrasound (IVUS) images. Upper panel: 2 perpendicular planes are used to reconstruct longitudinal sections (A and B) from the digitized IVUS images (step 1). Automated contour detection of the intimal leading edge of the vessel is performed on these longitudinal sections (step 2). The longitudinal contours are represented as individual edge points in the cross-sectional images. These points define center and range of the final contour detection process on the cross-sectional images (step 3). Lower right panel: The 2 reconstructed longitudinal sections (A and B), correspond to the perpendicular planes seen in the cross-section.

Manual IVUS analysis.

From each neck studied, 2 IVUS cross-sections were taken for manual analysis using an IBM compatible personal computer. One cross-section was taken at the beginning and one at end of the neck. The selected cross-sections were digitized, using a DT 2851 framegrabber (resolution 512 x 512 x 8 bits). The lumen diameter was calculated from the manual traced lumen area contour and its geometrical center using a digital video analyzer¹².

Data analysis.

From the two selected IVUS cross-sections, the minimum lumen diameter (intima to intima) obtained with manual analysis was compared with the minimum lumen diameter in the corresponding cross-sections obtained with automated analysis.

The minimum lumen diameter was chosen to present the actual diameter as non-coaxial IVUS imaging may overestimate the lumen diameter⁶. Using the

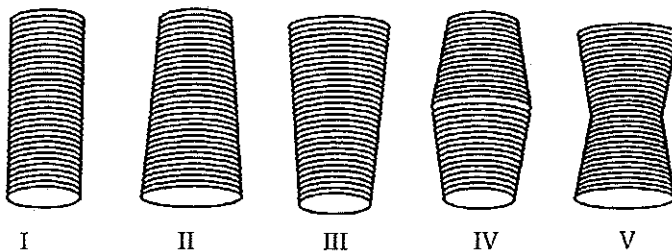


Fig. 3. Classification of the neck configuration in 5 categories. (Reproduced with permission from Balm R et al. Computed tomographic angiographic imaging of abdominal aortic aneurysms: implications for transfemoral endovascular aneurysm management. J Vasc Surg 1997; 26: 231-237)

automated analysis system, the length of the neck was calculated by multiplying the number of cross-sections, selected by the observer within the neck, with the interslice distance. The length of the neck was compared with the visual assessed length from video-tape, using the data obtained from the displacement sensing device. To assess the interobserver agreement the automated measurements were repeated by a second independent observer.

To identify additional features of 3D IVUS imaging, all necks were analyzed for shape and transition of neck to aneurysm. The shape of the neck was classified according to Balm et al.³ (Fig. 3).

Statistical analysis:

Measurements of quantitative data were compared with the paired sample t-test and linear regression analysis. Agreement was expressed as coefficient of variation, which was defined as the standard deviation of the paired differences divided by the mean of the absolute values¹³. Significance was defined as $p < 0.05$. Values are given as mean \pm SD.

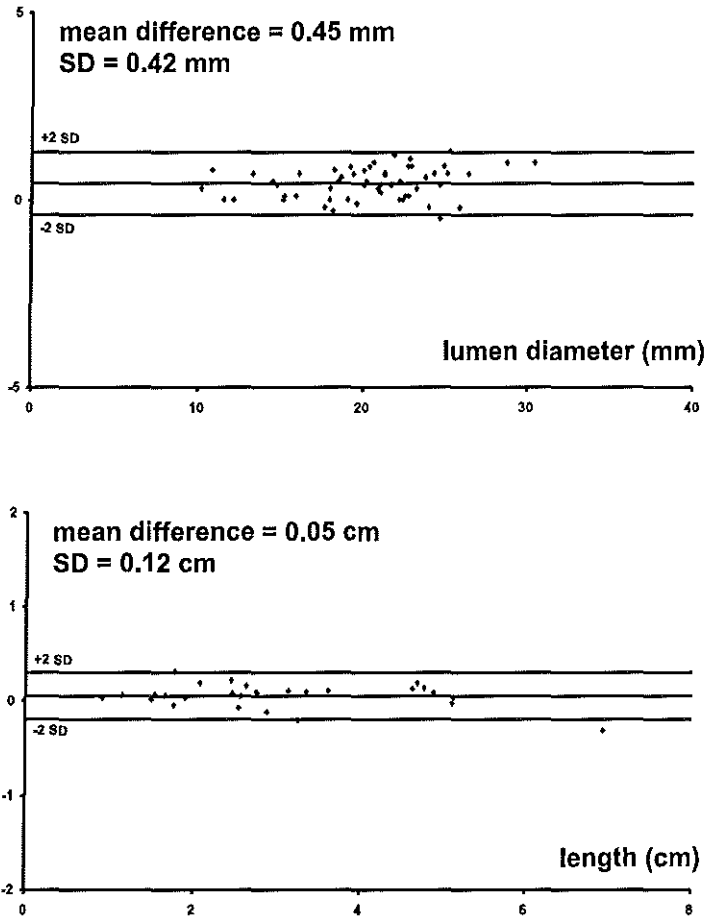


Fig. 4. Comparison between automated and manual analysis for lumen diameter of the proximal and distal neck (upper panel). Comparison between automated analysis and visual assessment for length of the proximal and distal neck (lower panel).

RESULTS

Of the 22 AAA studied, 20 proximal aortic necks, as well as six distal aortic necks and three iliac necks were available for analysis. The proximal neck

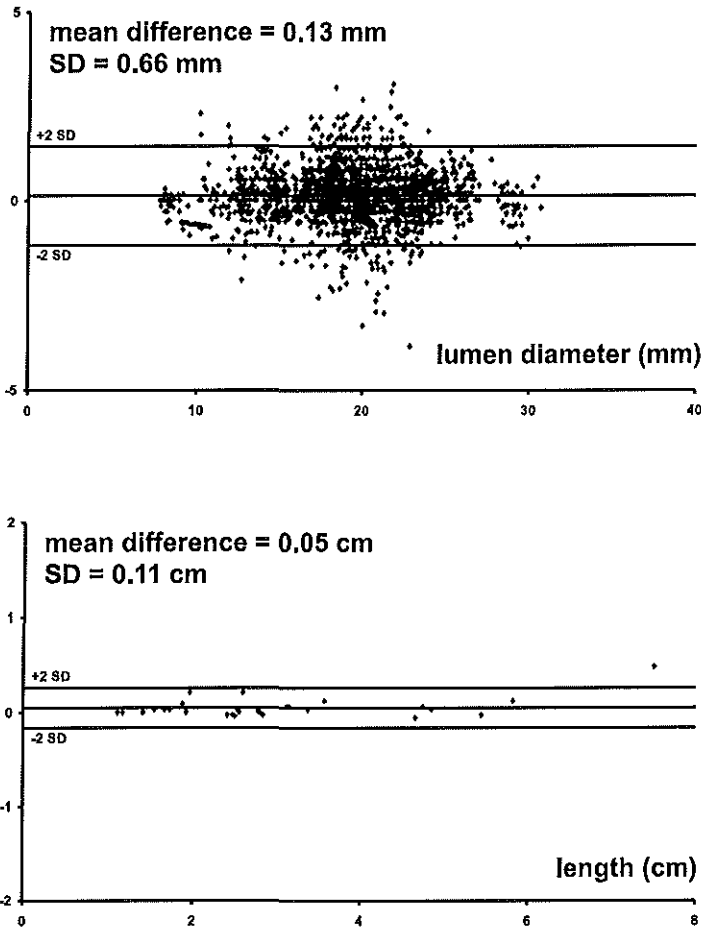


Fig. 5. Interobserver comparison for lumen diameter measurements (upper panel) and length measurements (lower panel).

was absent in two aneurysms; the distal aortic or iliac neck was absent in five aneurysms. In two aneurysms the distal aortic or iliac neck was not visualized with IVUS. In six aneurysms a change in reference scale during pull-back rendered the 3D IVUS analysis impossible, because the analysis system cannot compensate for scale adjustments.

Automated vs manual analysis:

A total of 58 IVUS cross-sections were available for comparison between the automated and manual analysis system. For lumen diameter a difference of 0.45 ± 0.42 mm ($p < 0.001$), with a correlation of 0.99 and a coefficient of variation of 2.1% was found, with automated measurements being larger than manual measurements. Comparison between automated and manual analysis for length measurements revealed a difference of 0.05 ± 0.12 cm ($p = 0.04$), with a correlation of 0.99 and a coefficient of variation of 4.1% (Fig. 4). Automated length measurements were larger than the visually assessed measurements.

Interobserver analysis.

For interobserver analysis of lumen diameter a total of 2595 cross-sections were available. Comparison between both observers showed a difference of 0.13 ± 0.66 mm ($p < 0.001$) for lumen diameter. A difference of 0.05 ± 0.11 cm ($p = 0.02$) was found for length measurements. Correlation was 0.99 for both lumen diameter and length measurements, coefficient of variation was 3.4% and 3.5% respectively (Fig. 5).

Table 1. Classification of proximal and distal aortic necks according to Balm et al.³.

Type neck	Proximal neck	Distal neck
Type I	2	0
Type II	7	1
Type III	1	3
Type IV	6	1
Type V	4	1
Total	20	6

Value of 3D IVUS imaging:

The 3D reconstructions showed the relationship between pertinent structures such as the renal arteries, the renal vein, the margins of the aneurysm and the aortic bifurcation. Furthermore, the longitudinal IVUS images improved the identification of the transition from

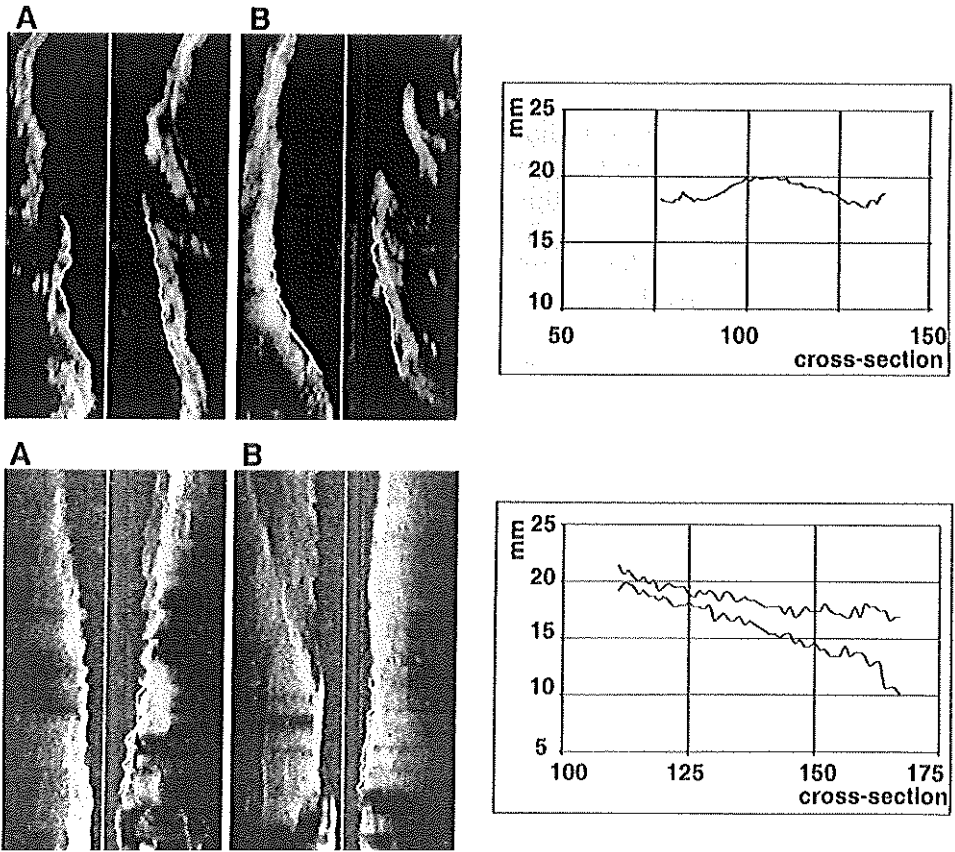


Fig. 6. Upper panel: Longitudinal IVUS images and graph containing the minimum lumen diameter of a proximal neck showing a type IV neck configuration. Lower panel: Longitudinal IVUS images and graph containing the minimum and maximum lumen diameter of a distal neck showing a type III neck configuration.

neck into aneurysm. Table 1 summarizes the shape of the aortic necks encountered, according to the classification of Balm et al.³. The majority of the proximal necks defined from the 3D analysis were of type II, IV and V, while distal necks usually presented as type III (Fig. 6). Neck of type II were found in short necks, and necks of type IV and V were found in long necks.

DISCUSSION

The introduction of endovascular stent-grafts for the treatment of AAA has highlighted the need for new peroperative imaging modalities. IVUS has become a valuable tool in clinical practice to assist in decision making during endovascular procedures. In validation studies using histology and computed tomographic angiography, we have recently shown that IVUS can accurately determine the lumen diameter and length of proximal and distal neck of AAA as well as the length of the aneurysm itself^{6,8}. In a clinical setting, others have proclaimed IVUS to be of inestimable value to determine key parameters of aortic morphology before and during intervention and for assessing the deployment after device placement^{4,7,8,14}. As yet, the assessment of minimum lumen diameter from IVUS images in the clinical setting is performed manually by visual estimation using a limited number of cross-sections. These diameters may be incorrect, particularly in the non circular cross-sectional images. Furthermore, measurements on a limited number of cross-sections may obscure the true nature of the shape of the neck. In contrast, automated contour analysis systems, designed to objectively determine lumen dimensions based on a multitude of IVUS cross-sections, uses the information from the entire cross-sectional image to acquire the minimum lumen diameter and can also provide information on the actual shape of the neck.

Assessment of length may be performed using a sterile ruler held against the catheter, an automated pull-back device, or a displacement sensing device. Using a displacement sensing device in the reconstruction of the longitudinal images we obtained additional insight in the length of the necks.

The present study showed that the overall agreement between the manual and automated analysis and between the two observers for both lumen diameter and length measurements was good, however, the differences were significant. The difference in lumen diameter between automated and manual analysis (0.45 mm) can be attributed to a simplification in lumen contour tracing applied by the automated analysis system. Similarly, the difference in length of the aortic neck between the automated and manual analysis and between the two observers was negligible (both 0.05 cm).

It is noteworthy that the agreement for lumen diameter measured with the automated analysis system between different observers in this study was high compared to the agreement between different observers found for manual analysis¹⁵. These findings underline that automated contour analysis has the potential to replace conventional manual analysis in the future. We opine that by using automated analysis in a clinical setting during endovascular surgery, multiple IVUS cross-sections assessed at once and continuous information on lumen diameter of the neck, may enable the selection of appropriately sized stent-grafts.

To date, research on the beneficial effects of 3D IVUS imaging in AAA is limited^{7,8,14}. White et al.⁷ reported that "3D IVUS images translated the cross-sectional tomographic views into easily interpreted longitudinal volumetric reconstructions". Reid et al.⁸ and White et al.¹⁴ reported that "3D IVUS, which provides better, more informative images than 2D IVUS, can be particularly useful intraprocedurally in detecting inaccurate deployment of intravascular stents and endoluminal grafts".

We experienced that 3D IVUS imaging provided an improved insight in the anatomy of the aortic neck. Shape of the AAA neck can be defined, and the location of anatomic markers, such as renal arteries and renal vein can be appreciated in relation to the aneurysm. Furthermore, the transition from neck into aneurysm was better appreciated. In longitudinal reconstructions, the position of the IVUS catheter in the vessel interrogated was better appreciated than during the pull-back maneuver. Therefore, we opine that the longitudinal reconstructions may serve as a reference guide for the tomographic IVUS images during endovascular intervention.

The significance of the shape of necks is as yet unknown. A conical shaped neck is considered by some as a contra-indication for endovascular repair. One may argue whether an optimized configuration of stent-grafts based on the shape of the individual neck may be beneficial for the healing response following endograft placement. Furthermore, it may be of interest to assess the effect of the shape of the neck on the expansion or displacement of the stent-graft attachment system.

Recently, particular concern has arisen regarding continued expansion of the proximal and distal aneurysm neck after endovascular repair^{16,17}. This expansion may be the result of ongoing degenerative changes or pressure from the stents on the attachment sites. Future studies using the automated analysis system may be aimed 1) to determine the relationship between initial diameter and shape of the proximal neck and its continued expansion after endovascular aneurysm repair and 2) to determine the behavior of endovascular grafts in different shaped necks in relation to the diameter of the stent-graft, the shape of the stent-graft inside the neck and the presence of endoleakage.

LIMITATIONS

3D IVUS imaging has 2 potential limitations: only 2D images, either cross-sectional or longitudinal, are displayed; and the images are centered along the IVUS catheter and, as such, the 3D stack does not represent the actual shape of the vessels studied. However, we feel that the analysis itself can still be regarded as 3D for the following reasons: 1) the analysis provides data in three dimensions, and 2) the longitudinal images can be rotated in the 3D stack.

CONCLUSIONS

Automated analysis of IVUS images provides accurate assessment of lumen diameter of the proximal and distal neck of AAA and gives similar length measurements compared to manual analysis. Longitudinal display of IVUS images facilitates anatomical understanding of the neck and can be used as a time-saving procedure during IVUS analysis of multiple cross-sections.

ACKNOWLEDGEMENTS

We thank Paul C. Huijsman for the interobserver analysis.

REFERENCES

1. May J, White GH, Yu W, et al. Endoluminal grafting of abdominal aortic aneurysms: causes of failure and their prevention. *J Endovasc Surg* 1994; 1: 44-52.
2. Parodi JC, Barone A, Piraino R, et al. Endovascular treatment of abdominal aortic aneurysms: lessons learned. *J Endovasc Surg* 1997; 4: 102-110.
3. Balm R, Stokking R, Kaatee R, et al. Computed tomographic angiographic imaging of abdominal aortic aneurysms: implications for transfemoral endovascular aneurysm management. *J Vasc Surg* 1997; 26: 231-237.
4. White RA, Donayre C, Kopchok G, et al. Intravascular ultrasound: the ultimate tool for abdominal aortic aneurysm assessment and endovascular graft delivery. *J Endovasc Surg* 1997; 4: 45-55.
5. Essen van JA, Lugt van der A, Gussenhoven EJ, et al. Intravascular ultrasonography allows accurate assessment of abdominal aortic aneurysm: an in vitro validation study. *J Vasc Surg* 1998; 27: 347-353.
6. Essen van JA, Gussenhoven EJ, Lugt van der A, et al. Accurate assessment of abdominal aortic aneurysm by intravascular ultrasound: validation with computed tomographic angiography. *J Vasc Surg* 1999; 29: 631-638.
7. White RA, Scoccianti M, Back M, et al. Innovations in vascular imaging: arteriography, three-dimensional CT scans, and two- and tree-dimensional intravascular ultrasound evaluation of an abdominal aortic aneurysm. *Ann Vasc Surg* 1994; 8: 285-289.
8. Reid DB, Douglas M, Dietrich EB. The clinical value of three-dimensional intravascular ultrasound imaging. *J Endovasc Surg* 1995; 2: 356-364.
9. Li W, Birgelen von C, Di Mario C, et al. Semi-automatic contour detection for volumetric quantification of intracoronary ultrasound. In: *Computers in Cardiology 1994*. Los Alamitos, CA: IEEE Comp Soc Press, 1994: 277-28.
10. Gussenhoven EJ, Lugt van der A, Strijen van M, et al. Displacement sensing device enabling accurate documentation of catheter tip position. In: Roelandt J, Gussenhoven EL, Bom N, eds. *Intravascular ultrasound*. Dordrecht: Kluwer Academic Press, 1993: 157-166.
11. Hagenaaers T, Gussenhoven EJ, Essen van JA, et al. Reproducibility of volumetric quantification in intravascular ultrasound images. *Ultrasound Med Biol* 2000; 26: 367-374.
12. Wenguang L, Gussenhoven EJ, Zhong Y, et al. Validation of quantitative analysis of intravascular ultrasound images. *Int J Card Imag* 1991; 6: 247-253.
13. Bland JM, Altman DG. Statistical methods for assessing agreement between two methods of clinical measurement. *Lancet* 1986; 1 (8476): 307-310.
14. White RA, Donayre CE, Walot I, et al. Preliminary clinical outcome and imaging criterion for endovascular prosthesis in high-risk patients who have aortoiliac and traumatic arterial lesions. *J Vasc Surg* 1996; 24: 556-571.
15. Lugt van der A, Gussenhoven EJ, Pasterkamp G, et al. Interobserver reproducibility of qualitative and quantitative analysis of intravascular ultrasound images before and after peripheral balloon angioplasty. *Ultrasound Med Biol* 1996; 22: 399-404.

16. Broeders IAMJ, Blankensteijn JD, Gvakharia A, et al. The efficacy of transfemoral endovascular aneurysm management: a study on size changes of the abdominal aorta during mid-term follow-up. *Eur J Vasc Endovasc Surg* 1997; 14: 84-90.
17. Matsumura JS, Chaikof EL. Continued expansion of aortic necks after endovascular repair of abdominal aortic aneurysms. *J Vasc Surg* 1998; 28: 422-431.

**INTRAVASCULAR ULTRASOUND TO GUIDE
ENDOVASCULAR TREATMENT OF
ABDOMINAL AORTIC ANEURYSM**

**Jeroen A. van Essen, MD^{1,8}, Elma J. Gussenhoven, MD, PhD^{1,8}
André A.E.A. de Smet, MD⁴, Jan D. Blankensteijn, MD, PhD⁵,
Alexander V. Tielbeek, MD, PhD⁶, Steven E. Kranendonk, MD, PhD⁷,
Lukas C. van Dijk, MD, PhD², Hero van Urk, MD, PhD³.**

From University Hospital Rotterdam-Dijkzigt and Erasmus University
Rotterdam departments of Cardiology¹, Radiology² and Vascular Surgery³,
St Clara Ziekenhuis Rotterdam department of Surgery⁴,
University Medical Center Utrecht department of Surgery⁵,
St Catharina Ziekenhuis Eindhoven department of Radiology⁶,
Twee Steden Ziekenhuis Tilburg department of Surgery⁷ and the
Interuniversity Cardiology Institute⁸, the Netherlands

Supported by a grant from the Interuniversity Cardiology Institute,
the Netherlands

Submitted

ABSTRACT

Purpose:

To evaluate the feasibility of intravascular ultrasound (IVUS) to guide endovascular treatment of abdominal aortic aneurysm (AAA).

Material and methods:

Patients (n=29) with AAA were treated with an endovascular graft using an AneuRx (n=13), an Ancure (n=11), an Excluder (n=3), a Talent (n=1) or a Vanguard (n=1) stent-graft. **Before placement**, IVUS was used to determine the location of the renal arteries and aortic bifurcation, the lumen diameter of proximal and distal fixation sites, and the length of the aneurysm. Based on these data the definitive size of the modular components of the AneuRx stent-graft was selected. **After placement**, IVUS was used to determine proximal and distal apposition of the stent-graft, and to rule out obstruction and/or occlusion of renal arteries, stenosis of the stent-graft, and potential damage to the iliac arteries due to the procedure.

Results:

IVUS images were available before (n=28) and after (n=26) intervention. Based on the data obtained with IVUS **before placement**, the proximal neck was deemed too wide for endovascular treatment in one patient and the definitive dimensions of the AneuRx stent-graft components were selected (n=12). In addition, IVUS influenced the definitive length of the Ancure stent-graft (n=1), altered the planned side of introduction (n=1), warranted predilatation of the common iliac artery (n=1) and detected an accessory renal artery (n=1). **After intervention**, IVUS revealed incomplete apposition at the proximal part of the stent-graft (n=1) and folding at the distal part of the stent-graft (n=1), for which no additional interventions were performed. Furthermore, IVUS revealed the iliac leg of the stent-graft to end in the aneurysm (n=1) and incomplete covering of the iliac part of the stent-graft (n=3), all of which were treated with appropriate extension cuffs. The bare part of the proximal attachment system was seen to be placed over a renal artery (n=1) and accessory renal arteries were seen to be intentionally covered (n=3). Stenosis in the iliac leg of the graft (n=5) detected with IVUS was treated with an additional balloon dilatation. Iliac artery dissection seen with IVUS after stent-graft placement (n=5) required no additional intervention. In one patient continuation of the dissection extending beyond the distal attachment system was missed on IVUS.

Conclusions:

Definitive dimensions required for modular endovascular prosthesis components can be determined adequately with IVUS. After placement, IVUS detects features that may negatively influence the outcome of the procedure and, therefore, allow additional interventions to handle these conditions, to be performed during the same session.

INTRODUCTION

The feasibility and short-term efficacy of endovascular treatment of abdominal aortic aneurysms (AAA) has been demonstrated¹⁻⁴. This type of endovascular intervention depends on accurate and detailed visualization of the anatomy of the abdominal aorta, before, during and after intervention⁵⁻⁸. Current imaging techniques, such as angiography and computed tomographic angiography (CTA), are widely used in the assessment of AAA before intervention. However, during endovascular intervention, angiography and fluoroscopy are the sole techniques to guide the placement of stent-grafts. Angiographic measurements may be hampered by thrombus, parallax and foreshortening of vascular structures, thus hampering the accurate placement of stent-grafts⁹. Intravascular ultrasound (IVUS) is proven to be a powerful imaging modality that provides information on lesion characteristics and vessel dimensions of coronary, peripheral and central arteries, and allows to assess the effect of endovascular interventions¹⁰⁻¹⁴. The aim of the present study was to assess the potential role of IVUS immediately before and after placement of an endovascular graft for AAA.

MATERIAL AND METHODS

Patients.

Between June 1997 and June 1999, 29 patients (27 males, age range 53-84 years, mean age 68.9 years) with AAA, eligible for open surgery were included in this multi-center study. Procedures were performed at the five centers, with one center supplying the IVUS system, personnel and analysis of IVUS data. At two centers, consecutive patients were studied with IVUS according to protocol, in three other centers patients were included based on availability of the IVUS system. All patients were considered suitable candidates for endovascular repair based on angiography and contrast enhanced computed tomography (CT) without 3-D reconstructions, or CTA combined with 3-D reconstructions^{8,15}. Patients were given detailed information on the risks of the procedure by their consulting specialists and have given written consent.

Stent-grafts.

Five types of stent-grafts were used, according to the individual hospital preference; i.e. the AneuRx stent-graft (Medtronic, Sunnyvale, CA, USA; n=13), the Ancure stent-graft (EndoVascular Technologies/Guidant, Menlo Park, CA, USA; n=11), the Excluder Endovascular Prosthesis (W.L. Gore & Associates, Inc. Sunny Vale, CA, USA; n=3), the Talent Endovascular Graft (World Medical Manufacturing Corp, Sunrise, FL, USA; n=1), and the Vanguard stent-graft (Boston Scientific Corp, Oakland, NJ, USA; n=1). Procedures were performed in the operating theater, under general

anesthesia (n=28) or local anesthesia (n=1). Detailed description of the AneuRx, Ancure, Talent and Vanguard stent-grafts have been published previously^{3,16-18}. The Excluder stent-graft is a self-expanding ePTFE coated graft with an external nitinol stent-structure along the entire length of the graft, with nitinol anchors and an ePTFE sleeve at the proximal end. The device consists of an 18F trunk-ipsilateral component and a 12F contralateral leg component that are assembled in situ. The device can be fitted with extender cuffs at both the proximal and distal side.

Intravascular ultrasound.

The IVUS systems used for the study were a mechanical (12.5 MHz, Boston Scientific Corp, Watertown, MA, USA) or a phased array system (10 MHz, Endosonics Corp, Rancho Cordova, CA, USA).

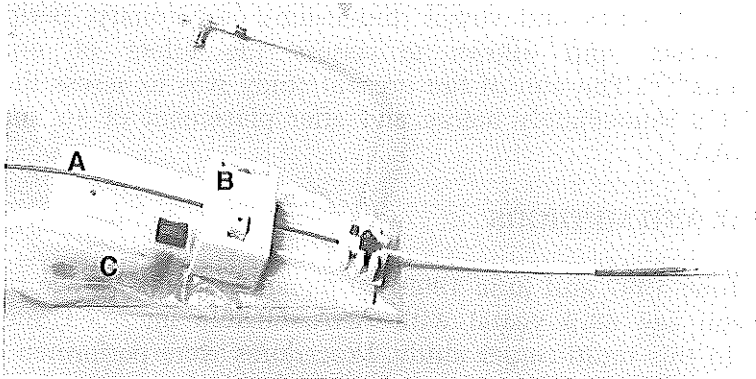


Fig.1. Displacement sensing device showing the ultrasound catheter (A) advanced via the sensing unit (B) into the sheath. C represents the registration unit which is packed in a plastic sterile bag.

After introduction of a guide-wire and baseline angiography, IVUS was used to determine the location of the renal arteries, the aortic bifurcation and the iliac bifurcation, and the diameter and length of the proximal and distal fixation sites as well as the length of the aneurysm. In case of the AneuRx stent-graft, these measurements were used to select the definitive dimensions of the modular components of the stent-graft. In case of the Ancure, Excluder, Talent and Vanguard stent-graft, the measurements were used to confirm the pre-operative measurements. After intervention, IVUS was used to determine the apposition at the proximal and distal edges of the stent-graft. Furthermore, IVUS was used to rule out occlusion of renal and/or accessory renal arteries, occlusion of the internal iliac arteries, stenosis in the iliac limbs of the stent-graft and damage to the iliac arteries as a result of

introduction of the device. If deemed necessary, additional interventions were performed during the same session and the effect of these interventions was, in turn, assessed with IVUS.

Lumen diameter measurements were performed on-line using the IVUS system software. Care was taken to select IVUS images during the systolic part of the cardiac cycle. Because non-coaxial positioning of the IVUS catheter may overestimate the lumen diameter, the smallest lumen diameter at any given level was taken to represent the actual diameter of the aorta and iliac arteries¹³.

Length measurements were performed using a displacement sensing device¹⁹ [Fig.1]. This device consists of a small sterile disposable sensing unit. Movement of the catheter activates a rotating wheel that converts the linear movement into an electronic pulse train signal. Advancement or withdrawal of the catheter is digitized and wirelessly registered by a sterilizable unit to which the sensing unit is mounted. The display of the displacement of the IVUS catheter tip in steps of 0.01 cm is mixed together with the ultrasound information on the videoscreen.

RESULTS

Intravascular studies were completed successfully before (n=28) and after (n=26) stent-graft placement. Failure of the IVUS system occurred in one patient. After intervention failure of the IVUS catheter occurred in another patient. In one patient the procedure was converted to open surgery. The essential and non-essential findings evidenced with IVUS and the modifications involved prior to and immediately following endovascular intervention are summarized in Table 1.

Before intervention.

Based on IVUS, the procedure was converted to open surgery because of a too large proximal aortic neck (diameter > 26 mm), exceeding the maximum diameter of the AneuRx stent-graft (maximum stent-graft diameter = 28 mm, recommended oversizing = 2 mm) (n=1) [Fig. 2], the size of modular components of the AneuRx stent-graft was chosen (n=12), as was the definitive length of an Ancure stent-graft (n=1). The side of introduction was modified (n=1) as IVUS revealed a calcified stenosis in the common iliac artery likely to complicate introduction of the Ancure stent-graft. For subtotal occlusion of a common iliac artery (n=1) predilatation was performed. The detection of an accessory renal artery missed on preoperative assessment was classified as a non-essential IVUS finding.

Table 1. Intravascular ultrasound findings and the modifications in management involved immediately before and after placement of endovascular stent-grafts for abdominal aortic aneurysm (AAA).

	Essential features		Non-essential features
	Finding	Action	Finding
Before intervention (n = 28)	Proximal aortic neck diameter > 26 mm (n=1) [Fig. 2]	Conversion to open surgery	Detection of accessory renal artery (n=1)
	Diameter/length of proximal and distal neck and AAA (n =12)	Selection of modular stent-graft components	
	Length of proximal and distal neck and AAA (n=1)	Selection of length of Ancure stent-graft	
	Calcified common iliac artery stenosis (n=1)	Modification of introduction side of Ancure stent-graft	
	Subtotal occlusion of common iliac artery (n=1)	Predilatation	
After intervention (n = 26)	Inadequate distal apposition (n=4)	Extension cuffs	Improper proximal apposition (n=1) [Fig. 7]
	Folding of distal part of Ancure tube graft (n=1) [Fig.3]	None	Iliac artery dissection (n=5)
	Stenosis and folding of iliac limb of stent-graft (n=5) [Fig. 4, 5]	Balloon angioplasty	Accessory renal artery occlusion (n = 3)
	Partial covering of renal artery (n=1) [Fig. 6]	None	

n = number of patients

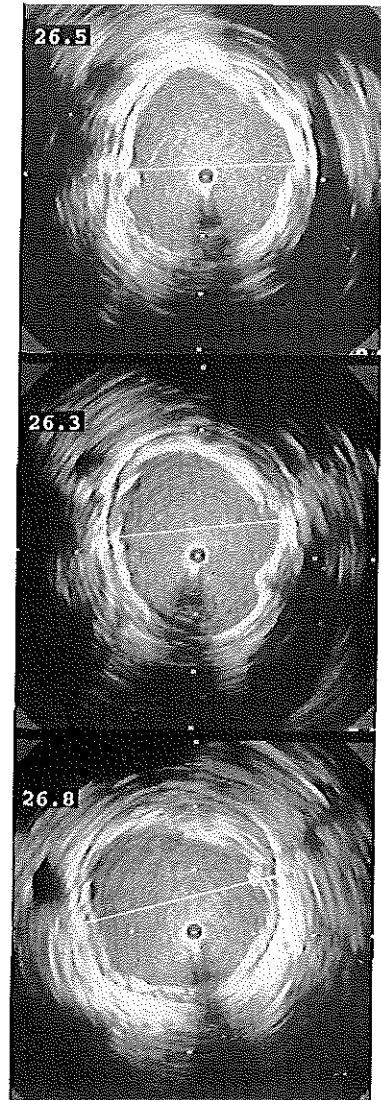
After intervention.

IVUS revealed inadequate distal apposition of the stent-graft (n=4): the stent-graft ended in the iliac part of the aneurysm (n=1) or the covering of the iliac leg was deemed too short (< 3 cm). These four patients were successfully treated with additional extension cuffs. For folding of a distal part of an Ancure tube stent-graft seen with IVUS in one patient, no additional intervention was performed [Fig. 3].

Stenosis with folding of abundant graft material in the iliac limb of the stent-graft (n=5) was treated with an additional balloon angioplasty [Fig. 4].

In one of these patients, treated with a aorto-uni-iliac stent-graft, IVUS showed stenosis and folding of the stent-graft, due to twisting of the stent-graft during the procedure. After additional balloon angioplasty, IVUS showed the stenosis and folding to be diminished [Fig. 5]. Within hours following the intervention, this patient developed thrombosis of the stent-graft and after a failed thrombectomy the stent-graft was subsequently explanted. In one patient IVUS detected a renal artery to be partially covered by a stent-strut of an Ancure stent-graft. On the intraoperative angiogram, no diminished filling of the renal artery was seen [Fig. 6], and no additional action was undertaken. For inadequate apposition of the proximal part of an Excluder stent-graft seen with IVUS (n=1), no additional intervention was performed [Fig. 7]. Similarly, for damage to the iliac arteries as a result of the intervention (e.g. dissection) detected with IVUS (n=5) no additional intervention was deemed necessary. In one of these patients the dissection continued beyond the distal attachment system, but this detail was missed by IVUS probably due to the presence of calcification; this patient developed an endoleak. Finally, in three patients accessory renal arteries seen before intervention with IVUS were deliberately sacrificed to warrant adequate apposition.

Fig.2. Intravascular ultrasound cross-sections showing the vessel diameter of the proximal neck of an abdominal aortic aneurysm obtained 0.5 cm, 1.0 cm and 1.5 cm distally from the renal arteries. As the diameter (> 26 mm) was considered too wide to be treated with an AneuRx stent-graft the procedure was converted to open surgery. Calibration = 5 mm.



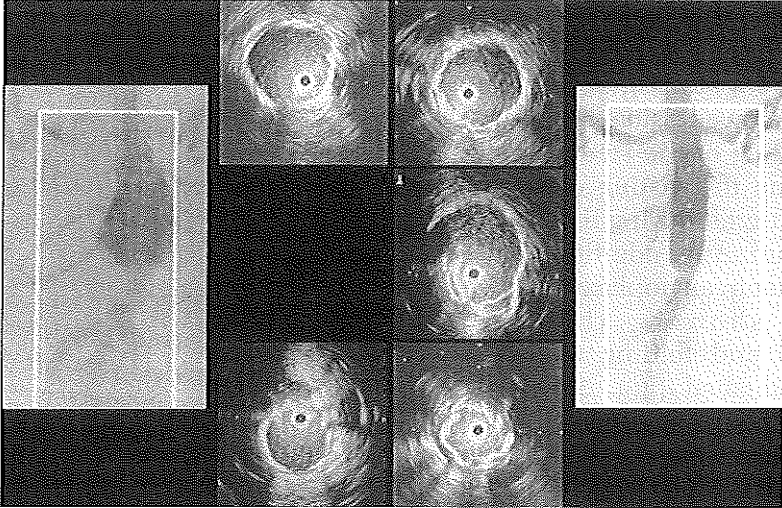


Fig.3. Intravascular ultrasound (IVUS) cross-sections from the proximal and distal neck before (left panel) and after placement (right panel) of an Ancure endovascular tube graft. Before intervention the diameter of the proximal neck was 18 mm and of the distal neck was 15 mm. Corresponding IVUS images obtained after implantation, showed good apposition at the proximal neck and folding of the stent-graft at the level of the distal neck. The inserts show the preoperative (left) and postoperative angiogram (right) showing the outline of the endovascular graft and tapering at the distal end. Calibration = 5 mm.

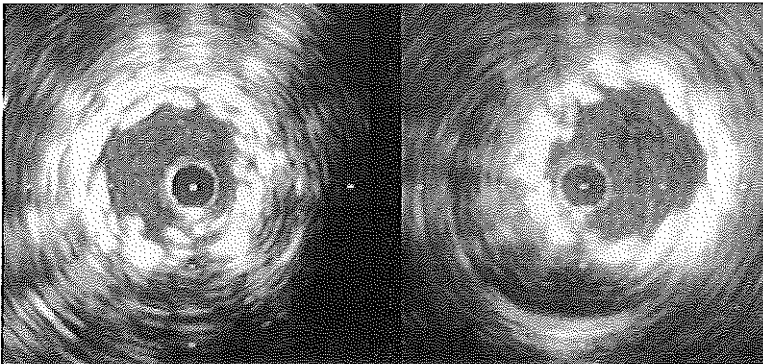


Fig.4. Corresponding intravascular ultrasound cross-sections obtained in the iliac part of an AneuRx stent-graft showing stenosis and folding. After additional balloon angioplasty mean lumen diameter increased from 6.5 to 8.5 mm and the folding diminished. Calibration = 5 mm.

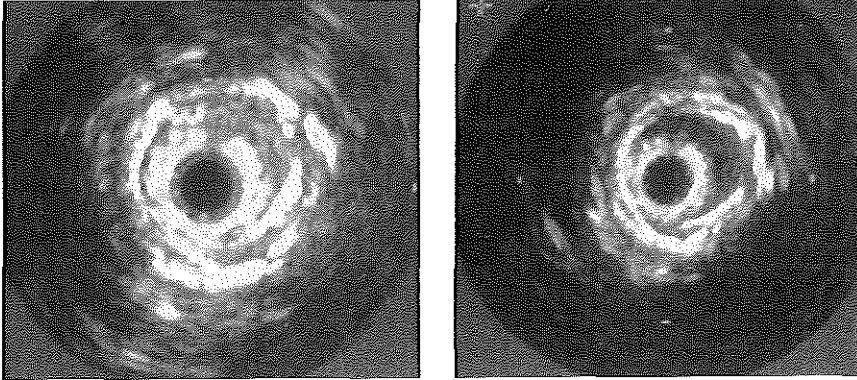


Fig.5. Corresponding intravascular ultrasound cross-sections from the iliac limb of an Ancure aorto-uni-iliac stent-graft showing stenosis and folding of abundant graft material. Although some folding remained, the result was considered satisfactory. The patient developed graft thrombosis a few hours after the intervention; re-intervention failed and the prosthesis was explanted. Calibration = 5 mm.

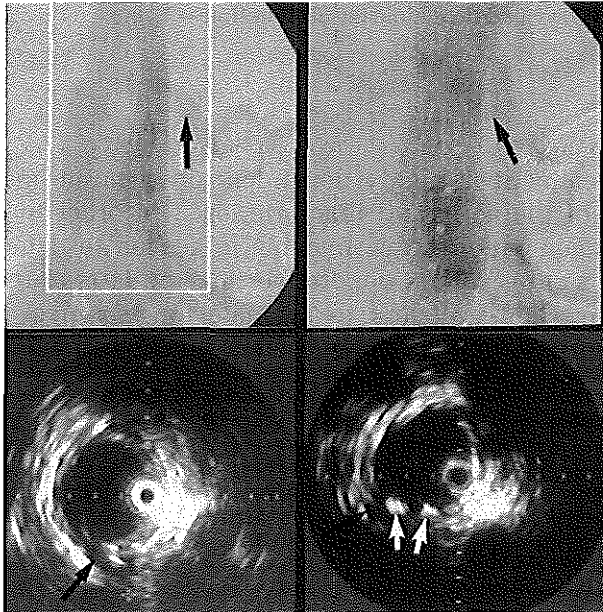


Fig.6. Intraoperative angiograms and intravascular ultrasound cross-sections from a renal artery obtained before and after placement of an Ancure stent-graft. On ultrasound the renal artery orifice (black arrow) is seen covered by bare stent-struts (white arrows). The angiogram revealed no diminished filling. Calibration = 5 mm.

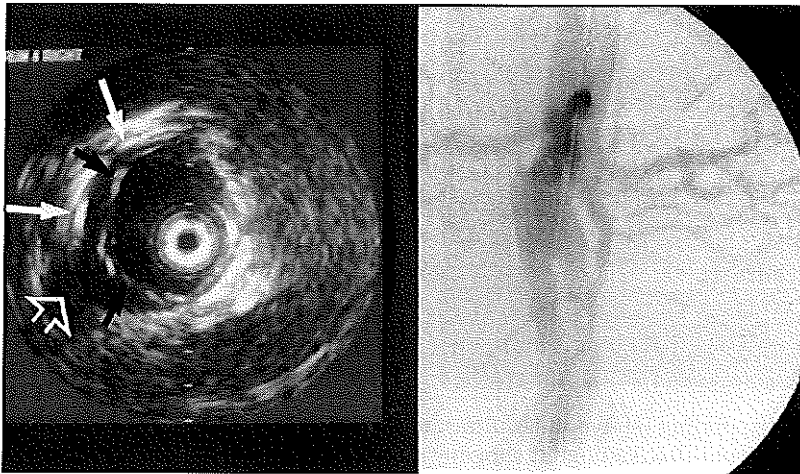


Fig.7. Intravascular ultrasound cross-section obtained after intervention showing a small gap between the aortic wall (white arrows) and the proximal border of the Excluder stent-graft (black arrows). The right renal artery is seen at 8 'o clock (open arrow). The angiogram revealed no endoleaks. Calibration = 5 mm.

DISCUSSION

Endovascular treatment is highly dependent on accurate measurements of the dimensions of the aorta and iliac arteries⁵⁻⁸. In order to safely perform endovascular repair, *preoperative* imaging is needed to determine the type and size of the stent-graft, *intraoperative* imaging is required to guide the placement of the stent-graft and to evaluate the technical success of the intervention, and *postoperative* imaging is needed to assess the short-, mid- and long-term effect (behavior, complications, dislodgement , etcetera) of the intervention.

Nowadays, several imaging techniques are available to assist in device sizing, decision making and follow-up of endovascular treatment. For *preoperative* imaging, calibrated angiography, CTA and 3-D reconstructed CTA are used to determine the feasibility of the individual patient for endovascular repair and to size the stent-graft^{7,8,15}. For *follow-up*, CTA has universally been determined as the imaging mode of choice^{2,20}. However, during the intervention itself, physicians have to rely on angiography to identify renal arteries, aortic and iliac bifurcation, and to determine the technical success of endovascular graft placement. From studies involving angiography we have learned that this technique has limitations with regard to assessment of AAA dimensions and to evaluate the success of

endovascular interventions^{15,21,22}. To provide instantaneous visualization intraoperatively, immediately before and after endovascular treatment of AAA, the use of IVUS has been promoted by several groups²³⁻²⁶.

White et al.²³ used IVUS to determine morphologic features of vascular structures, and to assure firm fixation of balloon-expanded stents. Lyon et al.²⁴ reported that after endovascular treatment, IVUS was more sensitive than angiography in detecting major arterial and graft lesions, which could result in graft thrombosis or technical failure, if not corrected. Vogt et al.²⁵ found that IVUS provided decisive information before and after stented graft deployment. In addition, Zajko et al.²⁶ reported that after deployment of an Ancure stent-graft, iliac limb stenosis or compression occurred in 41% of the patients. Most stenoses were caused by compression of the unsupported part of the stent-graft at the native aortic bifurcation or graft folding due to excess fabric in a small iliac artery. Such stenoses were easily and safely corrected with Wallstent placement. Since the authors used IVUS immediately after deployment, this problem was recognized and could be treated without delay by stent placement. At follow-up (1-27 months) all Wallstents reinforced Ancure stent-grafts remained patent²⁶.

After having established that IVUS is an accurate technique to document the anatomy of AAA^{12,13}, we conducted the present clinical feasibility study. It was shown that IVUS may provide essential and non-essential information both prior to and immediately after endovascular AAA treatment.

Despite preoperative assessment using either contrast enhanced CT without 3-D reconstructions and calibrated angiography, or CTA combined with 3-D reconstructions, IVUS revealed additional information prior to endovascular stent-grafting. As intraoperative IVUS assessment of the proximal aortic neck revealed a too large diameter in one patient, it was decided to convert the procedure to open surgery. In 12 other patients IVUS was used to determine the definitive dimensions of the AneuRx stent-graft as recommended by the manufacturer. In addition, using the displacement sensing device we were able to assess the length of the aortic neck, the aneurysm, and the iliac arteries. In one patient this information was used to select the definitive size of an Ancure stent-graft required. The identification of a circular calcified stenosis in the common iliac artery (diameter < 7 mm) seen on IVUS in one patient, warranted the use of the contralateral iliac artery for introduction of the stent-graft; although the stenosis was seen on the preoperative CTA, the extent of the calcification was unclear from that examination. Finally, for subtotal occlusion detected with IVUS in the iliac artery, predilatation was considered necessary in another patient.

Intraoperative use of IVUS in the present study immediately after stent-graft placement is unique and its additional value can only be compared with angiography obtained during the intervention. In four patients IVUS

detected inadequate distal apposition of the stent-graft. Although intraoperative IVUS measurements revealed that the length of the device would be insufficient, in all four patients the longest available type AneuRx stent-graft had already been selected. Consequently, based on these IVUS measurements extension cuffs were successfully implanted. In one patient with folding of the Ancure tube graft, a stent-graft with a diameter of 22 mm was used based on the preoperative CTA. Intraoperative IVUS showed that the diameter of the proximal neck was 18 mm and that of the distal neck 15 mm. It should be emphasized that this latter case was our first experience using intraoperative IVUS; as a result of our limited experience regrettably no additional intervention (i.e. balloon angioplasty) was performed. The patient developed an endoleak both at the proximal and distal attachment system; after six months the prosthesis was explanted because of continuous growth of the aneurysm. We now believe that such a patient could better be treated with a bifurcated graft.

IVUS evidenced a stenosis and folding in the iliac limb of the stent-graft in five patients. Three of these patients had an AneuRx stent-graft in whom after additional dilatation, lumen diameter increased and folding diminished. In the two other patients the stenosis and folding was found in the iliac limb of an Ancure stent-graft (one bifurcated, one aorto-uni-iliac); both stenoses were dilated with appropriately sized balloons. In one of these patients, the stenosis was the result of torsion of the stent-graft during introduction. This patient developed thrombosis of the aorto-uni-iliac stent-graft a few hours after the intervention. Thrombectomy was unsuccessful and the stent-graft was explanted. In retrospect, our opinion is that, although IVUS showed a good result after dilatation, this problem might have better been treated by a Wallstent as proposed by Zajko et al.²⁶.

In one patient, IVUS evidenced a renal artery overstented by the bare part of the struts of an Ancure stent-graft. The intraoperative angiogram showed undiminished filling of the renal artery. Postoperative CT scanning showed no renal infarction. In a preliminary study, Marin et al.²⁷, has shown no adverse effects of overstented renal orifices. Nowadays, stent-grafts are available that have intentionally bare and long stent-struts in order to acquire better fixation of the stent-graft in case of a short (12-15 mm) proximal neck.

Inadequate apposition at the proximal part of the stent-graft was recognized on IVUS in one patient as a small gap between the stent-graft and the aortic wall. The gap was the result of the angle between the proximal neck and the aneurysm.

No additional intervention was deemed necessary because:

- 1) the gap was considered too small to cause an endoleak
- 2) the ePTFE sleeve positioned at the proximal attachment system, might provide appropriate sealing at a more distal point in the proximal neck.

As yet, follow-up CTA has shown no endoleak along the proximal attachment.

Similarly, for a dissection of the iliac artery seen in five patients no additional intervention was performed. However, in one patient the dissection continued beyond the distal attachment system. This feature was missed on IVUS primarily due to extensive calcification at the level of the dissection. Follow-up CT scanning revealed an endoleak. This patient is now scheduled for placement of a Wallstent.

In three patients, accessory renal arteries were occluded intentionally to acquire sufficient sealing in a proximal neck that would otherwise have been too short.

Although CTA measurements combined with 3D reconstructions for AAA may provide sufficient detail to determine the length and diameter of endovascular stent-grafts, some hospitals may not have the hardware (e.g. workstation with capacity of central lumen line reconstruction) or the manpower to perform these time-consuming reconstructions. The introduction of modular devices may diminish the need for such precise measurements of AAA. On the basis of calibrated angiography and axial CT scans, appropriate patients can be selected for endovascular treatment.

The present study has shown that the additional value of IVUS immediately before stent-graft placement is beyond dispute: IVUS used during the procedure allows decision on the definitive dimensions of the endovascular graft components. In two centers IVUS was used during the start-up phase of endovascular treatment of AAA. The interventionalists experienced that the use of IVUS immediately before and after endovascular treatment, presents a unique opportunity to gain insight into the mechanism of the intervention, guide their actions during the procedure and appreciate the outcome.

Based on data from the present study, no answer can be given on the precise additional role of IVUS after intervention over angiography. Both IVUS and angiography were used for decision making during the procedure. To establish what conditions, possibly influencing the outcome of the intervention, IVUS may detect that are missed on angiography, a prospective comparative study is required in which IVUS findings after intervention are blinded to the operators who score of the postoperative angiograms. Based on angiography the outcome of the intervention can be assessed, which may either be affirmed or rejected by intraoperative IVUS. Such a study may also

reveal whether intraoperative IVUS is a cost-effective imaging tool to guide endovascular AAA repair.

CONCLUSIONS

This study showed that intraoperative IVUS used as a means of control of preoperative measurements immediately before endovascular stent-graft placement can optimize the intervention in the individual patient. Furthermore, IVUS measurements may definitively determine the dimensions of modular prosthesis components from a predefined range of components based on preoperative CT and angiography. Immediately after intervention, IVUS detects imperfections that may negatively influence the outcome of the procedure and thus allows additional interventions to be performed during the same session that may positively influence the outcome.

ACKNOWLEDGEMENTS

We thank Jan Honkoop for technical assistance.

REFERENCES

1. Parodi JC. Endovascular repair of abdominal aortic aneurysms and other arterial lesions. *J Vasc Surg* 1995; 21: 549-557.
2. Balm R, Eikelboom BC, May J, Swedenborg J, Collin J. Early experience with transfemoral endovascular aneurysm management (TEAM) in the treatment of abdominal aortic aneurysms. *Eur J Vasc Endovasc Surg* 1996; 11: 214-220.
3. Blum U, Langer M, Spillner G, Mialhe C, Beyersdorf F, Buitrago-Tellez C, et al. Abdominal aortic aneurysms: preliminary technical and clinical results with transfemoral placement of endovascular self-expanding stent-grafts. *Radiology* 1996; 198: 25-31.
4. May J, White GH, Yu W, Ly CN, Waugh R, Stephen MS, et al. Concurrent comparison of endoluminal versus open repair in the treatment of abdominal aortic aneurysms: analysis of 303 patients by life table method. *J Vasc Surg* 1998; 27: 213-221.
5. Beebe HG. Imaging modalities for aortic stent-grafting. *J Endovasc Surg* 1997; 4: 111-123.
6. Parodi JC, Barone A, Piriano R, Schonholz C. Endovascular treatment of abdominal aortic aneurysms: lessons learned. *J Endovasc Surg* 1997; 4: 102-110.
7. Schumacher H, Eckstein HH, Kallinowski F, Allenberg JR. Morphometry and classification in abdominal aortic aneurysms: patient selection for endovascular and open surgery. *J Endovasc Surg* 1997; 4: 39-44.
8. Dorros G, Parodi J, Schonholz C, Jaff M, Dietrich EB, White G, et al. Evaluation of endovascular abdominal aortic aneurysm repair: anatomical classification, procedural success, clinical assessment, and data collection. *J Endovasc Surg* 1997; 4: 203-225.
9. Beebe HG, Jackson T, Pigott JP. Aortic aneurysm morphology for planning endovascular aortic grafts: limitations of conventional imaging methods. *J Endovasc Surg* 1995; 2: 139-148.
10. Lugt van der A, Gussenhoven EJ, Stijnen T, Li W, Strijen van M, Driel van E, et al. Comparison of intravascular ultrasound findings after coronary balloon angioplasty evaluated in vitro with histology. *Am J Cardiol* 1995; 76: 661-666.
11. Gussenhoven EJ, Lugt van der A, Pasterkamp G, Berg van den FG, Sie LH, Vischjager M, et al. Intravascular ultrasound predictors of outcome after peripheral balloon angioplasty. *Eur J Vasc Endovasc Surg* 1995; 10: 279-288.
12. Essen van JA, Lugt van der A, Gussenhoven EJ, Leertouwer TC, Zondervan P, Sambeek van MRHM. Intravascular ultrasound allows accurate assessment of abdominal aortic aneurysm: an in vitro validation study. *J Vasc Surg* 1998; 27: 347-353.
13. Essen van JA, Gussenhoven EJ, Lugt van der A, Huijsman PC, Muiswinkel van JM, Sambeek van MRHM, et al. Accurate assessment of abdominal aortic aneurysm with intravascular ultrasound: validation with computed tomographic angiography. *J Vasc Surg* 1999; 29: 631-638.
14. Sambeek van MRHM, Gussenhoven EJ, Overhagen van H, Honkoop J, Lugt van der A, Bois du NA, et al. Intravascular ultrasound in endovascular stent-grafts for peripheral aneurysm: a clinical study. *J Endovasc Surg* 1998; 5: 106-112.

15. Broeders IAMJ, Blankensteijn JD, Olree M, Mali WPTHM, Eikelboom BC. Preoperative sizing of grafts for transfemoral endovascular aneurysm management; a prospective comparative study of spiral CT angiography, arterial angiography and conventional CT imaging. *J Endovasc Surg* 1997; 4: 252-261.
16. Zarins CK, White RA, Schwarten D, Kinney E, Dietrich EB, Hodgson KJ, et al. AneuRx stent graft versus open surgical repair of abdominal aortic aneurysms: multicenter prospective clinical trial. *J Vasc Surg* 1999; 29: 292-308.
17. Moore WS, Vescera CL. Repair of abdominal aortic aneurysm by transfemoral endovascular graft placement. *Ann Surg* 1994; 220: 331-341.
18. Uflacker R, Robison JG, Brothers TE, Pereira AH, Sanvitto PC. Abdominal aortic aneurysm treatment: preliminary results with the Talent Stent-Graft system. *JVIR* 1998; 9: 51-60.
19. Hagenshaars T, Gussenhoven EJ, Essen van JA, Seelen J, Honkoop J, Lugt van der A. Reproducibility of volumetric quantification in intravascular ultrasound images. *Ultrasound Med Biol* 2000; 26: 367-374.
20. Broeders IAMJ, Blankensteijn JD, Gvakharia A, May J, Bell PRF, Swedenborg J, et al. The efficacy of transfemoral endovascular aneurysm management: a study on size changes of the abdominal aorta at mid-term follow-up. *Eur J Vasc Endovasc Surg* 1997; 14: 84-90.
21. Quiñones-Baldrich WJ, Deaton DH, Mitchell S, Berry G, Piplani A, Quiachon D, et al. Preliminary experience with the Endovascular Technologies bifurcated endovascular aortic prosthesis in a calf model. *J Vasc Surg* 1995; 22: 370-381.
22. White RA, Verbin C, Kopchok G, Scocciati M, Virgilio de C, Donayre C. The role of cinefluoroscopy and intravascular ultrasonography in evaluating the deployment of experimental endovascular prosthesis. *J Vasc Surg* 1995; 21: 365-374.
23. White RA, Donayre CE, Walot I, Kopchok GE, Wilson EP, Buwalda R, et al. Preliminary clinical outcome and imaging criterion for endovascular prosthesis development in high-risk patients who have aortoiliac and traumatic arterial lesions. *J Vasc Surg* 1996; 24: 556-571.
24. Lyon RT, Veith FJ, Berdejo GL, Okhi T, Sanchez LA, Wain RA, et al. Utility of intravascular ultrasound for assessment of endovascular procedures. Joint Annual Meeting for the Society for Vascular Surgery and North American Chapter, International Society for Cardiovascular Surgery; 1997: 43.
25. Vogt KC, Brunkwall J, Malina M, Ivancev K, Lindblad B, Risberg B, et al. The use of intravascular ultrasound as control procedure for the deployment of endovascular stented grafts. *Eur J Vasc Endovasc Surg* 1997; 13: 592-596.
26. Zajko AB, Amesur NB, Orons PD, Makaroun M. Wallstent placement and/or thrombolysis for treatment of complicated endovascular aortic stent grafts: experience in 24 patient (abstract). *CVIR* 1999 (suppl 2); 22: S103-119.
27. Marin ML, Parsons RE, Hollier LH, Mitty HA, Ahn J, Parsons RE, et al. Impact of transrenal aortic stent-graft placement on endovascular graft repair of abdominal aortic aneurysms. *J Vasc Surg* 1998; 28: 638-646.

**ENDOVASCULAR REPAIR OF
ABDOMINAL AORTIC ANEURYSMS:
The role of intravascular ultrasound**

INTRODUCTION

In 1991 a new treatment for abdominal aortic aneurysm (AAA), using a combination of stents and grafts, was introduced^{1,2}. This endovascular approach intended to provide a less invasive way for treatment of AAA. It was expected that patients with serious co-morbidity, and thus at increased risk of fatal complications during open surgery, could be treated using endovascular techniques, thereby decreasing preoperative and postoperative morbidity and mortality. During the ensuing decade endovascular treatment of AAA was further developed and improved. Homemade stent-graft combinations were replaced by a number of commercial devices. Stent-grafts have become less rigid and requiring smaller introducer systems, easing the use of these devices. To date, the EUROSTAR database, a registry center for collection of data on endovascular treatment of AAA in Europe, registered over 2,400 stent-graft implantations³. The use of stent-grafts for the treatment of AAA has given rise to new problems and challenges which, in response, has generated a lot of research projects and clinical studies.

TECHNICAL SUCCESS OF ENDOVASCULAR REPAIR AND PROCEDURE-RELATED PROBLEMS

The SVS/ISCVS reporting standards⁴ define technical success of endovascular treatment as "*the proper placement of the graft using endovascular techniques [...] with successful access to the arterial system via a remote site; successful deployment of the endoluminal graft without persistent perigraft leakage ≥ 48 hours; and a patent endoluminal graft without significant twists, kinks or obstruction*". Recent reports on endovascular treatment of AAA have shown that technical success, as defined in the SVS/ISCVS reporting standards, ranges from 48-88%⁵⁻¹⁴. Using these criteria the success of the intervention seems relatively low. However, in practice the introduction of the device was successful in 85-100% of the patients. Perigraft leakage, or endoleak, significantly diminished the success rate. Conversion to open repair occurred in up to 0-10% of the cases⁵⁻¹⁴. Reasons for conversion were rupture of either the aortic neck or the iliac artery, access problems due to stenosis and angulation of the iliac artery, inability to deploy the stent-graft, stent-graft misplacement, or migration and thrombosis of the graft. Other problems encountered intraoperatively, but not leading to conversion, included nonalignment of proximal and distal stents, renal artery overstenting or occlusion, accessory renal artery occlusion, damage to iliac and femoral arteries, and embolization. The findings of different studies on success of introduction, technical success, conversion rate, and complications are summarized in Table 1.

Discussion

Table 1. Summary of the results of studies on endovascular treatment of AAA.

Author	Successful introduction	Technical success	Primary conversions	Intraoperative complications
Balm ⁵ (n=31)	100%	77%	0%	• Nonalignment of proximal attachment system (n=1)
Becquemin ¹³ (n=75)	100%	69%	0%	• Renal artery overstenting (n=5) • Microembolization (n=2) • Occlusion of internal iliac artery (n=1)
Blum ⁶ (n=154)	98%	86%	2%	• Macroembolization (n=3) • Femoral artery damage at access site (n=2) • Rupture of external iliac artery (n=1)
May ⁷ (n=121)	88%	83%	12%	• Femoral artery damage (n=4) • Iliac artery damage (n=5) • Graft stenosis (n=2) • Common iliac artery occlusion (n=4) • Renal artery covering (n=2)
Moore ⁸ (n=46)	85%	48%	13%	• Iliofemoral artery damage (n=8) • Thromboembolism (n=2)
Parodi ⁹ (n=109)	96%	81%	4%	• Malpositioning stent-graft (n=3) • Migration stent-graft (n=1) • Microembolization (n=7) • Iliac artery damage (n=1)
Uflacker ¹⁰ (n=10)	90%	70%	10%	• Migration of stent-graft (n=1) • Embolization (n=1) • Renal overstenting (n=1)
White ¹¹ (n=76)	91%	83%	9%	• Occlusion of renal arteries (n=1) • Rupture of proximal neck (n=1) • Stent-graft thrombosis (n=1) • Migration of stent-graft (n=1) • Iliac artery damage (n=2) • Embolization (n=1)
Zarins ¹² (n=190)	97%	77%	0%*	• Iliac artery damage (n=4) • Embolization (n=3) • Renal artery occlusion (n=1) • Internal iliac artery occlusion (n=6) • Iliac limb thrombosis (n=5)

*Although no surgical conversions were reported, in 5 patients the endovascular graft could not be deployed. All of these 5 patients declined further treatment.

The EUROSTAR database, a registry center for collection of data on endovascular treatment of AAA in Europe, reported a total of 2,310 patients treated from January 1994 to December 1999³. Of all intraoperative problems, inability to advance the delivery system was the most frequent complication (1.8%). In 1.3% of all endovascular procedures, conversion to open surgery was required. Endoleaks occurred in 16.3% of the patients.

Reports comparing the results of endovascular AAA repair with open surgery showed that endovascular repair has a perioperative mortality and morbidity that is comparable to open repair¹⁵⁻¹⁶. The early and late failure rate of endovascular repair is higher than that obtained with open repair. However, endovascular repair is associated with less severe systemic complications, shorter length of hospital stay, shorter duration of intensive care stay and less blood loss. Furthermore, endovascular repair appears to be an option for patients who, on the basis of their poor physical condition, are unfit to sustain open repair. In some institutions, endovascular repair of AAA has become the standard treatment for elective AAA exclusion. However, doubt exists about the long-term durability of endovascular treatment. Recent reports on late device failure have increased the growing concern about the long-term durability of endovascular repair of AAA¹⁷⁻²⁰. Apparently, the long-term stability of materials used for stent-grafts is at question, and either the stitches securing the stent to the graft, or the graft material itself, may not be enduring enough to last a lifetime. To date only one study has been published on this subject identifying the problems of one particular type of stent-graft (e.g. stent dislocation and tearing of graft material)¹⁹. It was suggested, however, that the EUROSTAR database already observed and identified this problem without stating the type of stent-graft in question²¹. Current initiatives to produce smaller stent-grafts using thinner stents and graft material may further increase the incidence of device failure. Therefore, extensive follow-up schedules remain mandatory to observe similar problems possibly developing in other stent-grafts.

IMAGING BEFORE AND AFTER ENDOVASCULAR REPAIR:

What are the Criteria?

In order to perform endovascular graft placement, an accurate measurement of aortic and iliac dimensions is necessary^{3,4,22} (Figure 1). Selection of the correct diameter and length of an endovascular graft is important to avoid complications such as perigraft endoleak and endovascular graft thrombosis. Undersizing the endovascular graft may lead to graft migration, or endoleak, while oversizing may lead to folding of abundant graft material, again giving rise to perigraft endoleak channels. A mismatch in length may lead to occlusion of renal arteries or internal iliac arteries. A too short endovascular graft may result in an insufficient covering of the proximal or distal neck,

which in turn may lead to dislodgement of the endovascular graft and endoleakage.

Current imaging techniques for preoperative assessment of AAA dimensions

Infra-Renal Abdominal Aortic Aneurysm worksheet

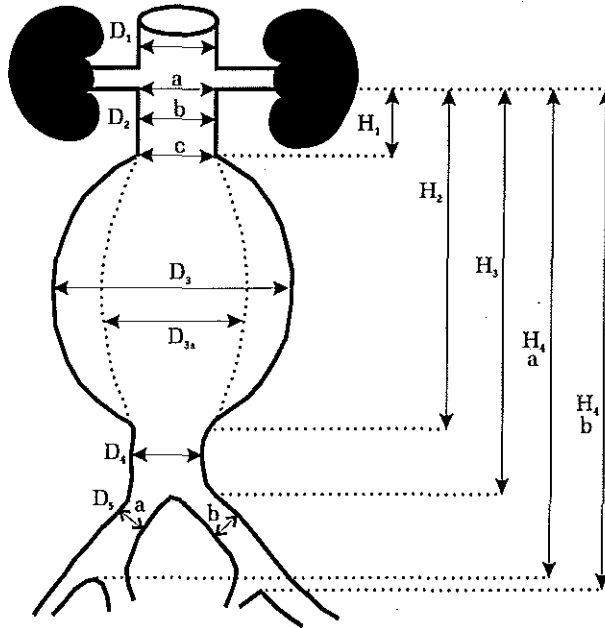


Fig. 1. Example sheet for preoperative evaluation of abdominal aortic aneurysm dimensions, as used by the EUROSTAR database. Reproduced with permission from EUROSTAR (Liverpool UK).

are calibrated angiography and CT angiography (CTA)²³⁻²⁵. Using these techniques, sufficient information on AAA dimensions and feasibility for endovascular repair can be obtained. Accurate endovascular graft measurements may be obtained using three-dimensional reconstruction and central lumen line reconstructions of CTA scans. Alternatively, a combination of CT scans and calibrated angiography may be sufficient to decide on the suitability of the individual patient for endovascular repair. The first generation of endovascular grafts were individually tailored for each patient before the intervention, using measurements obtained with the

above-described techniques. Using these endovascular grafts no intraoperative adjustments were possible. Nowadays, a range of modular endovascular grafts are available, enabling modifications in the planned intervention based on intraoperative findings. Patient selection for modular devices can be performed using calibrated angiography and axial CT scanning. Based on these measurements, an endovascular graft can be chosen within a certain range, using intraoperative measurements for completion and perfection of the process of selecting the size of the endovascular graft.

In selecting the appropriately-sized endovascular graft, intravascular ultrasound (IVUS) may play a major role. In both an *in vitro* and *in vivo* study our group has shown that IVUS allows to assess morphologic features of the abdominal aorta, and can assess diameter and length of the proximal neck and the length of AAA^{26,27} (Figure 2).

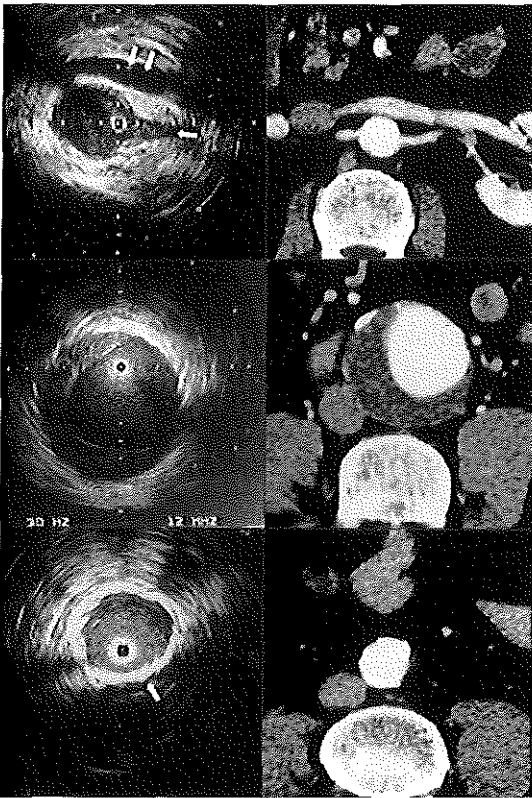


Fig. 2. Comparison of computed tomographic angiography images and intravascular ultrasound images (12.5 MHz) obtained in the proximal neck, the aneurysm and the iliac arteries.

Using these measurements, modular components may be selected from a range of predefined components during the intervention itself. In clinical studies, IVUS proved to be not only an adjunct but also a good alternative to

angiography during the intervention^{28,29}. White et al.²⁸ found IVUS to be "the most accurate way to determine the morphology of vascular structures". Furthermore, "the final choice of device dimensions was determined by IVUS interrogation". In one procedure IVUS identified a leak at the proximal landing zone apparently not seen on angiography. In this particular study, use of IVUS led to a decrease in the amount of contrast dye required²⁸. Altogether, it should be mentioned that, in this study, no actual overall results were given on the exact additional role of IVUS over angiography and CTA. Tutein Nolthenius et al.²⁹ used IVUS for the selection of final stent-graft size during the procedure. They found that in 65% of the procedures the expected stent-graft size based on preoperative CT scanning differed from the actual size chosen at the time of the procedure. Also, IVUS indicated a significantly smaller diameter and longer length, compared to preoperative CT scanning. However, in this study no three-dimensional CTA reconstructions were used for measurements, and therefore the length measurements obtained with preoperative CT scanning may not be corresponding to the actual length. They concluded that the 'last-minute' corrections based on intra-operative IVUS measurements did not result in high incidence of endoleaks at fixation zones. Based on these data no conclusive evidence can be given on the role of IVUS in diminishing the endoleak rate, since no fair comparison is possible between preoperative CTA measurements and intra-operative IVUS measurements.

In our hands, IVUS provided the dimensions of the proximal and distal landing zones for the endovascular graft³⁰. Based on measurements obtained with IVUS at the onset of the endovascular procedure in 29 patients, we decided to convert to open surgery in one case and in 12 patients we selected the size of the modular stent-graft components of the AneuRx stent-graft. Moreover, IVUS determined the definitive length of an Ancure stent-graft in one patient in whom the CTA measurements remained inconclusive. In another patient intraoperative IVUS investigation led to a change in the planned introduction side because of circular calcification in the common iliac artery, probably obstructing normal introduction of the delivery system. In the latter case extensive CTA measurements with three-dimensional reconstruction were available, but failed to recognize the true nature of the calcification. Finally, intraoperative IVUS investigation led to predilatation of a recently developed occlusion in one patient.

IVUS investigation immediately after endograft placement revealed the iliac leg of the stent-graft to end in the aneurysm in one patient and incomplete covering of the iliac part of the stent-graft in three other patients, all of which were treated with appropriate extension cuffs. The bare part of the proximal attachment system was seen to be placed over a renal artery (n=1) and accessory renal arteries were seen to be intentionally covered (n=3).

Stenosis in the iliac leg of the graft (n=5) detected with IVUS was treated with an additional balloon dilatation. For iliac artery dissections (n=5) no additional interventions were deemed required. Finally, no additional interventions were performed for incomplete apposition at the proximal part of the stent-graft (n=1) and folding at the distal part of the stent-graft (n=1). Our experience shows that there may be an important role for IVUS in/during endovascular treatment of AAA. This view seems to be supported by Zajko et al.³¹ who reported that after deployment of an Ancure stent-graft, iliac limb stenosis or compression occurred in 41% of the patients. Most of these stenoses were caused by compression of the unsupported part of the stent-graft at the native aortic bifurcation or by graft folding due to excess fabric in a small iliac artery. Such stenoses were easily and safely corrected with Wallstent placement. Since the authors used IVUS immediately after deployment, this problem was recognized and could be treated without delay by stent placement. At follow-up (1-27 months) all Wallstent reinforced Ancure stent-grafts remained patent.

IVUS BEFORE AND AFTER ENDOVASCULAR REPAIR:

What are the Costs?

Although IVUS has been proclaimed by some to be the imaging technique of choice for endovascular treatment, others are concerned about the additional costs using IVUS³². There are no specific reports on the cost-effectiveness of IVUS for endovascular repair of AAA. In our own experience with 29 patients, IVUS was used whenever feasible during the procedure. As our study was not designed to compare IVUS with angiography as routinely performed in a standardized fashion, no potential additional value of IVUS over angiography could be proven³⁰. To evaluate the additional value of IVUS in these circumstances, IVUS should be used only after standard peroperative angiography has shown the intervention to be completed as being successful. The results of angiography should than be blinded to the IVUS investigators. Based on both angiography and IVUS an independent decision should be made concerning the success of the intervention and the possible need for additional interventions. So far, a preliminary study on the additional role of IVUS in 10 patients, studied later, has shown angiography and IVUS to yield similar conclusions concerning clinical success in nine patients. In one patient, angiographic appearance after stent-graft placement was inconclusive; thereafter IVUS investigation revealed a stenosis of an iliac leg of the stent-graft and additional PTA was performed.

Eventually such studies will lead to conclusions concerning the value of IVUS over angiography. However, no conclusions can be drawn yet on the cost-effectiveness of IVUS, since it is not known to what extent additional procedures, based on IVUS interrogation, will prevent early complications such as stent-graft thrombosis or perigraft endoleaks.

A study on the costs of IVUS should include the costs for the IVUS console (including write-off of equipment), IVUS catheters and personnel to operate the IVUS equipment, as well as the additional costs taken up by the extra time needed for IVUS investigation (i.e. costs of OR personnel, costs of OR time). Such a study will show that IVUS will add up the already high costs of endovascular surgery.

In a number of reports the costs of endovascular treatment were compared with those for open surgery^{32,33}. Hölzenbein et al.³² calculated that endovascular treatment of AAA was cost-effective and less expensive than open surgery (ECU 22,269 vs. ECU 25,374), despite additional costs for evaluation of patients suitable for endovascular repair and a more costly endovascular procedure. The increased length of stay in ICU and the increased length of stay in hospital accounted for the higher costs of open surgery. The costs of follow-up needed for the endovascular group were not taken into account, meaning that the overall costs of endovascular repair will eventually be higher than those for open surgery. Seiwert et al.³³ reported the cost of endovascular repair to be similar to that for open repair (US\$12,905 ± 495 vs. US\$12,714 ± 1,116). In-hospital imaging costs specific for endovascular repair (e.g. guide-wires, catheters and fluoroscopy) were US\$1,370 ± 67. However, the costs for follow-up imaging were not taken into account, thus limiting the value of this study³³. Finally, Sternbergh et al.³⁴, reported in-hospital costs of endovascular repair to be significantly higher than that for open repair (US\$19,985 ± 7,396 vs. US\$12,546 ± 5,944). The costs of the endograft accounted for 52% of the total cost of endovascular repair. The contradiction between these three reports can probably be attributed to the costs of the endovascular grafts used. These costs ranged from US\$4,723 in the report by Hölzenbein et al.³² to US\$10,400 in the report by Sternbergh et al.³⁴. The costs of newly developed stent-grafts will be in the higher range, therefore the in-hospital costs of endovascular repair will remain higher than that for open repair. The total costs of endovascular repair, including follow-up and possible additional interventions, will even be higher, as long as a lifelong follow-up is deemed necessary.

In our opinion, regarding the total cost of endovascular repair, the cost of using IVUS should not be exaggerated (*vide supra*).

OTHER OPTIONS FOR IMAGING DURING ENDOVASCULAR REPAIR

A limitation of IVUS in the endovascular repair of AAA, is that during actual placement and deployment of the stent-graft imaging is not possible. It is during this part of the procedure that complications such as misplacement of the stent-graft or occlusion of renal and intestinal arteries may occur. A number of alternatives have been proposed to avoid the problem of this 'short-sightedness' during the actual placement. These include simultaneous IVUS interrogation from an intra-arterial position (either inside the device or next to the device), intravenous IVUS, IVUS guide-wires, and peroperative MR imaging³⁵⁻³⁹.

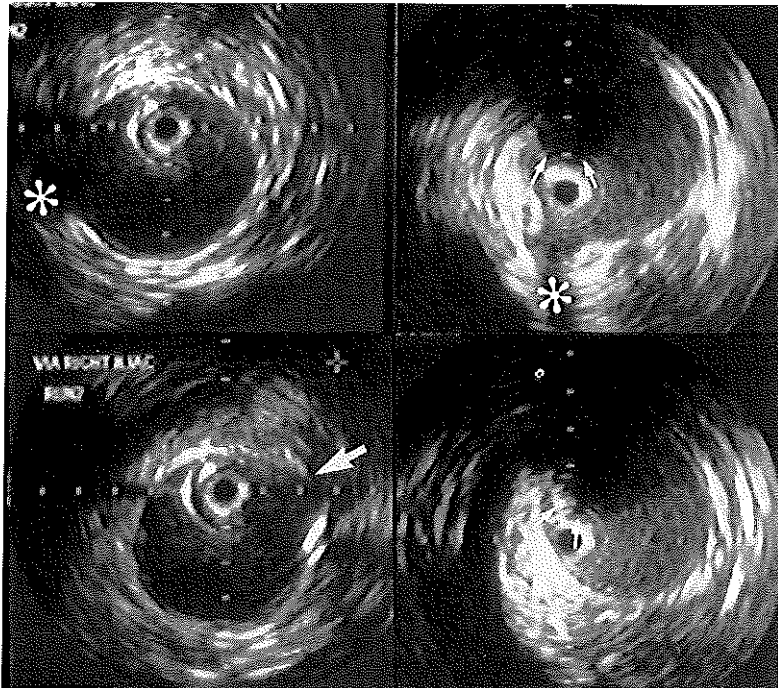


Fig. 3. Intravascular ultrasound images (10 MHz) showing the right renal artery and vein obtained immediately before placement of an endovascular graft. In the presence of the delivery system of an Ancure endovascular graft (EndoVascular Technologies/Guidant, Menlo Park, CA, USA), shadowing of 25% of the vessel wall occurs preventing visualization of the left renal artery.

For intra-arterial IVUS imaging, however, the IVUS catheter would be in the way of the device. Vogt et al.³⁵ tried to visualize the proximal stent during deployment by placing the IVUS catheter alongside the device. After three attempts this was stopped. Due to massive shadowing from the half-expanded stent only a segment of the aortic wall could be seen, and only one renal artery could be identified. Furthermore, the IVUS catheter was damaged by the hooks of the stents, preventing further imaging. In our experience, massive shadowing prevented visualization of about 25% of the vessel wall, including the most distal renal artery, and reliable positioning of the device in relation to the renal arteries, using IVUS, was impossible (Figure 3). As an alternative, the use of intravenous IVUS was explored^{35,36}. Kriegel et al.³⁵ compared intravenous IVUS with intra-arterial IVUS and external ultrasound in a sheep model; they succeeded in visualizing arterial branch ostia, measuring arterial diameter and assessing device placement.

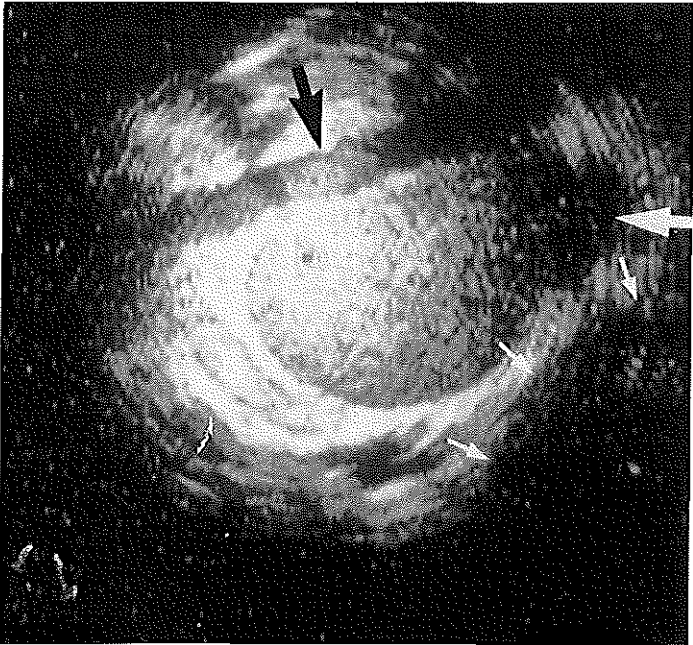


Fig. 4. Intravascular ultrasound image (20 MHz) obtained from within the vena cava showing the renal artery crossing over the vena cava and the left renal vein originating from the vena cava. The aorta could not be seen.

Vogt et al.³⁶ used a 10 MHz IVUS catheter in the inferior vena cava in one patient; the aorta could not be visualized from within the vena cava. Similarly, our own experience with intravenous IVUS was disappointing. We attempted to visualize the abdominal aorta from within the inferior vena cava with a 20 MHz IVUS catheter but the aorta did not come into viewing range (Figure 4). The discrepancy between our results and the animal model advocated by Kriegel et al.³⁵ may be due to the fact that the animal model used is of a smaller size compared to the human aorta, and did not have aneurysmal disease. It is likely that the vena cava is displaced in the presence of an aneurysm, thus making it difficult to see with a 20 MHz IVUS catheter. A solution to this problem may be to use a 10-12.5 MHz IVUS catheter or to introduce a pediatric transesophageal ultrasound probe into the vena cava, as was successfully demonstrated in sheep by Beebe et al.³⁷. Using a pediatric ultrasound probe, both B-mode and color flow pictures were obtained over linear segments of the aorta. A third alternative to intraoperative IVUS may be an IVUS guide-wire. An IVUS guide-wire is an ultrasonic imaging device that is of the same dimension as a standard guide-wire, allowing the device to be introduced through the guide-wire lumen of all sorts of endovascular devices. Both White et al.³⁸ and Hiro et al.³⁹, have shown that IVUS guide-wires are able to assess balloon inflation and stent-placement in iliac arteries and coronary arteries, respectively. White et al.³⁸ showed that for treatment of smaller-diameter arterial lesions an alternative deployment technique can be used, in which an 0.035-inch IVUS guide-wire was introduced after placement of the introduction system in the desired position. The imaging element was then used to observe the position of the proximal stent-device and to ensure complete expansion of the prosthesis. Hiro et al.³⁹ reported that the 0.018 inch IVUS guide-wire permitted clear visualization of the lumen-plaque interface and media-plaque interface both before, during and after balloon inflation. Currently, no imaging wires are available to use for aortic purposes. The dimensions of the abdominal aorta are too big for visualization by the available guide-wires. A low frequency (10-12.5 MHz) guide-wire may overcome this limitation. Using such an IVUS guide-wire, placement of endovascular grafts may be optimized, to be as proximal to the renal arteries as physically possible without occluding or overstenting them. It has recently been suggested that use of magnetic resonance imaging (MRI) during endovascular treatment may be an option for intraoperative imaging of endovascular treatment⁴⁰. However, at this time, only in vitro and animal experience is available on MR-guided balloon angioplasty. A major problem is that the devices, guide-wires and other material, are fundamentally unfit for MRI scanning due to the metal content, or because the imaging properties of the material used render it unfit for visualization.

FUTURE OF IVUS IN ENDOVASCULAR REPAIR OF AAA

The use of IVUS during endovascular repair of AAA remains a topic of discussion. Should IVUS be used in every endovascular intervention, or will its use be limited due to high costs. In our opinion IVUS may be used on demand in selected cases where problems during endovascular interventions may be suspected. Similarly, White et al.⁴¹ developed a grading scale to predict the degree of difficulty for endovascular graft procedures. Using anatomical and morphological features of AAA, such as length and angulation of the proximal neck, angulation of the aortic sack, and tortuosity, stenosis and calcification of the iliac arteries, three grades of difficulty can be established. If preoperative evaluation of AAA reveals a Grade III AAA (e.g. a difficult AAA presenting two or more of the above mentioned features), endovascular stent-grafting may present problems not seen on peroperative angiography. Similarly, postoperative assessment with IVUS may be warranted if angiography shows an ambiguous result. Altogether, our ultimate goal is to use IVUS during endovascular repair whenever indicated in order to improve the success of endovascular grafting of AAA.

REFERENCES

1. Parodi JC, Palmaz JC, Barone HD. Transfemoral intraluminal graft implantation for abdominal aortic aneurysms. *Ann Vasc Surg* 1991; 5: 491-499.
2. Volodos NL, Karpovich IP, Troyan VI, Kalashnikova YV, Shekhanin VE, Ternyuk NE, Neoneta AS, Ustinov NI, Yakovenko LF. Clinical experience of the use of self-fixing synthetic prostheses for remote endoprosthetics of the thoracic and the abdominal aorta and iliac arteries through the femoral artery and as intraoperative endoprosthesis for aorta reconstruction. *Vasa* 1991; 33 (suppl): 93-95.
3. Progress report EUROSTAR Data Registry Centre. January 2000.
4. Ahn SS, Rutherford RB, Johnston KW, May J, Veith FJ, Baker D, Ernst CB, Moore WS. Reporting standards for infrarenal endovascular abdominal aortic aneurysm repair. *J Vasc Surg* 1997; 25: 405-410.
5. Balm R, Eikelboom BC, May J, Bell PRF, Swedenborg J, Collin J. Early experience with Transfemoral Endovascular Aneurysm Management (TEAM) in the treatment of aortic aneurysms. *Eur J Vasc Endovasc Surg* 1996; 11: 214-220.
6. Blum U, Voshage G, Lammer J, Beyersdorf F, Töllner D, Kretschmer G, Spillner G, Polterauer P, Nagel G, Hölzenbein T, Thurnher S, Langer M. Endoluminal stent-grafts for infrarenal abdominal aortic aneurysms. *N Engl J Med* 1997; 336: 13-20.
7. May J, Woodburn K, White G. Endovascular treatment of infrarenal abdominal aortic aneurysms. *Ann Vasc Surg* 1998; 12: 391-395.
8. Moore WS, Rutherford RB. Transfemoral endovascular repair of abdominal aortic aneurysm: results of the North American EVT phase 1 trial. *J Vasc Surg* 1996; 23: 543-553.
9. Parodi JC, Barone A, Piraino R, Schonholz C. Endovascular treatment of abdominal aortic aneurysms: lessons learned. *J Endovasc Surg* 1997; 4: 102-110.
10. Uflacker R, Robison JG, Brothers TE, Pereira AH, Sanvittto PC. Abdominal aortic aneurysm treatment: preliminary results with the Talent Stent-Graft system. *JVIR* 1998; 9: 51-60.
11. White GH, Yu W, May J, Waugh R, Chaufour X, Harris JP, Stephen MS. Three-year experience with the White-Yu endovascular GAD graft for transluminal repair of aortic and iliac aneurysms. *J Endovasc Surg* 1997; 4: 124-136.
12. Zarins CK, White RA, Schwarten D, Kinney E, Dietrich EB, Hodgson KJ, Fogarty TJ. AneuRx stent graft versus open surgical repair of abdominal aortic aneurysms: multicenter prospective clinical trial. *J Vasc Surg* 1999; 29: 292-308.
13. Becquemin JP, Lapie V, Favre JP, Rousseau H. Mid-term results of a second generation bifurcated endovascular graft for abdominal aortic aneurysm repair: the French Vanguard trial. *J Vasc Surg* 1999; 30: 209-218.
14. Broeders IAMJ, Blankensteijn JD, Gvakharia A, May J, Bell PRF, Swedenborg J, Collin J, Eikelboom BC. The efficacy of transfemoral endovascular aneurysm management: a study on size changes of the abdominal aorta during mid-term follow-up. *Eur J Vasc Endovasc Surg* 1997; 14: 84-90.
15. May J, White GH, Yu W, Ly CN, Waugh R, Stephen MS, Arulchelvam M, Harris JP. Concurrent comparison of endoluminal versus open repair in the treatment

- of abdominal aortic aneurysms: analysis of 303 patients by life table method. *J Vasc Surg* 1998; 27: 213-221.
16. Brewster DC, Geller SC, Kaufman JA, Cambria RP, Gertler JP, LaMuraglia GM, Atamian S, Abbott WM. Initial experience with endovascular aneurysm repair: comparison of early results with outcome of conventional open repair. *J Vasc Surg* 1998; 27: 992-1005.
 17. Alimi YS, Chakfe N, Rivoal E, Slimane KK, Valerio N, Riepe G, Kretz JG, Juhan C. Rupture of an abdominal aortic aneurysm after endovascular graft placement and aneurysm size reduction. *J Vasc Surg* 1998; 28: 178-183.
 18. Torsello GB, Klenk E, Kasprzak B, Umscheid T. Rupture of abdominal aortic aneurysm previously treated by endovascular stent-graft. *J Vasc Surg* 1998; 28: 184-187.
 19. Riepe G, Heilberger P, Umscheid T, Chakfe N, Raithel D, Stelter W, Morlock M, Kretz JG, Schröder A, Imig H. Frame dislocation of body middle rings in endovascular stent-tube grafts. *Eur J Vasc Endovasc Surg* 1999; 17: 28-34.
 20. Krogh-Sørensen K, Brekke M, Drolsum A, Kvernebo K. Periprosthetic leak and rupture after endovascular repair of abdominal aortic aneurysm: the significance of device design for long-term results. *J Vasc Surg* 1999; 29: 1152-1158.
 21. Rutherford RB. Problems with the dissemination of up-to-date information on the results of endograft repair for abdominal aortic aneurysm. *J Vasc Surg* 1999; 29: 1167-1169.
 22. Dorros G, Parodi J, Schonholz C, Jaff M, Dietrich EB, White G, et al. Evaluation of endovascular abdominal aortic aneurysm repair: anatomical classification, procedural success, clinical assessment, and data collection. *J Endovasc Surg* 1997; 4: 203-225.
 23. Beebe HG. Imaging modalities for aortic stent-grafting. *J Endovasc Surg* 1997; 4: 111-123.
 24. Schumacher H, Eckstein HH, Kallinowski F, Allenberg JR. Morphometry and classification in abdominal aortic aneurysms: patient selection for endovascular and open surgery. *J Endovasc Surg* 1997; 4: 39-44.
 25. Broeders IAMJ, Blankensteijn JD, Olree M, Mali WPTM, Eikelboom BC. Preoperative sizing of grafts for transfemoral endovascular aneurysm management; a prospective comparative study of spiral CT angiography, arterial angiography and conventional CT imaging. *J Endovasc Surg* 1997; 4: 252-261.
 26. Essen van JA, Lugt van der A, Gussenhoven EJ, Leertouwer TC, Zondervan P, Sambeek van MRHM. Intravascular ultrasound allows accurate assessment of abdominal aortic aneurysm: an in vitro validation study. *J Vasc Surg* 1998; 27: 347-353.
 27. Essen van JA, Gussenhoven EJ, Lugt van der A, Huijsman PC, Muiswinkel van JM, Sambeek van MRHM, Dijk van LC, Urk van H. Accurate assessment of abdominal aortic aneurysm with intravascular ultrasound: validation with computed tomographic angiography. *J Vasc Surg* 1999; 29: 631-638.

28. White RA, Donayre C, Kopchok G, Walot I, Wilson E, Virgilio de C. Intravascular ultrasound: the ultimate tool for abdominal aortic aneurysm assessment and endovascular graft delivery. *J Endovasc Surg* 1997; 4: 45-55.
29. Tutein Nolthenius RP, Berg van der JC, Moll FL. The value of intraoperative IVUS in stent-graft sizing excluding AAA with a modular system. In press: *Ann Vasc Surg*.
30. Essen van JA, Gussenhoven EJ, Smet de AAEA, Blankensteijn JD, Tielbeek AV, Kranendonk SE, Dijk van LC, Urk van H. Intravascular ultrasound to guide endovascular treatment of abdominal aortic aneurysm. Submitted.
31. Zajko AB, Amesur NB, Orons PD, Makaroun M. Wallstent placement and/or thrombolysis for treatment of complicated endovascular aortic stent grafts: experience in 24 patients (abstract). *CVIR* 1999 (suppl 2); 22: S103-119.
32. Hölzenbein TJ, Kretschmer G, Schön A, Thurnher S, Winkelbauer F, Trubel W, Minar E, Ahmadi A, Huk I, Ingruber H, Erhinger H, Lammer J, Polterauer P. Endovascular AAA treatment: expensive prestige or economic alternative. *Eur J Vasc Endovasc Surg* 1997; 14: 265-272.
33. Seiwert AJ, Wolfe J, Whalen RC, Pigott JP, Kritpracha B, Beebe HG. Cost comparison of aortic aneurysm endograft exclusion versus open surgical repair. *Am J Surg* 1999; 178: 117-120.
34. Sternbergh WC 3rd, Money SR. Hospital cost of endovascular versus open repair of abdominal aortic aneurysms: a multicenter study. *J Vasc Surg* 2000; 31: 237-244.
35. Kriegel AV, Salles-Cunha S, Pigott JP, Beebe HG. Intravenous intravascular ultrasound for arterial visualization: a feasibility study. *J Endovasc Surg* 1996; 3: 429-434.
36. Vogt KC, Brunkwall J, Malina M, Ivancev K, Lindblad B, Risberg B, Schroeder TV. The use of intravascular ultrasound as control procedure for the deployment of endovascular stented grafts. *Eur J Vasc Endovasc Surg* 1997; 13: 592-596.
37. Beebe HG, Assadnia S, Kriegel AV, Salles-Cunha SX. Biplane color flow duplex intravenous intravascular ultrasound for arterial visualization. *J Endovasc Surg* 1998; 5: 101-105.
38. White RA, Donayre CE, Walot I, Kopchok GE, Wilson EP, Buwalda R, deVirgilio C, Ayres B, Zalewski M, Mehringer CM. Preliminary clinical outcome and imaging criterion for endovascular prosthesis development in high-risk patients who have aortoiliac and traumatic arterial lesions. *J Vasc Surg* 1996; 24: 556-571.
39. Hiro T, Hall P, Maiello L, Itoh A, Colombo A, Jang YT, Salmon SM, Tobis JM. Clinical feasibility of 0.018-inch intravascular ultrasound imaging device. *Am Heart J* 1998; 136: 1017-1020.
40. Smits HFM, Bos C, Weide van der R, Bakker CJG. Interventional MR: vascular applications. *Eur Radiol*; 1999; 9: 1488-1495.
41. White GH, May J, Petrasek P, Yu W, Waugh RC, Choufour X. A grading scale to predict the degree of difficulty for endovascular AAA graft procedures. *J Endovasc Surg* 1998; 5: 380-381.

SUMMARY

Summary

SUMMARY

Endovascular treatment of abdominal aortic aneurysms (AAA) by means of a stent-graft is feasible and effective. Accurate knowledge of the dimensions of AAA is important for planning endovascular treatment. Imaging techniques, such as angiography and computed tomographic angiography (CTA), are widely used in the assessment of AAA before intervention. During endovascular intervention angiography is the sole technique to guide the placement of endografts. Angiographic measurements, however, may be hampered by thrombus, parallax and foreshortening, thus limiting the accurate placement of endografts. Intravascular ultrasound (IVUS) is a powerful imaging modality that provides information on lesion characteristics and vessel dimensions of coronary, peripheral and central arteries, and allows to assess the success of endovascular interventions. This thesis describes the validation and application of IVUS in the endovascular treatment of AAA.

Chapter 1 gives an introduction to the scope of the thesis.

Chapter 2 describes the results of an in vitro validation study in which histologic sections of normal, atherosclerotic and aneurysmal aortae were compared with corresponding IVUS cross-sections. Fifteen abdominal aortic specimens were studied (5 normal, 5 atherosclerotic and 5 aneurysmal) in an in vitro set-up. After IVUS study, the specimens were fixated and studied histologically. Ultrasonic images were compared with histologic counterparts for vessel wall characteristics, lesion morphology and lumen diameter. Length of the aneurysm and the proximal and distal neck were measured using a displacement sensing device and compared to external measurements.

This study showed that normal aortic wall can be seen as a 2 or 3 layered structure corresponding with intima, media and adventitia. A clear distinction could be made between fibrous lesion, calcified lesion, and thrombus in the aneurysm sac, and between normal and aneurysmal aorta. For lumen diameter measurements a high correlation was found between histologic sections and IVUS cross-sections ($r=0.93$; $p<0.001$). Similarly, a high correlation was found for length measurements of the aneurysm and its proximal and distal necks ($r=0.99$; $p<0.001$).

Thus, this in vitro study showed that IVUS may be an accurate imaging tool for the assessment of AAA in a clinical setting.

Chapter 3 describes the results of a clinical validation study in which IVUS measurements of the proximal and distal neck and the aneurysm were

compared with data obtained with angiography and CTA. A total of 16 patients with AAA were studied with angiography and IVUS. Shortly after the IVUS examination all patients underwent CTA. Measurements included the length of the aneurysm, and the length and diameter of the proximal and distal neck. CTA measurements were performed along a so-called "central lumen line". IVUS was able to identify 97% of the renal arteries and 80% of the accessory renal arteries. Comparison of measurements of the length of the aneurysm and of the proximal and distal necks obtained with IVUS and CTA showed a correlation of 0.99 ($p < 0.001$) and a coefficient of variation of 9%. IVUS tended to underestimate the length measurements as compared to CTA. This difference may be attributed to the non-coaxial position of the IVUS catheter, and to the stiffness of the IVUS catheter, leading to a different path between the IVUS catheter and the "central lumen line". Comparison of the lumen diameter measurements obtained with IVUS and CTA showed a correlation of 0.93 ($p < 0.001$) and a coefficient of variation of 9%; again IVUS underestimated luminal diameter of the neck as compared to CTA. The latter difference may be due to the fact that on IVUS the minimum lumen diameter was taken to represent the actual lumen diameter to avoid overestimation due to the non-coaxial position of the IVUS catheter. Interobserver analysis of length and diameter measurements showed a correlation of 1.0 and a coefficient of variation of 3% and 2%, respectively. Altogether, this clinical study showed that IVUS in a clinical setting provides accurate and reproducible measurements of AAA.

Chapter 4 describes the use of an automated contour analysis system developed to increase reproducibility and facilitate quantitative analyses of multiple IVUS images, in IVUS images derived from femoropopliteal arteries before vascular intervention. First, measurements obtained with automated analysis were compared with those obtained by conventional manual contour tracing. Second, the intra- and interobserver variability of the measurements was determined.

Area measurements obtained with automated analysis agreed well with those obtained with manual analysis, displaying high correlation coefficients ($r = 0.92-0.98$) and low coefficients of variation (8.5%-15.7%). Intra- and interobserver analysis showed high correlation coefficients (both: $r = 0.93-0.99$) and low coefficients of variation (6.0%-15.3% and 5.7%-14.0%). This study showed that automated analysis of multiple IVUS images is reliable for the quantitative assessment of vessel dimensions obtained in peripheral arteries before a vascular intervention.

Chapter 5 describes the use of the automated contour analysis system for quantitative analysis of IVUS images obtained after vascular intervention in femoropopliteal arteries, including percutaneous transluminal angioplasty (PTA; $n=10$), stent placement ($n=10$) or stent-graft placement ($n=10$). Comparison was made between lumen diameter obtained with automated analysis and manual analysis. The location showing the smallest lumen area derived from automated analysis was compared with the smallest lumen area selected by visual estimation.

It became clear that IVUS images containing a dissection, a common feature after PTA, could not be analyzed by the automated analysis system. For images obtained within stents and stent-grafts, a high correlation (both: $r = 1.0$) and low coefficients of variation were obtained for lumen diameter (2.7% and 2.1%, respectively). The location of the smallest lumen area determined by both systems was the same (< 1 cm) in 16 of the 20 patients studied and differed more than 1 cm in 4 patients. This study showed that the automated analysis system can accurately determine the lumen diameter as well as the smallest lumen area in stents and stent-grafts. However, the analysis system is not able to analyze an irregular-shaped lumen area caused by dissection.

After validation of the automated analysis system for quantitative assessment of vessel dimensions, **Chapter 6** describes the use of the automated analysis system in assessment of the lumen diameter and length of the proximal and distal neck of an AAA, and the additional features associated with three-dimensional (3D) IVUS imaging. Lumen diameter obtained with both systems was compared. The length of the neck obtained with automated analysis was compared with the length assessed by visual estimation using the displacement sensing device.

Comparison of lumen diameter and length showed good correlation (both: $r = 0.99$) and low coefficients of variation (2.1% and 4.1%, respectively). Interobserver analysis of the automated analysis also showed good correlation (both: $r = 0.99$) and low coefficients of variation (3.4% and 3.5%, respectively). 3D IVUS analysis allowed identification of the shape of the neck. This study showed that automated analysis of the proximal and distal neck of AAA is feasible. Additional information on neck anatomy can be acquired with 3D IVUS analysis.

Chapter 7 describes a feasibility study on the role of IVUS immediately before and after endovascular repair of AAA performed in 29 patients. In this multi-center study different endovascular grafts were used. Before intervention, IVUS was used to assess the diameter and length of the stent-graft to be used. In case of a modular stent-graft the final dimensions of

the stent-graft were chosen based on the IVUS measurements. After intervention IVUS was used to assess parameters known to be critical for the success of the treatment.

Based on IVUS data obtained *before* intervention, one procedure was converted to open surgery, modules of the AneuRx stent-graft were chosen (n=12), as was the length of one Ancure stent-graft, the introduction side for one Ancure stent-graft was changed due to a critical stenosis in the common iliac artery, and a stenosis of the common iliac artery was dilated (n=1). *After* intervention, IVUS revealed incomplete apposition at the proximal side (n=1) and folding of a tube graft at the distal side (n=1) for which no additional intervention was performed. Furthermore, IVUS showed the leg of a stent-graft to end inside the aneurysm (n=1) and incomplete covering by the iliac part of the stent-graft (n=3), which were, all 4, treated successfully with extension cuffs. IVUS revealed that the bare part of the proximal attachment system of an Ancure stent-graft was placed over a renal artery (n=1), while in 3 other patients accessory renal arteries were intentionally occluded. For stenosis in an iliac leg of a stent-graft (n=5) additional PTA was performed. For dissection seen with IVUS (n=5) no additional intervention was deemed necessary. In conclusion, this study showed that IVUS may play a major role in the endovascular treatment of AAA. Before intervention IVUS can be used to assess definitive dimensions of modular stent-graft components. After intervention IVUS may be used to assess the outcome of the procedure and allow additional interventions to be performed during the same session.

Finally, **Chapter 8**, addresses the current state of endovascular treatment and describes different perspectives on the use of IVUS during endovascular repair. Topics such as additional costs of IVUS for endovascular treatment, and selection of patients who may benefit from using IVUS, are discussed. A few remarks on future developments in vascular imaging are given.

SAMENVATTING

SAMENVATTING

Een aneurysma van de abdominale aorta (AAA) is een locale, permanente, verwijding van de aorta. Het grootste gevaar van deze afwijking, die in feite een onderdeel is van aderverkalking, is ruptuur. De kans op ruptuur neemt toe met de diameter van het AAA. Ruptuur van het AAA gaat gepaard met een hoge mortaliteit; 60-70% van deze patiënten haalt het ziekenhuis niet levend. Een chirurgische behandeling van een geruptureerd AAA heeft een mortaliteit van 45-55%. In verband met deze hoge mortaliteit wordt een AAA behandeld als het groter dan 5 cm in doorsnede is. De traditionele behandeling van het AAA is een operatie waarbij het zieke verwijde deel wordt vervangen door een kunststof prothese. Deze behandeling heeft een mortaliteit van 5-7%, waarbij patiënten met hartklachten, ritme stoornissen en long problemen een verhoogde kans op complicaties hebben. Recentelijk is een nieuwe 'endovasculaire' behandeling voor het AAA geïntroduceerd. Bij deze endovasculaire behandeling wordt de prothese niet meer via een buikoperatie geplaatst, maar wordt deze in opgevouwen toestand, via een slagader in de lies ingebracht en in de aorta geplaatst. Met behulp van een ballon en een stent wordt de prothese ontplooid en vastgezet in een gezond deel van de aorta. Met deze behandeling wordt het aneurysma van binnenuit behandeld. Het plaatsen van een endovasculaire prothese is millimeterwerk. De slagaders naar de nieren, die meestal vlak boven de verwijding liggen mogen niet worden afgesloten door de prothese. Verschillende onderzoekers hebben inmiddels aangetoond dat endovasculaire protheses een effectieve en veilige behandeling van het AAA vormen.

Om een endovasculaire procedure te plannen en uit te voeren is uitgebreide informatie nodig over de dimensies van het aneurysma. Huidige technieken die gebruikt worden om de anatomie van het AAA voor de interventie in beeld te brengen zijn angiografie (Röntgencontrast foto) en computer tomografische angiografie (CTA; een CT scan met contrastmiddel). Om de plaatsing van stent-grafts te begeleiden is men, tijdens de interventie zelf, aangewezen op angiografie. Het probleem van angiografie is echter dat deze relatief eenvoudige techniek bemoeilijkt kan worden door de aanwezigheid van trombus, parallax en verkorting van schuin afgebeelde bloedvaten. Intravasculaire echografie (IVUS) is een afbeeldingstechniek die informatie kan verschaffen over de morfologie van de plaque in de vaatwand en over de afmeting van het bloedvat, zowel van coronaire, perifere en centrale arteriën. Ook kan met deze techniek het effect van de endovasculaire behandeling worden vastgelegd. Het onderzoek beschreven in dit proefschrift heeft tot doel het gebruik van IVUS voor de diagnostiek van het AAA te valideren, alsmede een automatisch contour analyse station voor de bepaling van vasculaire dimensies te valideren. Tenslotte worden de mogelijkheden van

het gebruik van IVUS tijdens endovasculaire behandeling van het AAA besproken.

Hoofdstuk 1 geeft een introductie van de inhoud van het proefschrift.

Hoofdstuk 2 beschrijft de resultaten van een in vitro validatie studie waarbij IVUS beelden verkregen bij normale, atherosclerotische en aneurysmatische aorta's werden vergeleken met corresponderende histologische coupes. Vijftien, bij obductie verkregen, aorta segmenten werden in een in vitro opstelling onderzocht onder fysiologische druk. Na de IVUS studie werden de segmenten gefixeerd en werden er histologische coupes van gemaakt. Echobeelden werden vergeleken met bijbehorende histologische coupes voor vaatwand karakteristieken, lesie morfologie en lumen diameter. De lengte van het aneurysma en de lengte van de proximale en distale hals werd gemeten met de catheter verplaatsingsmeter en vergeleken met de uitwendig gemeten lengte.

De studie liet zien dat normale aorta wand gezien kan worden als 2 of 3 lagige structuur overeenkomend met intima, media en adventitia. Een duidelijk onderscheid werd gevonden tussen fibreuze afwijkingen, verkalkte afwijkingen en trombus en tussen een normale en aneurysmatische aorta. De correlatie gevonden tussen IVUS diameter metingen en histologische diameter metingen was hoog ($r=0,93$; $p<0,001$). Ook tussen de IVUS lengte metingen en uitwendige lengte metingen werd een goede correlatie gevonden ($r=0,99$; $p<0,001$). Gezien de resultaten van dit onderzoek mag verwacht worden dat IVUS bij klinisch gebruik een betrouwbare techniek kan zijn voor de diagnostiek van het AAA.

Na de in vitro validatie van IVUS, beschrijft **Hoofdstuk 3** een klinische validatie studie waarbij IVUS metingen van de lengte en diameter van de proximale en distale hals van het AAA en de lengte van het aneurysma werden vergeleken met angiografische metingen en CTA metingen. Zestien patiënten met een AAA werden bestudeerd met angiografie en IVUS. Daarnaast werden de patiënten onderzocht met CTA.

IVUS identificeerde 97% van de nier arteriën en 80% van de accessoire nier arteriën. De vergelijking van lengtemetingen verkregen met IVUS en CTA lieten een goede correlatie zien ($r=0,99$; $p<0,001$) en een lage variatie coëfficiënt (9%). De lengte gemeten met IVUS was consequent korter dan de lengte gemeten met CTA. Wij nemen aan dat door de stijfheid van de IVUS catheter een kortere afstand door de aorta gemeten wordt dan gemeten wordt met de centrale lumen lijn waarlangs de metingen met CTA worden verricht. Vergelijking van de diametermetingen verkregen met IVUS en CTA toonde een goede correlatie ($r=0,93$); $p<0,001$) en een lage variatie coëfficiënt (9%).

IVUS onderschatte de lumen diameter vergeleken met CTA. Dit kan worden verklaard door het feit dat de minimum lumen diameter verkregen met IVUS is gekozen om de diameter van het bloedvat te bepalen om te voorkomen dat door de non coaxiale (scheve) positie van de echocatheter de diameter van het bloedvat overschat zou kunnen worden.

Deze klinische validatie studie toonde aan dat IVUS accurate en reproduceerbare metingen kan leveren van het AAA.

In **Hoofdstuk 4** wordt een automatisch contour analyse station beschreven dat de reproduceerbaarheid van handmatige IVUS metingen moet vergroten en de kwantitatieve analyse van een grote hoeveelheid IVUS beelden mogelijk moet maken. In deze studie werden IVUS beelden verkregen voor interventie van de arteria femoralis superficialis geanalyseerd. Metingen verkregen met behulp van het automatische analyse station werden vergeleken met handmatig geanalyseerde IVUS beelden. Daarnaast werd de intraobserver en de interobserver variabiliteit van automatische analyse bepaald.

Oppervlakte metingen verkregen met automatische analyse kwamen goed overeen met handmatige verkregen metingen, en lieten hoge correlatie coëfficiënten zien ($r=0,92-0,98$) en lage variatie coëfficiënten (8,5%-15,7%). De intra- en interobserver analyses toonden hoge correlatie coëfficiënten ($r=0,93-0,99$) en lage variatie coëfficiënten (6,0%-13,5% en 5,7% en 14,0%).

Vervolgens wordt in **Hoofdstuk 5** de toepassing van het automatisch contour analyse station beschreven voor de kwantitatieve analyse van IVUS cross-secties verkregen na vasculaire interventie (ballon dilatatie, stent plaatsing en stent-graft plaatsing) in de arteria femoralis superficialis. Lumen diameter verkregen met automatische analyse werd vergeleken met lumen diameter verkregen met handmatige analyse. De positie van het kleinste lumenoppervlak gezien met behulp van automatische analyse werd vergeleken met de positie van deze plek gevonden met visuele benadering. IVUS cross-secties met een dissectie, een niet ongebruikelijke bevinding na ballon dilatatie, konden niet worden geanalyseerd met het automatische analyse station. IVUS cross-secties verkregen in stents en stent-grafts vertoonden een hoge correlatie en lage variatie tussen automatische en handmatige analyse (beiden $r=1,0$; variatie coëfficiënt 2,7% en 2,1%). De positie van het kleinste lumen oppervlak gemeten met beide systemen was gelijk (< 1 cm) bij 16 van de 20 onderzochte patiënten en verschilde meer dan 1 cm bij 4 patiënten.

Dit onderzoek toonde aan dat de analyses verkregen met een automatische contour analyse station betrouwbaar en reproduceerbaar de dimensies van

bloedvaten kan bepalen voor en na een endovasculaire behandeling van perifere bloedvaten.

Na de validatie studies van het automatisch contour analyse station wordt in **Hoofdstuk 6** de toepassing van dit systeem beschreven voor de analyse van de proximale en distale hals van het AAA en de additionele toepassing van drie dimensionale beeldverwerking. Diameter metingen van de proximale en distale hals werden zowel automatisch als handmatig bepaald. De lengte van de hals gemeten met automatische analyse met behulp van de catheter verplaatsingsmeter werd vergeleken met de lengte verkregen door visuele benadering.

Vergelijking van de lumen diameter en de lengte vertoonde hoge correlatie coëfficiënten (beiden: $r=0,99$) en lage variatie coëfficiënten (2,1% en 4,1%). Interobserver analyse toonde hoge correlatie (beiden: $r=0,99$) en lage variatie coëfficiënten (3,4% en 3,5%). Drie dimensionale IVUS analyse maakte een onderscheid mogelijk tussen verschillende vormen van de halzen.

Deze studie heeft duidelijk gemaakt dat automatische analyse van de proximale en distale hals van een AAA mogelijk is. De gegevens verkregen met behulp van automatische analyse kunnen mogelijk gebruikt worden tijdens endovasculaire behandeling van AAA.

Hoofdstuk 7 beschrijft een 'feasibility' studie naar de aanvullende rol van IVUS tijdens endovasculaire behandeling van AAA. In deze multi-center studie werden verschillende soorten stent-grafts gebruikt. Voorafgaand aan de interventie werd IVUS gebruikt om de diameter en lengte van de stent-graft te bepalen. In het geval van modulaire stent-grafts werd de uiteindelijke maat bepaald met de IVUS metingen. Na de interventie werd IVUS gebruikt om het succes van de ingreep te bepalen. Meer specifiek werd er gekeken naar de appositie (aanligging) aan de proximale en distale zijde van de stent-graft, en werden factoren die het succes van de ingreep kunnen bedreigen uitgesloten.

Voor de interventie werden gebaseerd op IVUS data bij 12 patiënten de modules van modulaire stent-grafts gekozen. Bij 1 patiënt werd de procedure geconverteerd naar open chirurgie nadat IVUS had aangetoond dat de proximale hals niet geschikt (te groot) was voor endovasculaire behandeling. Bij 1 patiënt werd IVUS gebruikt om een keuze te maken tussen 2 verschillende lengtematen stent-graft. Bij 1 patiënt werd de introductiekant voor de stent-graft veranderd nadat met IVUS een ernstige stenose werd gezien in de arteria iliaca. Tenslotte werd bij 1 patiënt een predilatatie verricht van een stenose van de arteria iliaca communis.

Na interventie onthulde IVUS incomplete appositie aan de proximale zijde bij 1 patiënt en een vouw in een tube-graft bij een andere patiënt: in beide

gevallen werd geen aanvullende interventie verricht. Bij 1 patiënt werd met IVUS gezien dat het iliacale deel van een stent-graft eindigde in het aneurysma en werd een incomplete bekleding van de arteria iliaca communis gezien in 3 andere patiënten; al deze 4 patiënten werden met succes behandeld door een verlengstuk te plaatsen.

Ook werd met IVUS gezien dat het onbeklede gedeelte van een stent-graft bij 1 patiënt over een nier slagader was geplaatst, en bij 3 andere patiënten een accessoire nier arterie opzettelijk was afgesloten. Bij 5 patiënten werd een stenose in het iliacale been van de stent-graft gevonden waarvoor met succes een aanvullende ballon dilatatie werd verricht. Tenslotte werd voor een dissectie van de arteria iliaca met IVUS gezien in 5 patiënten, geen additionele behandeling nodig geacht.

Kort samengevat kunnen we stellen dat deze studie heeft aangetoond dat IVUS *voor* de interventie gebruikt kan worden voor de maatvoering van modulaire stent-grafts, en *na* de interventie om het succes van de procedure te bepalen, waarna aanvullende interventies gedurende de zelfde sessie kunnen worden verricht.

Tenslotte wordt in **Hoofdstuk 8** de huidige stand van zaken met betrekking tot endovasculaire behandeling van AAA besproken en de verschillende perspectieven over het gebruik van IVUS tijdens endovasculaire behandeling van AAA uiteen gezet. Onderwerpen, zoals de kosten van IVUS en de selectie van patiënten die het meest baat zullen hebben bij het gebruik van IVUS worden behandeld. Enkele noten over de toekomst van vasculaire afbeeldingstechnieken worden besproken.

LIST OF PUBLICATIONS

Jeroen A. van Essen

List of publications

ARTICLES

1. Gussenhoven EJ, Lugt van der A, **Essen van J**, Pieterman H, Urk van H. What can we learn from intravascular ultrasound? *Medizin im Bild* 1995; 10: 9-15.
2. Lugt van der A, Gussenhoven EJ, **Essen van J**, Pieterman H, Honkoop J, Urk van H. Can intravascular ultrasound supplement angiographic diagnosis? *Critical Ischemia* 1995; 5(2):45-51.
3. Lugt van der A, Gussenhoven EJ, The SHK, **Essen van J**, Honkoop J, Blankensteijn JD, Bois du NAJJ, Urk van H. Femorodistal venous bypass evaluated with intravascular ultrasound. *Eur J Vasc Endovasc Surg* 1995; 9: 394-402.
4. Lugt van der A, Hartlooper A, **Essen van JA**, Li W, Birgelen von C, Reiber JHC, Gussenhoven EJ. Reliability and reproducibility of automated contour analysis in intravascular ultrasound images of femoropopliteal arteries. *Ultrasound Med Biol* 1998; 24: 43-50.
5. **Essen van JA**, Lugt van der A, Gussenhoven EJ, Leertouwer TC, Zondervan P, Sambeek van MRHM. Intravascular ultrasonography allows accurate assessment of abdominal aortic aneurysm: an in vitro validation study. *J Vasc Surg* 1998; 27: 347-353.
6. Hartlooper A, **Essen van JA**, Lugt van der A, Gussenhoven EJ, Sambeek van MRHM, Overhagen van H. Validation of automated contour analysis of intravascular ultrasound images following vascular intervention. *J Vasc Surg* 1998; 27: 486-491.
7. Gussenhoven EJ, Hagens T, **Essen van JA**, Honkoop J, Lugt van der A, Lankeren van W, Overhagen van H, Bom N. What has been learnt from 10 years of peripheral IVUS? *Intravascular Imaging* 1998; 2: 43-50.
8. **Essen van JA**, Huijsman PC, Lugt van der A, Honkoop J, Sambeek van MRHM, Dijk van LC, Gussenhoven EJ. Intravascular ultrasound assessment of abdominal aortic aneurysm. *CVI-Online* 1998; 1: 32..
9. **Essen van JA**, Gussenhoven EJ, Lugt van der A, Huijsman PC, Muiswinkel van JM, Sambeek van MRHM, Dijk van LC, Urk van H. Accurate assessment of abdominal aortic aneurysm by intravascular ultrasound scanning: validation with computed tomographic angiography. *J Vasc Surg* 1999; 29: 631-638.
10. Leertouwer TC, Gussenhoven EJ, Dijk van LC, **Essen van JA**, Honkoop J, Deinum J, Pattynama PMT. Intravascular ultrasound evidence for renal artery coarctation causing symptomatic renal artery stenosis. *Circulation* 1999; 99: 2976-2978.
11. Gussenhoven EJ, Honkoop J, Athanassopoulos P, Goedbloed Y, Hagens T, Bom N, **Essen van JA**. Intravasculaire echografie als kijkdraad. *Vakblad voor vaatdiagnostiek* 1999; 12 (3): 16-21.
12. Hagens T, Gussenhoven EJ, **Essen van JA**, Seelen J, Honkoop J, Lugt van der A. Reproducibility of volumetric quantification in intravascular ultrasound images. *Ultrasound Med Biol* 2000; 26: 367-374.
13. Sambeek van MRHM, Segeren CM, Dijk van LC, **Essen van JA**, Dippel DWJ, Urk van H. Endovascular repair of an extracranial aneurysm of the internal carotid artery complicated by heparin induced thrombocytopenia and thrombosis. In press; *J Endovasc Ther*.

List of publications

14. **Essen van JA**, Gussenhoven EJ, Blankensteijn JD, Honkoop J, Dijk van LC, Sambeek van MRHM, Lugt van der A. Three-dimensional intravascular ultrasound assessment of the proximal and distal neck of abdominal aortic aneurysms. In press; *J Endovasc Ther*.

BOOKS

1. Lugt van der A, Gussenhoven EJ, **Essen van J**, Pieterman H, Urk van H. Venous bypass imaging with intravascular ultrasound. In: *Vascular imaging for surgeons*. Greenhalgh RM (ed). WB Saunders Comp. Ltd. 1995: 361-375.
2. Gussenhoven EJ, Hagenaaars T, **Essen van JA**, Leertouwer TC, Bom N. Intravascular ultrasound for peripheral application. In: *Theory and practice of vascular medicine*. Lanzer P, Topol EJ (eds). Springer-Verlag GmbH & Co. KG, Heidelberg. In press.

ABSTRACTS

1. Gussenhoven EJ, The SHK, Lugt van der A, **Essen van J**, Pasterkamp G, Berg van den F, Sie LWS, Tielbeek AS, Gerritsen GP, Li W, Pieterman H, Urk van H. Intravascular ultrasound as predictor of restenosis after successful peripheral balloon angioplasty: a multicenter trial. *ESVS '94, VIII Annual Meeting, Berlin, 3-6 September*; 102.
2. Gussenhoven EJ, Lugt van der A, The SHK, Li W, Stijnen T, Egmond van FC, **Essen van J**, Urk van H, Bom N. Balloon angioplasty evaluated in vitro by intracoronary ultrasound: a validation with histology. *J Am Coll Cardiol* 1995; 916-84: 74A.
3. Lugt van der A, Gussenhoven EJ, The SHK, **Essen van J**, Pasterkamp G, Berg van den FG, Vischjager M, Bom N, Urk van H, Pieterman H. Qualitative and quantitative effects of balloon angioplasty in peripheral vessels assessed by intravascular ultrasound. *11th Symposium of echocardiology, Rotterdam, June 1995*; 136.
4. Lugt van der A, Gussenhoven EJ, The SHK, **Essen van J**, Pasterkamp G, Berg van den FG, Vischjager M, Pieterman H, Urk van H. The mechanism of balloon angioplasty in peripheral vessels assessed by intravascular ultrasound. *Eur Surg Res* 1995; 27 (1): 137.
5. Lugt van der A, Gussenhoven EJ, **Essen van J**, Pasterkamp G, Vischjager M, The SHK, Pieterman H, Urk van H. The mechanism of balloon angioplasty in peripheral vessels assessed by intravascular ultrasound. *Eur Heart J* 1995; 18: 209.
6. Lugt van der A, Gussenhoven EJ, Stijnen T, Li W, **Essen van J**, Bom N, Urk van H. Balloon angioplasty evaluated in vitro by intracoronary ultrasound: a validation with histology. *Eur Heart J* 1995; 203: 1201.
7. **Essen van JA**, Lugt van der A, Gussenhoven EJ, Leertouwer TC, Hartlooper A, Honkoop J, Urk van H. In vitro validation of intravascular ultrasonic findings in abdominal aortic aneurysm. *Nederlands Vereniging voor Vaatchirurgie, Voorjaarsvergadering 18 april 1997, Utrecht*.

8. **Essen van J**, Lugt van der A, Gussenhoven E, Suylen van R, Leertouwer T, Honkoop J, Hartlooper A. Intravascular ultrasound of abdominal aortic aneurysm: in vitro validation study. *Thoraxcenter J* 1997; June: 22.
9. Lugt van der A, **Essen van JA**, Gussenhoven EJ, Leertouwer T, Hartlooper A. In vitro validation of intravascular ultrasonic findings in abdominal aortic aneurysm. *Memorad* 1997; 2: 14.
10. Lugt van der A, Gussenhoven EJ, **Essen van JA**, Hartlooper A, Birgelen von C, Li W. Automated contour analysis of lumen and vessel area in intravascular ultrasound images obtained in peripheral arteries: a validation study. *Radiology* 1997; 205(P): 546-1712.
11. **Essen van JA**, Lugt van der A, Gussenhoven EJ, Muiswinkel van JM, Overhagen van H, Urk van H. Intravascular ultrasound allows accurate assessment of abdominal aortic aneurysm: comparison with spiral computed tomographic angiography. *J Endovasc Surg* 1998; 5: I-34.
12. Gussenhoven EJ, **Essen van JA**, Lankeren van W, Lugt van der A, Bom N. Tissue analysis: will it change our interventional approach? *Current Concepts in Therapy of Coronary Heart Disease*, 1998.
13. Gussenhoven EJ, **Essen van JA**, Lankeren van W, Lugt van der A, Hartlooper A, Wenguang L. Can intravascular ultrasound (IVUS) be used to assess effect of antisclerotic agents? *J Molec Cell Cardiol* 1998; 30: A186.
14. **Essen van JA**, Gussenhoven EJ, Lugt van der A, Huijsman P, Sambeek van MRHM, Overhagen van H, Urk van H. Intravasculaire echografie voor de diagnostiek van het abdominale aorta aneurysma: validatie met CT angiografie. *Chirurgendagen 1998, Samenvattingen*: 68.
15. **Essen van JA**, Huijsman P, Lugt van der A, Blankensteijn JD, Sambeek van MRHM, Dijk van LC, Gussenhoven EJ. Three-dimensional intravascular ultrasound assessment of the proximal and distal neck of abdominal aortic aneurysms. *European Society for Vascular Surgery, XII Annual Meeting, Paris 1-4 October 1998*: 128.
16. Hagens T, Gussenhoven EJ, Lugt van der A, **Essen van JA**, Honkoop J. Can intravascular ultrasound be used to assess the effect on atherosclerotic plaque by lipid-lowering agents? *Echocardiography* 1998; 15 (6) Part 2: S49-326.
17. Gussenhoven EJ, Hagens T, **Essen van JA**, Wittens CHA, Kranendonk SE, Honkoop J, Lugt van der A. Reproducible assessment of lumen, vessel and plaque volume in serially acquired intravascular ultrasound (IVUS) images obtained from femoropopliteal arteries. *J Am Coll Cardiol* 1999; 33: 78A.
18. Gussenhoven EJ, **Essen van JA**, Honkoop J, Seyen van A, Seelen J, Lankeren van W. Intimal hyperplasia and vascular remodelling contribute to lumen area change following balloon angioplasty of the femoropopliteal artery: an intravascular ultrasound study. *J Am Coll Cardiol* 1999; 33: 292A.
19. Hagens T, Gussenhoven EJ, **Essen van JA**, Honkoop J, Lugt van der A. Can intravascular ultrasound be used to assess effect on atherosclerotic plaque by lipid-lowering agents? *Cardiovasc Drugs Ther* 1999; 13: 25.

List of publications

20. **Essen van JA**, Smet de AAEA, Blankensteijn JD, Kranendonk SE, Tielbeek AV, Sambeek van MRHM, Gussenhoven EJ. Intravasculaire echografie (IVUS) bij de endovasculaire behandeling van het abdominale aorta aneurysma (AAA). Vaatdagen 1999, Samenvattingen: 19.
21. **Essen van JA**, Urk van H, Gussenhoven EJ, Blankensteijn JD, Honkoop J, Tielbeek AV, Dijk van LC, Yo TI. Intravascular ultrasound (IVUS) to guide endovascular stent-graft placement in abdominal aortic aneurysms (AAA). 13th Rotterdam Symposium on Echocardiology; 76.
22. Gussenhoven EJ, **Essen van JA**, Honkoop J, Seyen van A, Seelen J, Lankeren van W. Intimal hyperplasia and vascular remodeling contribute to lumen area change following balloon angioplasty (PTA) of the femoropopliteal artery: and intravascular ultrasound (IVUS) study. 13th Rotterdam Symposium on Echocardiology; 79.
23. Leertouwer TC, Gussenhoven EJ, Dijk van LC, **Essen van JA**, Honkoop J, Deinum J, Pattynama PMT. Intravascular ultrasound evidence for coarctation causing symptomatic renal artery stenosis. 13th Rotterdam Symposium on Echocardiology; 86.
24. **Essen van JA**, Smet de AAEA, Blankensteijn JD, Tielbeek AV, Sambeek van MRHM, Gussenhoven EJ. Intravascular ultrasound (IVUS) to guide endovascular stent-graft placement in abdominal aortic aneurysms (AAA). CVIR 1999; 22 (suppl 2): S112-155.
25. **Essen van JA**, Hagens T, Gussenhoven EJ, Seyen van A, Seelen J, Honkoop J, Lugt van der A. Volumetric change of lumen, vessel and plaque seen at 1-year follow-up with intravascular ultrasound. CVIR 1999; 22 (suppl 2): S158-339.
26. Leertouwer TC, Gussenhoven EJ, Dijk van LC, **Essen van JA**, Honkoop J, Pattynama PMT. Intravascular ultrasound evidence for coarctation causing symptomatic renal artery stenosis. Memorad 1999; 4: 30.
27. Lugt van der A, Hagens T, **Essen van JA**, Seelen JL, Gussenhoven EJ. Reproducible assessment of lumen, vessel and plaque volume in serially acquired intravascular ultrasound images obtained from femoropopliteal arteries. Memorad 1999; 4: 51-52.
28. Lugt van der A, **Essen van JA**, Zondervan P, Muiswinkel van JM, Dijk van LC, Gussenhoven EJ. Validation of intravascular ultrasound images obtained in abdominal aortic aneurysm. Radiology 1999; 213(p): 569-1134VI.
29. Leertouwer TC, Gussenhoven EJ, Dijk van LC, **Essen van JA**, Honkoop J, Pattynama PMT. Intravascular ultrasound evidence for coarctation causing symptomatic renal artery stenosis. Radiology 1999; 213(p): 434-1444.

DANKWOORD

Jeroen A. van Essen

Dankwoord

DANKWOORD

Een proefschrift is niet het werk van één persoon. De afdeling Experimentele Echocardiografie staat temidden van vaatchirurgen en radiologen. Alle betrokken medewerkers van die afdelingen, in het Dijkzigt Ziekenhuis, het Universitair Medisch Centrum Utrecht, het St. Clara Ziekenhuis te Rotterdam, het St. Catharina Ziekenhuis te Eindhoven en het Twee Steden Ziekenhuis te Tilburg, dank ik voor de ondersteuning van mijn onderzoek.

In het bijzonder wil ik bedanken:

Mijn promotoren, Prof.dr. H. van Urk en Prof.dr. P.M.T. Pattynama, voor hun aanwijzingen, hun commentaar op mijn manuscripten en de vrijheid om op hun afdelingen mijn onderzoek te kunnen verrichten.

Mijn co-promotor, Elma Gussenhoven, die, met haar enorme kennis en ervaring op het gebied van de intravasculaire echografie, mijn onderzoek in sneltreinvaart geregisseerd heeft. Dat na mijn promotie haar slapeloze nachten voorbij zullen zijn.

De leden van de kleine commissie, Prof.dr. N. Bom, Prof.dr. J. Jeekel en Prof.dr. J.A. Reekers, voor de snelle beoordeling van mijn proefschrift.

Aad van der Lugt, Winnifred van Lankeren, Aran Hartlooper, Trude Leertouwer en Tjebbe Hagenaars, voor hun gezelschap en morele ondersteuning.

De medewerkers van het echolab, in het bijzonder Jan Honkoop en Frans van Egmond, voor de technische ondersteuning van mijn onderzoek. Hun kundige handen hebben menigmaal het door mij kapotgemaakte materiaal weten te herstellen.

Vaatchirurgen en radiologen betrokken bij mijn onderzoek, Marc van Sambeek, Lukas van Dijk, Hans van Muiswinkel, Jan Blankensteijn, André de Smet, Xander Tielbeek, Steven Kranendonk en Jan Seelen, voor het bedienen van mijn echocatheters, de genoten gastvrijheid op operatiekamers en angiokamers, en hun commentaar op mijn manuscripten.

Laraine Visser is acknowledged for her speedy corrections of my manuscripts.

Andries Zwamborn en Teun van Rijsdijk, voor het maken van posters, dia's, foto's en dit proefschrift.

Het Interuniversitair Cardiologisch Instituut Nederland, met name Manja Helmers en Erwin van de Ridder, voor de ondersteuning van de verschillende studies.

Mijn paranimfen, Wouter en Mark, voor hun vriendschap en steun tijdens studietijd en daarna.

Mijn familie en vrienden, tenslotte, voor hun grenzeloze vertrouwen.

CURRICULUM VITAE

Jeroen A. van Essen

Curriculum vitae

CURRICULUM VITAE

- 18 september 1970 Geboren te Haarlem.
- 1982 - 1989 VWO, Scholen Gemeenschap Sint Michiel, Geleen.
- 1989 - 1994 Doctoraal examen geneeskunde, Erasmus Universiteit Rotterdam.
- 1994 Student-assistent Afdeling Experimentele Echocardiografie. Onderwerp: Ballondilatatie van de arteria femoralis superficialis.
Begeleider: Dr. E.J. Gussenhoven
- 1995 - 1996 Arts examen, Erasmus Universiteit Rotterdam.
- 1997 - 1999 Wetenschappelijk onderzoeker Afdeling Experimentele Echocardiografie, Erasmus Universiteit Rotterdam.
Onderwerp: Intravasculaire echografie van het abdominale aorta aneurysma.
Begeleider: Dr. E.J. Gussenhoven.
- 1999 - heden Arts-assistent chirurgie, Academisch Ziekenhuis Rotterdam.
Hoofd: Prof.dr. J. Jeekel.

Curriculum vitae
